Published for SISSA by Springer

Received: August 31, 2017
Revised: October 20, 2017
Accepted: November 21, 2017
Published: November 29, 2017

Search for supersymmetry in events with b-tagged jets and missing transverse momentum in pp collisions at $\sqrt{s} = 13$ TeV with the ATLAS detector



The ATLAS collaboration

E-mail: atlas.publications@cern.ch

Abstract: A search for the supersymmetric partners of the Standard Model bottom and top quarks is presented. The search uses 36.1 fb^{-1} of pp collision data at $\sqrt{s} = 13$ TeV collected by the ATLAS experiment at the Large Hadron Collider. Direct production of pairs of bottom and top squarks ($\bar{b}_1$ and $\bar{t}_1$) is searched for in final states with b-tagged jets and missing transverse momentum. Distinctive selections are defined with either no charged leptons (electrons or muons) in the final state, or one charged lepton. The zero-lepton selection targets models in which the $\bar{b}_1$ is the lightest squark and decays via $\bar{b}_1 \to b\bar{\chi}_1^0$, where $\bar{\chi}_1^0$ is the lightest neutralino. The one-lepton final state targets models where bottom or top squarks are produced and can decay into multiple channels, $\bar{b}_1 \to b\bar{\chi}_1^0$ and $\bar{b}_1 \to t\bar{\chi}_1^\pm$, or $\bar{t}_1 \to t\bar{\chi}_1^0$ and $\bar{t}_1 \to b\bar{\chi}_1^\pm$, where $\bar{\chi}_1^\pm$ is the lightest chargino and the mass difference $m_{\bar{\chi}_1^\pm} - m_{\bar{\chi}_1^0}$ is set to 1 GeV. No excess above the expected Standard Model background is observed. Exclusion limits at 95% confidence level on the mass of third-generation squarks are derived in various supersymmetry-inspired simplified models.

Keywords: Hadron-Hadron scattering (experiments)

ArXiv ePrint: 1708.09266

Open Access, Copyright CERN,
for the benefit of the ATLAS Collaboration.
Article funded by SCOAP^3.

https://doi.org/10.1007/JHEP11(2017)195

Contents

1 Introduction **1**

2 ATLAS detector **2**

3 Data and simulated event samples **3**

4 Event reconstruction **5**

5 Event selection **7**
5.1 Discriminating variables 7
5.2 Zero-lepton channel selections 10
5.3 One-lepton channel selections 11

6 Background estimation **12**
6.1 Background estimation in the zero-lepton signal regions 13
6.2 Background estimation in the one-lepton signal regions 16
6.3 Validation regions 16

7 Systematic uncertainties **18**

8 Results and interpretation **21**

9 Conclusion **26**

The ATLAS collaboration **33**

JHEP11(2017)195

1 Introduction

Supersymmetry (SUSY) [1–6] provides an extension of the Standard Model (SM) that solves the hierarchy problem [7–10] by introducing partners of the known bosons and fermions. In the framework of R-parity-conserving models, SUSY particles are produced in pairs and the lightest supersymmetric particle (LSP) is stable, providing a possible candidate for dark matter [11, 12]. In a large variety of models the LSP is the lightest neutralino ($\tilde{\chi}_1^0$). Naturalness considerations [13, 14] suggest that the supersymmetric partners of the third-generation SM quarks are the lightest coloured supersymmetric particles. This may lead to the lightest bottom squark ($\tilde{b}_1$) and top squark ($\tilde{t}_1$) mass eigenstates[1] being significantly lighter than the other squarks and the gluinos. As a consequence, $\tilde{b}_1$ and $\tilde{t}_1$ could be pair-produced with relatively large cross-sections at the Large Hadron Collider (LHC).

[1]Scalar partners of the left-handed and right-handed chiral components of the bottom quark ($\tilde{b}_{\mathrm{L,R}}$) or top quark ($\tilde{t}_{\mathrm{L,R}}$) mix to form mass eigenstates for which $\tilde{b}_1$ and $\tilde{t}_1$are defined as the lighter of the two.

This paper presents a search for the direct pair production of bottom and top squarks decaying into final states with jets, two of them originating from the fragmentation of b-quarks (b-jets), and missing transverse momentum ($p_{\mathrm{T}}^{\mathrm{miss}}$, whose magnitude is referred to as $E_{\mathrm{T}}^{\mathrm{miss}}$). The dataset analysed corresponds to 36.1 fb^{-1} of proton-proton (pp) collisions data at $\sqrt{s} = 13$ TeV collected by the ATLAS experiment during Run 2 of the LHC in 2015 and 2016. The third-generation squarks are assumed to decay to the lightest neutralino (LSP) directly or through one intermediate stage. The search is based on simplified models inspired by the minimal supersymmetric extension of the SM (MSSM) [15–17], where the $\tilde{b}_1$ exclusively decays as $\tilde{b}_1 \to b\tilde{\chi}_1^0$ or where two decay modes for the bottom (top) squark are allowed and direct decays to the LSP, $\tilde{b}_1 \to b\tilde{\chi}_1^0$ ($\tilde{t}_1 \to t\tilde{\chi}_1^0$) compete with decays via an intermediate chargino ($\tilde{\chi}_1^{\pm}$) state, $\tilde{b}_1 \to t\tilde{\chi}_1^{\pm}$ ($\tilde{t}_1 \to b\tilde{\chi}_1^{\pm}$). In this case it is assumed that the $\tilde{\chi}_1^{\pm}$ is the next-to-lightest supersymmetric particle (NLSP) and is almost degenerate with $\tilde{\chi}_1^0$, such that other decay products are too low in momentum to be efficiently reconstructed. The first set of models lead to final-state events from bottom squark pair production characterized by the presence of two b-jets, $E_{\mathrm{T}}^{\mathrm{miss}}$ and no charged leptons ($\ell = e, \mu$), referred to as the zero-lepton channel (figure 1a). For mixed decays models (intended as models where both direct decays and decays through an intermediate stage are kinematically allowed), the final state of bottom or top squark pair production depends on the branching ratios of the competing decay modes. If the decay modes are equally probable, a large fraction of the signal events are characterized by the presence of a top quark, a bottom quark, and neutralinos. Hadronic decays of the top quark are targeted by the zero-lepton channel, whilst novel dedicated selections requiring one charged lepton, two b-jets and $E_{\mathrm{T}}^{\mathrm{miss}}$ are developed for semi-leptonic decays of the top quark, referred to as the one-lepton channel (figure 1b). A statistical combination of the two channels is performed when interpreting the results in terms of exclusion limits on the third-generation squark masses.

Previous searches for the exclusive decay $\tilde{b}_1 \to b\tilde{\chi}_1^0$ with the $\sqrt{s} = 13$ TeV LHC Run-2 dataset at ATLAS and CMS have set exclusion limits at 95% confidence level (CL) on $\tilde{b}_1$ masses in such scenarios [18, 19]. Searches in the context of mixed-decay models were performed only by ATLAS using the Run-1 $\sqrt{s} = 8$ TeV dataset and resulted in exclusion limits on the third-generation squark mass that depend on the branching ratios of the competing decay modes [20].

2 ATLAS detector

The ATLAS detector [21] is a multi-purpose particle physics detector with a forward-backward symmetric cylindrical geometry and nearly 4π coverage in solid angle.[2] The

[2] ATLAS uses a right-handed coordinate system with its origin at the nominal interaction point in the centre of the detector. The positive x-axis is defined by the direction from the interaction point to the centre of the LHC ring, with the positive y-axis pointing upwards, while the beam direction defines the z-axis. Cylindrical coordinates (r, ϕ) are used in the transverse plane, ϕ being the azimuthal angle around the z-axis. The pseudorapidity η is defined in terms of the polar angle θ by $\eta = -\ln\tan(\theta/2)$. Rapidity is defined as $y = 0.5\ln[(E + p_z)/(E - p_z)]$ where E denotes the energy and p_z is the component of the momentum along the beam direction.

JHEP11(2017)195

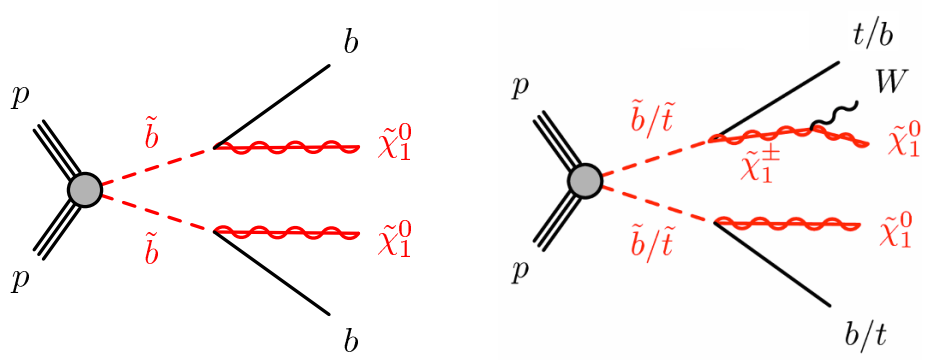


Figure 1. Diagrams illustrating the most relevant signal scenarios considered for the pair production of bottom and top squarks targeted by the (a) zero-lepton and (b) one-lepton channel selections. In (a) bottom squarks decay to a bottom quark and the lightest neutralino. In (b), decays via intermediate charginos are kinematically available and compete. If the mass difference $\Delta m(\tilde{\chi}_1^{\pm}, \tilde{\chi}_1^0)$ is small, the W bosons from chargino decays are off-shell.

inner tracking detector consists of pixel and silicon microstrip detectors covering the pseudorapidity region $|\eta| < 2.5$, surrounded by a transition radiation tracker which enhances electron identification in the region $|\eta| < 2.0$. Between Run 1 and Run 2, a new inner pixel layer, the insertable B-layer [22], was added at a mean sensor radius of 3.3 cm. The inner detector is surrounded by a thin superconducting solenoid providing an axial 2 T magnetic field and by a fine-granularity lead/liquid-argon (LAr) electromagnetic calorimeter covering $|\eta| < 3.2$. A steel/scintillator-tile calorimeter provides hadronic coverage in the central pseudorapidity range ($|\eta| < 1.7$). The endcap and forward regions ($1.5 < |\eta| < 4.9$) of the hadronic calorimeter are made of LAr active layers with either copper or tungsten as the absorber material. An extensive muon spectrometer with an air-core toroidal magnet system surrounds the calorimeters. Three layers of high-precision tracking chambers provide coverage in the range $|\eta| < 2.7$, while dedicated fast chambers allow triggering in the region $|\eta| < 2.4$. The ATLAS trigger system consists of a hardware-based level-1 trigger followed by a software-based high-level trigger [23].

3 Data and simulated event samples

The data used in this analysis were collected by the ATLAS detector in pp collisions at the LHC with a centre-of-mass energy of 13 TeV and a 25 ns proton bunch crossing interval during 2015 and 2016. The full dataset corresponds to an integrated luminosity of 36.1 fb^{-1} after requiring that all detector subsystems were operational during data recording. The uncertainty in the combined 2015+2016 integrated luminosity is 3.2%. It is derived following a methodology similar to that detailed in ref. [24] from a preliminary calibration of the luminosity scale using x–y beam-separation scans performed in August 2015 and May 2016. Each event includes on average 13.7 and 24.9 inelastic pp collisions ("pile-up") in the same bunch crossing in the 2015 and 2016 dataset, respectively. In the zero-lepton channel, events are required to pass an $E_{\mathrm{T}}^{\mathrm{miss}}$ trigger [25]. This trigger is

JHEP11(2017)195

fully efficient for events passing the preselection defined in section 5, which requires the offline reconstructed $E_{\mathrm{T}}^{\mathrm{miss}}$ to exceed 200 GeV. Events in the one-lepton channel, as well as events used for control regions, are selected online by a trigger requiring the presence of one electron or muon. The online selection thresholds are such that a plateau of the efficiency is reached for charged-lepton transverse momenta of 27 GeV and above.

Monte Carlo (MC) samples of simulated events are used to model the signal and to aid in the estimation of SM background processes, except multijet processes, which are estimated from data only.

All simulated samples were produced using the ATLAS simulation infrastructure [26] using GEANT4 [27], or a faster simulation [28] based on a parameterization of the calorimeter response and GEANT4 for the other detector systems. The simulated events are reconstructed with the same algorithm as that used for data.

SUSY signal samples were generated with MadGraph5_aMC@NLO [29] v2.2.3 at leading order (LO) and interfaced to Pythia v8.186 [30] with the A14 [31] set of tuned parameters (tune) for the modelling of the parton showering (PS), hadronization and underlying event. The matrix element (ME) calculation was performed at tree level and includes the emission of up to two additional partons. The ME-PS matching was done using the CKKW-L [32] prescription, with a matching scale set to one quarter of the third-generation squark mass. The NNPDF23LO [33] parton distribution function (PDF) set was used. The cross-sections used to evaluate the signal yields are calculated to next-to-leading-order (NLO) accuracy in the strong coupling constant, adding the resummation of soft gluon emission at next-to-leading-logarithmic accuracy (NLO+NLL) [34–36]. The nominal cross-section and uncertainty are taken as the midpoint and half-width of an envelope of cross-section predictions using different PDF sets and factorization and renormalization scales, as described in ref. [37].

SM background samples were simulated using different MC event generator programs depending on the process. The generation of $t\bar{t}$ was performed by the Powheg-Box [38] v2 generator with the CT10 [39] PDF set for the matrix element calculations. Single-top-quark events in the Wt, s-, and $t-$ channels were generated using the Powheg-Box v1 generator. For all processes involving top quarks, top quark spin correlations were preserved. The parton shower, fragmentation and the underlying event were simulated using Pythia v6.428 [40] with the CTEQ6L1 PDF set and the Perugia 2012 [41] tune for the underlying event. The h_{damp} parameter in Powheg, which controls the p_{T} of the first additional emission beyond the Born level and thus regulates the p_{T} of the recoil emission against the $t\bar{t}$ system, was set to the mass of the top quark ($m_t = 172.5$ GeV). All events with at least one leptonically decaying W boson are retained. Fully hadronic $t\bar{t}$ and single-top events do not contain sufficient $E_{\mathrm{T}}^{\mathrm{miss}}$ to contribute significantly to the background. The $t\bar{t}$ samples are normalized using their next-to-NLO (NNLO) cross-section including the resummation of soft gluon emission at next-to-NLL accuracy using Top++2.0 [42]. Samples of single-top-quark events are normalized using the NLO cross-sections reported in refs. [43–45] for the s-, t- and Wt-channels, respectively.

Events containing W or Z bosons with associated jets, including jets from the fragmentation of b- and c-quarks, were simulated using the Sherpa v2.2.1 [46] generator.

JHEP11(2017)195

Matrix elements were calculated for up to two additional partons at NLO and four partons at LO using the Comix [47] and OpenLoops [48] matrix element event generators and merged with the Sherpa PS [49] using the ME+PS@NLO prescription [50]. The NNPDF30NNLO [33] PDF set was used in conjunction with a dedicated PS tune developed by the Sherpa authors. Additional Sherpa Z+jets samples were produced with similar settings but with up to four partons LO, for the γ+jets studies detailed in section 6. The W/Z+jets events are normalized using their NNLO QCD theoretical cross-sections [51].

Diboson processes were also simulated using the Sherpa generator using the NNPDF30NNLO PDF set in conjunction with a dedicated PS tune developed by the Sherpa authors. They were calculated for up to one (ZZ) or zero (WW, WZ) additional partons at NLO and up to three additional partons at LO. Additional contributions to the SM backgrounds in the signal regions arise from the production of top quark pairs in association with $W/Z/h$ bosons and possibly additional jets. The production of top quark pairs in association with electroweak vector bosons (W, Z) or Higgs bosons was modeled by samples generated at NLO using MadGraph5_aMC@NLO v2.2.3 and showered with Pythia v8.212. Other potential sources of backgrounds, such as the production of three or four top quarks or three gauge bosons, are found to be negligible.

For all samples, except the ones generated using Sherpa, the EvtGen v1.2.0 program [52] was used to simulate the properties of the bottom- and charm-hadron decays. In-time and out-of-time pile-up interactions from the same or nearby bunch-crossings were simulated by overlaying additional pp collisions generated by Pythia v8.186, with the MSTW2008LO [53] PDF set, superimposed onto the hard-scattering events to reproduce the observed distribution of the average number of interactions per bunch crossing [54].

Several samples produced without detector simulation are employed to estimate systematic uncertainties associated with the specific configuration of the MC event generators used for the nominal SM background samples. They include variations of the renormalization and factorization scales, the CKKW-L matching scale, as well as different PDF sets and fragmentation/hadronization models. Details of the MC modelling uncertainties are discussed in section 7.

4 Event reconstruction

The search for pair production of bottom and top squarks is based on two distinct selections of events with b-jets and large missing transverse momentum, with either no charged leptons in the final state, or requiring exactly one electron or muon (for details, see section 5). For the zero-lepton channel selection, events containing charged leptons are explicitly vetoed in the signal and validation regions. Events characterized by the presence of exactly one electron or muon with transverse momentum above 27 GeV are retained in the one-lepton selection and are also used to define control regions for the zero-lepton channel. Finally, same-flavour opposite-sign (SFOS) two-lepton (electron or muon) events with dilepton invariant mass near the Z boson mass are used for control regions employed to aid in the estimation of the Z+jets background for the zero-lepton channel. The details of the reconstruction and selection, as well as the overlap removal procedure are given below.

JHEP11(2017)195

Selected events are required to have a reconstructed primary vertex consistent with the beamspot envelope and to consist of at least two tracks in the inner detector with $p_{\mathrm{T}} > 0.4$ GeV. When more than one such vertex is found, the one with the largest sum of the squares of transverse momenta of associated tracks [55] is chosen.

Jet candidates are reconstructed from three-dimensional energy clusters [56] in the calorimeter using the anti-k_t jet algorithm [57, 58] with a radius parameter of 0.4. The reconstructed jets are then calibrated to the particle level by the application of a jet energy scale (JES) derived from $\sqrt{s} = 13$ TeV data and simulation [59]. Quality criteria are imposed to identify jets arising from non-collision sources or detector noise, and any event containing such a jet is removed [60]. Further track-based selections are applied to reject jets with $p_{\mathrm{T}} < 60$ GeV and $|\eta| < 2.4$ that originate from pile-up interactions [61], and the jet momentum is corrected by subtracting the expected average energy contribution from pile-up using the jet area method [62]. Jets are classified as "baseline" and "signal". Baseline jets are required to have $p_{\mathrm{T}} > 20$ GeV and $|\eta| < 4.8$. Signal jets, selected after resolving overlaps with electrons and muons, are required to pass the stricter requirement of $p_{\mathrm{T}} > 35$ GeV and $|\eta| < 2.8$.

Jets are identified as b-jets if tagged by a multivariate algorithm which uses information about the impact parameters of inner detector tracks matched to the jet, the presence of displaced secondary vertices, and the reconstructed flight paths of b- and c-hadrons inside the jet [63]. The b-tagging working point with a 77% efficiency, as determined in a sample of simulated $t\bar{t}$ events, was chosen as part of the optimization procedure. The corresponding rejection factors against jets originating from c-quarks and from light quarks and gluons at this working point are 6.2 and 134, respectively [64]. To compensate for differences between data and MC simulation in the b-tagging efficiencies and mis-tag rates, correction factors are derived from data and applied to the samples of simulated events [63]. Candidate b-jets are required to have $p_{\mathrm{T}} > 20$ GeV and $|\eta| < 2.5$.

Electron candidates are reconstructed from energy clusters in the electromagnetic calorimeter matched to a track in the inner detector and are required to satisfy a set of "loose" quality criteria [65–67]. They are also required to lie within the fiducial volume $|\eta| < 2.47$. Muon candidates are reconstructed by matching tracks in the inner detector with tracks in the muon spectrometer. Events containing one or more muon candidates that have a transverse (longitudinal) impact parameter with respect to the primary vertex larger than 0.2 mm (1 mm) are rejected to suppress muons from cosmic rays. Muon candidates are also required to satisfy "medium" quality criteria [68] and have $|\eta|$ ¡ 2.5. All electron and muon candidates must have $p_{\mathrm{T}} > 10$ GeV. Lepton candidates remaining after resolving overlaps with baseline jets (see next paragraph) are called "baseline" leptons. In the control and signal regions where lepton identification is required, "signal" leptons are chosen from the baseline set with $p_{\mathrm{T}} > 27$ GeV to ensure full efficiency of the trigger and are required to be isolated from other activity in the detector using a criterion designed to accept at least 95% of leptons from Z boson decays as detailed in ref. [69]. The angular separation between the lepton and the b-jet arising from a semi-leptonically decaying top quark narrows as the top quark's p_{T} increases. This increased collimation is accounted for by varying the radius of the isolation cone as $\max(0.2, 10\ \mathrm{GeV}/p_{\mathrm{T}}^{\mathrm{lep}})$, where $p_{\mathrm{T}}^{\mathrm{lep}}$ is the

JHEP11(2017)195

lepton p_{T}. Signal electrons are further required to satisfy "tight" quality criteria. Electrons (muons) are matched to the primary vertex by requiring the transverse impact parameter (d_0) to satisfy $|d_0|/\sigma(d_0) < 5$ (3), and the longitudinal impact parameter (z_0) to satisfy $|z_0 \sin\theta| < 0.5$ mm for both the electrons and muons. The MC events are corrected to account for differences in the lepton trigger, reconstruction and identification efficiencies between data and MC simulation.

The sequence to resolve overlapping electrons, muons and jets begins by removing electron candidates sharing an inner detector track with a muon candidate. Next, jet candidates within $\Delta R = \sqrt{(\Delta y)^2 + (\Delta\phi)^2} = 0.2$ of an electron candidate are discarded, unless the jet is b-tagged, in which case the electron is discarded since it is likely to originate from a semileptonic b-hadron decay. Electrons are discarded if they lie within $\Delta R = 0.4$ of a jet. Muons with p_{T} below (above) 50 GeV are discarded if they lie within $\Delta R = 0.4$ ($\Delta R = 0.04 + 10$ GeV$/p_{\mathrm{T}}$) of any remaining jet, except for the case where the number of tracks associated with the jet is less than three.

The missing transverse momentum is defined as the negative vector sum of the p_{T} of all selected and calibrated physics objects (electrons, muons and jets) in the event, with an extra term added to account for soft energy in the event which is not associated with any of the selected objects. This soft term is calculated from inner detector tracks with p_{T} above 0.4 GeV matched to the primary vertex to make it more robust against pile-up contamination [70, 71].

Reconstructed photons are not used in the main signal event selections but are selected in the regions employed in one of the alternative methods used to estimate the Z+jets background, as explained in section 6. Photon candidates are required to have $p_{\mathrm{T}} > 145$ GeV and $|\eta| < 2.37$, whilst being outside the transition region $1.37 < |\eta| < 1.52$, to satisfy the tight photon shower shape and electron rejection criteria [72], and to be isolated.

5 Event selection

Two sets of signal regions (SRs) are defined and optimized to target different third-generation squark decay modes and mass hierarchies of the particles involved. The zero-lepton channel SRs (b0L) are designed to maximize the efficiency to retain bottom-squark pair production events where $\tilde{b}_1 \to b\tilde{\chi}_1^0$. The one-lepton channel selections (b1L) target SUSY models where bottom squarks decay with a significant branching ratio as $\tilde{b}_1 \to t\tilde{\chi}_1^\pm$ and the lightest chargino is almost degenerate with the lightest neutralino. With these assumptions, the final decay products of the off-shell W boson from $\tilde{\chi}_1^\pm \to \tilde{\chi}_1^0 W^*$ are too soft to be detected. If the branching ratios of the two competing decay modes ($b\tilde{\chi}_1^0, t\tilde{\chi}_1^\pm$) are around 50%, the final state for the largest fraction of signal events is characterized by the presence of a top quark, a bottom quark, and neutralinos escaping the detector. Similarly, $\tilde{t}_1$ pair production can lead to an equivalent final state if the $\tilde{t}_1 \to t\tilde{\chi}_1^0$ and $\tilde{t}_1 \to b\tilde{\chi}_1^\pm$ decay modes compete.

5.1 Discriminating variables

Several kinematic variables and angular correlations, built from the physics objects defined in the previous section, are employed to discriminate SUSY from SM background events

JHEP11(2017)195

and are reported below. In the following, signal jets are used and are ordered according to decreasing p_{T}.

- $\Delta\phi^{j}_{\mathrm{min}}$, $\mathrm{min}[\Delta\phi(\mathrm{jet}_{1-4}, E_{\mathrm{T}}^{\mathrm{miss}})]$, $\mathrm{min}[\Delta\phi(\mathrm{jet}_{1-2}, E_{\mathrm{T}}^{\mathrm{miss}})]$: these variables are the minimum $\Delta\phi$ between any of the leading jets and the missing transverse momentum vector. The background from multijet processes is characterized by small values of this variable. Depending on the signal regions, all, four or two jets are used.

- H_{T}: this is defined as the scalar sum of the p_{T} of all jets in the event

$$H_{\mathrm{T}} = \sum_{i} (p_{\mathrm{T}}^{\mathrm{jet}})_i,$$

  where the number of jets involved depends on the signal region. In addition, the modified form of H_{T}, referred to as the H_{T4} variable, is used to reject events with extra-jet activity in signal regions targeting models characterized by small mass-splitting between the bottom squark and the neutralino. In H_{T4} the sum starts with the fourth jet (if any).

- m_{eff}: this is defined as the scalar sum of the p_{T} of the jets and the $E_{\mathrm{T}}^{\mathrm{miss}}$, i.e.:

$$m_{\mathrm{eff}} = \sum (p_{\mathrm{T}}^{\mathrm{jet}})_i + E_{\mathrm{T}}^{\mathrm{miss}}.$$

  The m_{eff} observable is correlated with the mass of the pair-produced SUSY particles and is employed as a discriminating variable in some of the zero-lepton and one-lepton channel selections, as well as in the computation of other composite observables.

- $E_{\mathrm{T}}^{\mathrm{miss}}/m_{\mathrm{eff}}$, $E_{\mathrm{T}}^{\mathrm{miss}}/\sqrt{H_{\mathrm{T}}}$: the first ratio is the $E_{\mathrm{T}}^{\mathrm{miss}}$ divided by the m_{eff}, while the second emulates the global $E_{\mathrm{T}}^{\mathrm{miss}}$ significance, given that the $E_{\mathrm{T}}^{\mathrm{miss}}$ resolution scales approximately with the square root of the total hadronic energy in the event. Events with low values for these variables are rejected as it is most probable that $E_{\mathrm{T}}^{\mathrm{miss}}$ arises from jets mismeasurements, caused by instrumental and resolution effects.

- m_{jj}: this variable is calculated as the invariant mass of the leading two jets. In events where at least one of the leading jets is b-tagged, this variable aids in reducing the contamination from $t\bar{t}$ events. It is referred to as m_{bb} for events where the two leading jets are b-tagged.

- m_{T}: the event transverse mass m_{T} is defined as $m_{\mathrm{T}} = \sqrt{2p_{\mathrm{T}}^{\mathrm{lep}} E_{\mathrm{T}}^{\mathrm{miss}} - 2\boldsymbol{p}_{\mathrm{T}}^{\mathrm{lep}} \cdot \boldsymbol{p}_{\mathrm{T}}^{\mathrm{miss}}}$ and is used in the one-lepton control and signal regions to reduce the W+jets and $t\bar{t}$ backgrounds.

- $m_{b\ell}^{\mathrm{min}}$: the minimum invariant mass of the lepton and one of the two b-jets is defined as:

$$m_{b\ell}^{\mathrm{min}} = \mathrm{min}_{i=1,2} \left(m_{\ell b_i} \right).$$

  This variable is bound from above by $\sqrt{m_t^2 - m_W^2}$ for $t\bar{t}$ production, and it is used to distinguish $t\bar{t}$ contributions from Wt-channel single-top-quark events in the one-lepton control regions.

JHEP11(2017)195

- Contransverse mass (m_{CT}) [73]: this is the main discriminating variable in some of the zero-lepton channel signal regions [74]. It is used to measure the masses of pair-produced semi-invisibly decaying heavy particles. For identical decays of two heavy particles (e.g. the bottom squarks decaying exclusively as $\tilde{b}_1 \to b\tilde{\chi}_1^0$) into two visible particles v_1 and v_2 (the b-quarks), and two invisible particles X_1 and X_2 (the $\tilde{\chi}_1^0$ for the signal), m_{CT} is defined as

$$m_{\mathrm{CT}}^2(v_1,\ v_2) = [E_{\mathrm{T}}(v_1) + E_{\mathrm{T}}(v_2)]^2 - [\mathbf{p}_{\mathrm{T}}(v_1) - \mathbf{p}_{\mathrm{T}}(v_2)]^2,$$

  with $E_{\mathrm{T}} = \sqrt{p_{\mathrm{T}}^2 + m^2}$, and it has a kinematical endpoint at $m_{\mathrm{CT}}^{\mathrm{max}} = (m_i^2 - m_X^2)/m_i$ where i is the initially pair-produced particle. This variable is effective in suppressing the top-quark pair production background ($i = t, X = W$), for which the endpoint is at 135 GeV.

- $m_{\mathrm{T}}^{\mathrm{min}}(\mathrm{jet}_{1-4}, E_{\mathrm{T}}^{\mathrm{miss}})$: this is the minimum of the transverse masses calculated using any of the leading four jets and the $E_{\mathrm{T}}^{\mathrm{miss}}$ in the event. For signal scenarios with low values of $m_{\mathrm{CT}}^{\mathrm{max}}$, this kinematic variable is an alternative discriminating variable to reduce the $t\bar{t}$ background.

- am_{T2}: the asymmetric transverse mass [75, 76] is a kinematic variable which can be used to separate processes in which two decays giving missing transverse momentum occur, and it is the main discriminating observable in the one-lepton channel signal regions. The am_{T2} definition is based on the stransverse mass (m_{T2}) [77]:

$$m_{\mathrm{T2}}^2(\chi) = \min_{\mathbf{q}_{\mathrm{T}}^{(1)}+\mathbf{q}_{\mathrm{T}}^{(2)}=\mathbf{p}_{\mathrm{T}}^{miss}} \left[\max\left\{m_{\mathrm{T}}^2(\mathbf{p}_{\mathrm{T}}(v_1), \mathbf{q}_{\mathrm{T}}^{(1)}; \chi), m_{\mathrm{T}}^2(\mathbf{p}_{\mathrm{T}}(v_2), \mathbf{q}_{\mathrm{T}}^{(2)}; \chi)\right\}\right],$$

  where $\mathbf{p}_{\mathrm{T}}(v_i)$ are reconstructed transverse momenta vectors and $\mathbf{q}_{\mathrm{T}}^{(i)}$ represent the missing transverse momenta from the two decays, with a total missing transverse momentum, $p_{\mathrm{T}}^{\mathrm{miss}}$; χ is a free parameter representing the unknown mass of the invisible particles — here assumed to be zero. The a in am_{T2} indicates that the two visible decay legs are asymmetric, i.e. not composed of the same particles.

  In the case of events with one lepton (electron or muon) and two b-jets, the m_{T2} variable is calculated for different values of $\mathbf{p}_{\mathrm{T}}(v_1)$ and $\mathbf{p}_{\mathrm{T}}(v_2)$, by grouping the lepton and the two b-jets into two visible objects v_1 and v_2. The lepton needs to be paired with one of the two b-jets and the choice is driven by the value of $m_{b\ell}(n)$ — the invariant mass of the n^{th} b-tagged jet and the lepton. If the two particles are correctly associated, this value has an upper bound given by the top quark mass. The value of am_{T2} is thus computed accordingly:

  – If $m_{b\ell}(1)$ and $m_{b\ell}(2)$ are both > 170 GeV, neither of the two associations is compatible with the b-jet and the lepton originating from a top decay, so the event is rejected since all control, validation and signal regions require the smaller value of $m_{b\ell}$ to be < 170 GeV.

JHEP11(2017)195

– If $m_{b\ell}(1)$ is < 170 GeV and $m_{b\ell}(2)$ is > 170 GeV, am_{T2} is calculated with $v_1 = b_1 + \ell$ and $v_2 = b_2$. This is done because only the first pairing is compatible with a top quark decay.

– Similarly, if $m_{b\ell}(1)$ is > 170 GeV and $m_{b\ell}(2)$ is < 170 GeV, am_{T2} is calculated with $v_1 = b_1$ and $v_2 = b_2 + \ell$.

– If $m_{b\ell}(1)$ and $m_{b\ell}(2)$ are both < 170 GeV, am_{T2} is calculated in both configurations and its value is taken to be the smaller of the two. This must be done because, according to the $m_{b\ell}$ check, both pairings would be acceptable.

- $\mathcal{A}$: this is the p_{T} asymmetry of the leading two jets and is defined as:

$$\mathcal{A} = \frac{p_{\mathrm{T}}(j_1) - p_{\mathrm{T}}(j_2)}{p_{\mathrm{T}}(j_1) + p_{\mathrm{T}}(j_2)}.$$

The $\mathcal{A}$ variable is employed in scenarios where the mass-splitting between the bottom squark and the neutralino is small (< 20 GeV) and the selection exploits the presence of a high-momentum jet from initial-state radiation (ISR).

5.2 Zero-lepton channel selections

The selection criteria for the zero-lepton channel SRs are summarized in table 1 and have the main requirement of no baseline leptons with $p_{\mathrm{T}} > 10$ GeV and two b-tagged jets. To exploit the kinematic properties over the large range of $\tilde{b}_1$ and $\tilde{\chi}_1^0$ masses explored, three sets of SRs are defined.

The b0L-SRA regions are optimized to be sensitive to models with large mass-splitting between the $\tilde{b}_1$ and the $\tilde{\chi}_1^0$, $\Delta m(\tilde{b}_1, \tilde{\chi}_1^0) > 250$ GeV. Incremental thresholds are imposed on the main discriminating variable, m_{CT}, resulting in three overlapping regions (m_{CT} >350, 450 and 550 GeV). Only events with $E_{\mathrm{T}}^{\mathrm{miss}} > 250$ GeV are retained to ensure full efficiency of the trigger and comply with the expected signal topology. The two leading jets are required to be b-tagged whilst contamination from backgrounds with high jet multiplicity, particularly $t\bar{t}$ production, is suppressed by vetoing events with a fourth jet with $p_{\mathrm{T}} >$ 50 GeV. To discriminate against multijet background, events where $E_{\mathrm{T}}^{\mathrm{miss}}$ is aligned with a jet in the transverse plane are rejected by requiring $\min[\Delta\phi(\mathrm{jet}_{1-4}, E_{\mathrm{T}}^{\mathrm{miss}})] > 0.4$, and $E_{\mathrm{T}}^{\mathrm{miss}}/m_{\mathrm{eff}} > 0.25$. A selection on the invariant mass of the two b-jets ($m_{bb} > 200$ GeV) is applied to further enhance the signal yield over the SM background contributions.

The b0L-SRB region targets intermediate mass-splitting between $\tilde{b}_1$ and $\tilde{\chi}_1^0$, $50 < \Delta m(\tilde{b}_1, \tilde{\chi}_1^0) < 250$ GeV. In these scenarios, the selections based on the m_{CT} and m_{bb} variables are no longer effective and the variable $m_{\mathrm{T}}^{\mathrm{min}}(\mathrm{jet}_{1-4}, E_{\mathrm{T}}^{\mathrm{miss}})$ is employed to reduce SM background contributions from $t\bar{t}$ production, with events selected if $m_{\mathrm{T}}^{\mathrm{min}}(\mathrm{jet}_{1-4}, E_{\mathrm{T}}^{\mathrm{miss}}) >$ 250 GeV. No more than four signal jets are allowed, to reduce additional hadronic activity in the selected events. As opposed to the b0L-SRA criteria, no veto based on the fourth jet p_{T} is applied. A series of selections on the azimuthal angle between the two b-tagged jets and the $E_{\mathrm{T}}^{\mathrm{miss}}$ are implemented ($|\Delta\phi(b_1, E_{\mathrm{T}}^{\mathrm{miss}})| < 2.0$ and $|\Delta\phi(b_2, E_{\mathrm{T}}^{\mathrm{miss}})| < 2.5$) to reduce Z+jets background events.

JHEP11(2017)195

	b0L-SRAx	b0L-SRB	b0L-SRC
Lepton veto	No e/μ with p_{T} >10 GeV after overlap removal		
N_{jets} ($p_{\mathrm{T}} > 35$ GeV)	2–4	2–4	—
N_{jets} ($p_{\mathrm{T}} > 20$ GeV)	—	—	2–5
$p_{\mathrm{T}}(j_1)$ [GeV]	> 130	> 50	> 500
$p_{\mathrm{T}}(j_2)$ [GeV]	> 50	> 50	> 20
$p_{\mathrm{T}}(j_4)$ [GeV]	< 50	—	—
H_{T4} [GeV]	—	—	< 70
b-jets	j_1 and j_2	any 2	j_2 and (j_3 or j_4 or j_5)
$E_{\mathrm{T}}^{\mathrm{miss}}$ [GeV]	> 250	> 250	> 500
$E_{\mathrm{T}}^{\mathrm{miss}}/m_{\mathrm{eff}}$	> 0.25	-	—
$\min[\Delta\phi(\mathrm{jet}_{1-4}, E_{\mathrm{T}}^{\mathrm{miss}})]$	> 0.4	> 0.4	—
$\min[\Delta\phi(\mathrm{jet}_{1-2}, E_{\mathrm{T}}^{\mathrm{miss}})]$	—	-	> 0.2
$\Delta\phi(b_1, E_{\mathrm{T}}^{\mathrm{miss}})$	—	< 2.0	—
$\Delta\phi(b_2, E_{\mathrm{T}}^{\mathrm{miss}})$	—	< 2.5	—
$\Delta\phi(j_1, E_{\mathrm{T}}^{\mathrm{miss}})$	—	-	> 2.5
m_{jj} [GeV]	> 200	—	> 200
m_{CT} [GeV]	>350, 450, 550	—	—
$m_{\mathrm{T}}^{\mathrm{min}}(\mathrm{jet}_{1-4}, E_{\mathrm{T}}^{\mathrm{miss}})$ [GeV]	—	> 250	—
m_{eff} [GeV]	—	—	> 1300
$\mathcal{A}$	—	—	> 0.8

Table 1. Summary of the event selection in each signal region for the zero-lepton channel. For SRA, the "x" denotes the m_{CT} selection used. The term lepton is used in the table to refer to baseline electrons and muons. Jets (j_1, j_2, j_3, j_4 and j_5) are labelled with an index corresponding to their decreasing order in p_{T}.

Finally, the b0L-SRC region targets events where a bottom squark pair is produced in association with a jet from ISR. This selection provides sensitivity to models with a small mass difference between the $\tilde{b}_1$ and the $\tilde{\chi}_1^0$, $\Delta m(\tilde{b}_1, \tilde{\chi}_1^0) < 50$ GeV, such that a boosted bottom squark pair would satisfy the trigger requirements. To efficiently suppress $t\bar{t}$ and W+jets backgrounds, events are selected with one high-p_{T} non-b-tagged jet and $E_{\mathrm{T}}^{\mathrm{miss}} > 500$ GeV such that $\Delta\phi(j_1, E_{\mathrm{T}}^{\mathrm{miss}}) > 2.5$. Stringent requirements on the minimum azimuthal angle between the jets and $E_{\mathrm{T}}^{\mathrm{miss}}$ are not suited for these scenarios where b-jets have softer momenta and are possibly aligned with $E_{\mathrm{T}}^{\mathrm{miss}}$. A large asymmetry $\mathcal{A}$ is required to reduce the multijet background while loosening the selection on the minimum azimuthal angle between the jets and $E_{\mathrm{T}}^{\mathrm{miss}}$ to $\min[\Delta\phi(\mathrm{jet}_{1-2}, E_{\mathrm{T}}^{\mathrm{miss}})]$ >0.2, and relaxing the p_{T} threshold on signal jets to 20 GeV.

5.3 One-lepton channel selections

The selection criteria for the one-lepton channel SRs are summarized in table 2. Events are required to have exactly one signal electron or muon and no additional baseline leptons, two b-tagged jets and a large $E_{\mathrm{T}}^{\mathrm{miss}}$. Similarly to the zero-lepton channel, three sets of SRs are defined to maximize the sensitivity depending on the mass hierarchy between $\tilde{b}_1(\tilde{t}_1)$ and $\tilde{\chi}_1^{\pm} \approx \tilde{\chi}_1^0$.

JHEP11(2017)195

	b1L-SRAx	b1L-SRA300-2j	b1L-SRB
Number of leptons (e, μ)	1	1	1
N_{jets} ($p_{\text{T}} > 35$ GeV)	≥ 2	$= 2$	≥ 2
b-jets	any 2	j_1 and j_2	any 2
$E_{\text{T}}^{\text{miss}}$ [GeV]	> 200	> 200	> 200
$E_{\text{T}}^{\text{miss}}/\sqrt{H_{\text{T}}}$ [GeV$^{1/2}$]	> 8	> 8	> 8
$m_{b\ell}^{\text{min}}$ [GeV]	< 170	< 170	< 170
$\Delta\phi_{\text{min}}^{j}$	> 0.4	—	> 0.4
$\min[\Delta\phi(\text{jet}_{1-2}, E_{\text{T}}^{\text{miss}})]$	—	> 0.4	—
am_{T2} [GeV]	> 250	> 250	> 200
m_{T} [GeV]	> 140	> 140	> 120
m_{bb} [GeV]	> 200	> 200	< 200
m_{eff} [GeV]	$> 600, 750$	> 300	> 300
$m_{\text{T}}^{\text{min}}(b\text{-jet}_{1-2}, E_{\text{T}}^{\text{miss}})$ [GeV]	—	—	> 200
$\Delta\phi(b_1, E_{\text{T}}^{\text{miss}})$	—	—	> 2.0

Table 2. Summary of the event selection in each signal region for the one-lepton channel. For SRA, the "x" denotes the m_{eff} selection used. The term lepton is used in the table to refer to signal electrons and muons. Jets (j_1, j_2) are labelled with an index corresponding to their decreasing order in p_{T}.

The b1L-SRA regions are optimized for models with large $\Delta m(\tilde{b}_1, \tilde{\chi}_1^0)$: events are required to have large $E_{\text{T}}^{\text{miss}}$ and $E_{\text{T}}^{\text{miss}}/\sqrt{H_{\text{T}}}$ and $\Delta\phi_{\text{min}}^{j}$ above 0.4 to reduce the multijet background contributions to negligible levels. Requirements on the m_{T} and am_{T2} variables to be above 140 GeV and 250 GeV, respectively, are set to reject W+jets and $t\bar{t}$ events whilst the selection on the invariant mass of the two b-jets ($m_{bb} > 200$ GeV) is applied to further enhance the signal yield over the SM background contributions. Two incremental thresholds are finally imposed on m_{eff} (600 and 750 GeV) to define two overlapping signal regions.

The b1L-SRB region is designed to be sensitive to compressed mass spectra, hence low m_{bb} is expected, and the selections on the m_{T} and am_{T2} variables must be relaxed to avoid loss of signal events. The $\min[m_{\text{T}}(b\text{-jet}, E_{\text{T}}^{\text{miss}})]$ is employed to discriminate signal from $t\bar{t}$ events, which is the dominant SM background contribution.

A third region, referred to as b1L-SRA300-2j, is defined similarly to the b1L-SRAs but requiring no extra jets beside the two b-jets and m_{eff} above 300 GeV. Such a selection also targets SUSY models characterized by compressed mass spectra. It is kinematically similar to the signal region in the Run-1 analysis [20] with a veto requirement on the number of jets with $p_{\text{T}} > 50$ GeV.

6 Background estimation

Monte Carlo simulation is used to estimate the background yield in the signal regions. The MC prediction for the major backgrounds is normalized to data in control regions

JHEP11(2017)195

(CR) constructed to enhance a particular background and to be kinematically similar but mutually exclusive to the signal regions. The control regions are defined by explicitly requiring the presence of one or two leptons (electrons or muons) in the final state together with further selection criteria similar to those of the corresponding signal region. To ensure that the b0L and b1L analyses can be statistically combined, the CRs associated with b0L and b1L SRs are mutually exclusive, with the exception of the single-top CR, where the same CR is used for both channels.

The expected SM backgrounds are determined separately for each SR with a profile likelihood fit [78], referred to as the background-only fit. The fit uses as a constraint the observed event yields in a set of associated CRs to adjust the normalization of the main backgrounds, assuming that no signal is present. The inputs to the fit for each SR include the number of events observed in its associated CRs and the number of events predicted by simulation in each region for all background processes. The latter are described by Poisson statistics. The systematic uncertainties in the expected values are included in the fit as nuisance parameters. They are constrained by Gaussian distributions with widths corresponding to the sizes of the uncertainties and are treated as correlated, when appropriate, between the various regions. The product of the various probability density functions forms the likelihood, which the fit maximizes by adjusting the background normalization and the nuisance parameters. Finally, the reliability of the MC extrapolation of the SM background estimate outside of the control regions is evaluated in several validation regions (VRs).

6.1 Background estimation in the zero-lepton signal regions

The main SM background in the b0L signal regions is from the production of Z+jets followed by invisible decays of the Z boson. The production of top quark pairs, single top quarks and W+jets also results in important backgrounds, with their relative contributions depending on the specific SR considered. Full details of the CR definitions are given in tables 3 and 4.

Three same-flavour opposite-sign (SFOS) two-lepton (electron or muon) control regions with dilepton invariant mass near the Z boson mass ($76 < m_{\ell\ell} < 106$ GeV) and two b-tagged jets provide data samples dominated by Z boson production. Signal leptons are considered, with the threshold for the second lepton p_{T} loosened to 20 GeV. For these control regions, labelled in the following as b0L-CRzA, b0L-CRzB and b0L-CRzC, the p_{T} of the leptons is added vectorially to the $p_{\mathrm{T}}^{\mathrm{miss}}$ to mimic the expected missing transverse momentum spectrum of $Z \to \nu\bar{\nu}$ events, and is indicated in the following as $E_{\mathrm{T}}^{\mathrm{miss,cor}}$ (lepton corrected). In addition, a selection is applied to the uncorrected $E_{\mathrm{T}}^{\mathrm{miss}}$ of the event, in order to further enhance the Z boson contribution.

Events with one charged lepton in the final state are used to define control regions dominated by W+jets and top quark production by requiring either one or two b-tagged jets, respectively. Selections on the variable m_{T} are used to ensure that the lepton originates from a W decay. For the CRs corresponding to b0L-SRA, the contribution from $t\bar{t}$ and single top quark production are separated by applying the selection $m_{bb} < 200$ GeV and $m_{bb} > 200$ GeV, respectively. To further enhance the single-top-quark contribution, a selection on the minimum invariant mass of the lepton and one of the b-jets, $m_{b\ell}^{\mathrm{min}} >$

JHEP11(2017)195

b0L-	CRzA	CRttA	CRstA	CRwA	CRzB	CRttB	CRwB
Number of leptons ($\ell = e,\ \mu$)	2 SFOS	1	1	1	2 SFOS	1	1
$p_{\mathrm{T}}(\ell_1)$ [GeV]	> 90	> 27	> 27	> 27	> 27	> 27	> 27
$p_{\mathrm{T}}(\ell_2)$ [GeV]	> 20	—	—	—	> 20	—	—
$m_{\ell\ell}$ [GeV]	[76 –106]	—	—	—	[76–106]	—	—
N_{jets} ($p_{\mathrm{T}} > 35$ GeV)	2–4	2–4	2–4	2–4	2–4	2–4	2–4
$p_{\mathrm{T}}(j_1)$ [GeV]	> 50	> 130	–	> 130	> 50	> 50	> 50
$p_{\mathrm{T}}(j_2)$ [GeV]	> 50	> 50	> 50	> 50	> 50	> 50	> 50
$p_{\mathrm{T}}(j_4)$ [GeV]	< 50	< 50	< 50	< 50	—	—	—
b-jets	j_1 and $j_2 j_1$ and j_2	j_1 and j_2	j_1	any 2	any 2	any 2	
$E_{\mathrm{T}}^{\mathrm{miss}}$ [GeV]	< 100	> 200	> 200	> 200	< 100	> 100	> 100
$E_{\mathrm{T}}^{\mathrm{miss,cor}}$ [GeV]	> 100	—	—	—	> 200	—	—
$E_{\mathrm{T}}^{\mathrm{miss}}/m_{\mathrm{eff}}$	> 0.25	> 0.25	> 0.25	> 0.25	—	—	—
$\min[\Delta\phi(\mathrm{jet}_{1-4}, E_{\mathrm{T}}^{\mathrm{miss}})]$	—	> 0.4	> 0.4	> 0.4	> 0.4	> 0.4	> 0.4
m_{T} [GeV]	—	—	—	> 30	—	> 30	> 30
m_{bb} [GeV]	> 200	< 200	> 200	$m_{bj} > 200$	—	—	—
m_{CT} [GeV]	> 250	> 250	> 250	> 250	—	—	—
$m_{b\ell}^{\mathrm{min}}$ [GeV]	—	—	> 170	—	—	—	—
$m_{\mathrm{T}}^{\mathrm{min}}(\mathrm{jet}_{1-4}, E_{\mathrm{T}}^{\mathrm{miss}})$ [GeV]	—	—	—	—	> 200	> 200	> 250
$\Delta\phi(b_1, E_{\mathrm{T}}^{\mathrm{miss}})$	—	—	—	—	—	< 2.0	< 2.0
$\Delta\phi(b_2, E_{\mathrm{T}}^{\mathrm{miss}})$	—	—	—	—	—	< 2.5	—

Table 3. Summary of the event selection in each control region corresponding to b0L-SRA and b0L-SRB. The term lepton is used in the table to refer to signal electrons and muons. Jets (j_1, j_2, j_3 and j_4) and leptons (ℓ_1 and ℓ_2) are labelled with an index corresponding to their decreasing order in p_{T}.

b0L-	CRzC	CRttC	CRwC
Number of leptons ($\ell = e,\ \mu$)	2 SFOS	1	1
$p_{\mathrm{T}}(\ell_1)$ [GeV]	> 27	> 27	> 27
$p_{\mathrm{T}}(\ell_2)$ [GeV]	> 20	—	—
$m_{\ell\ell}$ [GeV]	[76 –106]	—	—
N_{jets} ($p_{\mathrm{T}} > 20$ GeV)	2–5	2–5	2–5
Leading jet p_{T} [GeV]	> 250	> 500	> 500
b-jets	j_2 and (j_3 or j_4)	j_2 and (j_3 or j_4)	j_2
$E_{\mathrm{T}}^{\mathrm{miss}}$ [GeV]	< 100	> 100	> 100
$E_{\mathrm{T}}^{\mathrm{miss,cor}}$ [GeV]	> 200	—	—
m_{T} [GeV]	—	> 30	[30–120]
m_{eff} [GeV]	> 500	> 1300	> 500
m_{jj} [GeV]	> 200	> 200	> 200
H_{T4} [GeV]	< 70	< 70	< 70
$\mathcal{A}$	> 0.5	> 0.5	> 0.8
$\Delta\phi(j_1, E_{\mathrm{T}}^{\mathrm{miss}})$	> 2.5	> 2.5	> 2.5

Table 4. Summary of the event selection in each control region corresponding to b0L-SRC. The term lepton is used in the table to refer to signal electrons and muons. Jets (j_1, j_2, j_3 and j_4) and leptons (ℓ_1 and ℓ_2) are labelled with an index corresponding to their decreasing order in p_{T}.

JHEP11(2017)195

170 GeV is applied. For the CRs corresponding to b0L-SRB, selections on the azimuthal angle between the b-jets and the $E_{\mathrm{T}}^{\mathrm{miss}}$ value are applied to enhance the $t\bar{t}$ and W+jets contributions, while the single-top-quark background is estimated from MC simulation. The CRs corresponding to the b0L-SRC are defined with one or two b-jets to enhance the $t\bar{t}$ and W+jets contributions, respectively. Finally, the single top quark production is estimated using the MC normalization.

The contributions from dibosons (WW, WZ, ZZ), $t\bar{t}$ production associated with W and Z bosons, and other rare backgrounds are estimated from MC simulation for both the signal and the control regions and included in the fit procedure, and are allowed to vary within their normalization uncertainty. The background from multijet production is estimated from data using a procedure described in detail in ref. [79] and modified to account for the heavy flavour of the jets. The contribution from multijet production in all regions is found to be negligible.

In total, four CRs are defined for the b0L-SRA to estimate the contributions from W+jets, Z+jets, $t\bar{t}$ and single top quark production independently, while three CRs are defined for each of the b0L-SRB and b0L-SRC to estimate W+jets, Z+jets and $t\bar{t}$. The $E_{\mathrm{T}}^{\mathrm{miss}}$ distribution in b0L-CRwA and b0L-CRzC is shown in figures 2a and 2b, where good agreement with the SM prediction is achieved after the background-only fit. The yields in all these CRs are shown in figure 3 and compared to the MC predictions before the likelihood fit is performed, including only the statistical uncertainty of the MC samples. The bottom panel shows the value of the normalization factors, μ, used for each of the backgrounds fitted and given taking into account statistical and detector-related systematic uncertainties.

As a further validation, two alternative methods are used to estimate the Z+jets contribution. The first method exploits the similarity of the Z+jets and γ+jets processes [79]. For a photon with p_{T} significantly larger than the mass of the Z boson, the kinematics of γ+jets events strongly resemble those of Z+jets events. A set of dedicated control regions is defined by requiring one isolated photon with $p_{\mathrm{T}} > 145$ GeV. The p_{T} of the photon is vectorially added to the $p_{\mathrm{T}}^{\mathrm{miss}}$, and the magnitude of this sum is used to replace the $E_{\mathrm{T}}^{\mathrm{miss}}$-based selections. The yields are then propagated to the SRs using a reweighting factor derived using the MC simulation. This factor takes into account the different kinematics of the two processes and residual effects arising from the different geometrical acceptance and reconstruction efficiency for photons. In the second alternative method, applied to b0L-SRA only, the MC simulation is used to verify that the shape of the m_{CT} distribution for events with no b-tagged jets is compatible with the shape of the m_{CT} distribution for events where two b-tagged jets are present. A new highly populated Z+jets CR is defined, selecting $Z \to \ell\ell$ events with no b-tagged jets. The m_{CT} distribution in this CR is constructed using the two leading jets and is used to estimate the shape of the m_{CT} distribution in the b0L-SRA, whilst the normalization in SRA is rescaled based on the ratio in data of $Z \to \ell\ell$ events with no b-tagged jets to events with two b-tagged jets. Additional MC-based corrections are applied to take into account the two-lepton selection in this CR. The two alternative methods are in agreement within uncertainties with the estimates obtained with the profile likelihood fit to the control regions. Experimental and theoretical

JHEP11(2017)195

systematic uncertainties in the estimates from the nominal and alternative methods are taken into account (see section 7).

6.2 Background estimation in the one-lepton signal regions

The main SM background in the b1L signal regions is the production of $t\bar{t}$ and single-top-quark events in the Wt channel. Two control regions (b1L-CRttA and b1L-CRttB) where the $t\bar{t}$ production is enhanced are defined by inverting the am_{T2} selection. In the case of b1L-CRttA the m_{bb} selection is also inverted, while for b1L-CRttB the $\min[m_{\mathrm{T}}(b\text{-jet}, E_{\mathrm{T}}^{\mathrm{miss}})]$ requirement is inverted. To allow a statistical combination of the results from the b0L-SRA and b1L-SRA regions the corresponding $t\bar{t}$ CRs are defined to be orthogonal via the m_{CT} selection. The single-top-quark contribution is estimated with the same CR employed by the b0L analysis. In the case of b1L-SRB the production of W+jets is no longer negligible, and is estimated by using a dedicated control region b1L-CRwB, where only one b-tagged jet is required. In total, two CRs are used to estimate the event yields in b1L-SRA and three CRs to estimate the yields in b1L-SRB. Full details of the CR selections are given in table 5. The distribution of m_{bb} in b1L-CRstA and of m_{T} in b1L-CRttB are presented in figures 2c and 2d to show the level of agreement achieved after the background-only fit.

The yields in all these CRs are also shown in figure 3 and compared to the direct MC prediction before the likelihood fit is performed. The normalization parameters reported for each SR and SM background process include the statistical and detector-related systematic uncertainties. The decrease of the $\mu_{t\bar{t}}$ parameter from SRA to SRC is related to mismodelling in the description of $t\bar{t}$ processes by Powheg +Pythia 6 MC samples. Previous analyses [80] also found normalization factors considerably smaller than unity for $t\bar{t}$ background processes in similar regions of phase space. The W+jets and Z+jets normalization factors are larger than unity. This is possibly related to the fact that in the default Sherpa 2.2.1 the heavy-flavour production fractions are not consistent with the measured values [81].

6.3 Validation regions

The results of the background-only fit to the CRs are extrapolated to a set of VRs defined to be similar to the SRs, with some of the selection criteria modified to enhance the background contribution, while maintaining a small signal contribution. For each SR, one or more VRs are defined starting from the SR definition and inverting or changing some of the selections as summarized in table 6.

The number of events predicted by the background-only fit is compared to the data in the upper panel of figure 4. The pull, defined by the difference between the observed number of events (n_{obs}) and the predicted background yield (n_{pred}) divided by the total uncertainty (σ_{tot}), is shown for each region in the lower panel. No evidence of significant background mismodelling is observed in the VRs.

JHEP11(2017)195

b1L-	CRttA	CRstA	CRttB	CRstB	CRwB
Number of leptons ($\ell = e,\ \mu$)	1	1	1	1	1
$p_{\mathrm{T}}(\ell)$ [GeV]	> 27	> 27	> 27	> 27	> 27
N_{jets} ($p_{\mathrm{T}} > 35$ GeV)	≥ 2	[2–4]	≥ 2	≥ 2	≥ 2
$p_{\mathrm{T}}(j_1)$ [GeV]	> 35	> 130	> 35	> 35	> 35
$p_{\mathrm{T}}(j_2)$ [GeV]	> 35	> 50	> 35	> 35	> 35
$p_{\mathrm{T}}(j_4)$ [GeV]	> 35	[35–50]	—	—	—
$\min[\Delta\phi(\mathrm{jet}_{1-4}, E_{\mathrm{T}}^{\mathrm{miss}})]$	> 0.4	> 0.4	> 0.4	> 0.4	> 0.4
b-jets	any 2 j_1 and (j_2 or j_3 or j_4)		any 2	any 2	any 1
m_{bb} [GeV]	< 200	> 200	< 200	> 200	> 200
$m_{b\ell}^{\mathrm{min}}$ [GeV]	< 170	> 170	< 170	> 170	< 170
$E_{\mathrm{T}}^{\mathrm{miss}}$ [GeV]	> 200	> 200	> 200	> 200	> 200
m_{T} [GeV]	> 140	—	> 120	[30–120]	[30–120]
am_{T2} [GeV]	< 250	—	< 200	—	> 200
m_{eff} [GeV]	> 300	—	—	—	—
m_{CT} [GeV]	< 250	> 250	—	—	—
$E_{\mathrm{T}}^{\mathrm{miss}}/\sqrt{H_{\mathrm{T}}}$ [GeV$^{1/2}$]	> 8	—	> 8	> 8	> 8
$E_{\mathrm{T}}^{\mathrm{miss}}/m_{\mathrm{eff}}$	—	> 0.25	—	—	—
$m_{\mathrm{T}}^{\mathrm{min}}(b\text{-jet}_{1-2}, E_{\mathrm{T}}^{\mathrm{miss}})$ [GeV]	—	—	< 200	> 200	> 200
$\Delta\phi(b_1, E_{\mathrm{T}}^{\mathrm{miss}})$	—	—	> 2.0	> 2.0	> 2.0

Table 5. Summary of the event selection in each control region corresponding to the b1L signal regions. The term lepton is used in the table to refer to signal electrons and muons. Jets (j_1, j_2, j_3 and j_4) are labelled with an index corresponding to their decreasing order in p_{T}.

VR	Corresponding SR	Selection changes
b0L-VRmctA	b0L-SRA	$m_{\mathrm{T}}^{\mathrm{min}}(\mathrm{jet}_{1-4}, E_{\mathrm{T}}^{\mathrm{miss}}) < 250$ GeV, $150 < m_{\mathrm{CT}} < 250$ GeV
b0L-VRmbbA	b0L-SRA	$m_{\mathrm{T}}^{\mathrm{min}}(\mathrm{jet}_{1-4}, E_{\mathrm{T}}^{\mathrm{miss}}) < 250$ GeV, $100 < m_{bb} < 200$ GeV
b0L-VRzB	b0L-SRB	$m_{\mathrm{CT}} < 250$ GeV, $200 < m_{\mathrm{T}}^{\mathrm{min}}(\mathrm{jet}_{1-4}, E_{\mathrm{T}}^{\mathrm{miss}}) < 250$ GeV, $\mathcal{A} < 0.8$, no selection on $\Delta\phi(b_1, E_{\mathrm{T}}^{\mathrm{miss}})$ and $\Delta\phi(b_2, E_{\mathrm{T}}^{\mathrm{miss}})$
b0L-VRttB	b0L-SRB	$m_{\mathrm{CT}} < 250$ GeV, $150 < m_{\mathrm{T}}^{\mathrm{min}}(\mathrm{jet}_{1-4}, E_{\mathrm{T}}^{\mathrm{miss}}) < 200$ GeV, $\mathcal{A} < 0.8$
b0L-VRttC	b0L-SRC	$m_{\mathrm{CT}} < 250$ GeV, $m_{\mathrm{T}}^{\mathrm{min}}(\mathrm{jet}_{1-4}, E_{\mathrm{T}}^{\mathrm{miss}}) < 250$ GeV, $0.6 < \mathcal{A} < 0.8$
b1L-VRamt2A	b1L-SRA300-2j	$30 < m_{\mathrm{T}} < 140$ GeV, $m_{bb} < 200$ GeV
b1L-VRmbbA	b1L-SRA300-2j	$am_{\mathrm{T2}} < 250$ GeV
b1L-VRamt2B	b1L-SRB	$\Delta\phi(b_1, E_{\mathrm{T}}^{\mathrm{miss}}) > 2.0$, $m_{bb} > 200$ GeV
b1L-VRmbbB	b1L-SRB	$\Delta\phi(b_1, E_{\mathrm{T}}^{\mathrm{miss}}) > 2.0$, $30 < m_{\mathrm{T}} < 120$ GeV

Table 6. Summary of the VRs used in the analysis. Each VR (left column) corresponds to a SR (middle column) defined in tables 1 and 2, with a few selection requirements changed (right column) to ensure the selection has low efficiency for the expected signal.

JHEP11(2017)195

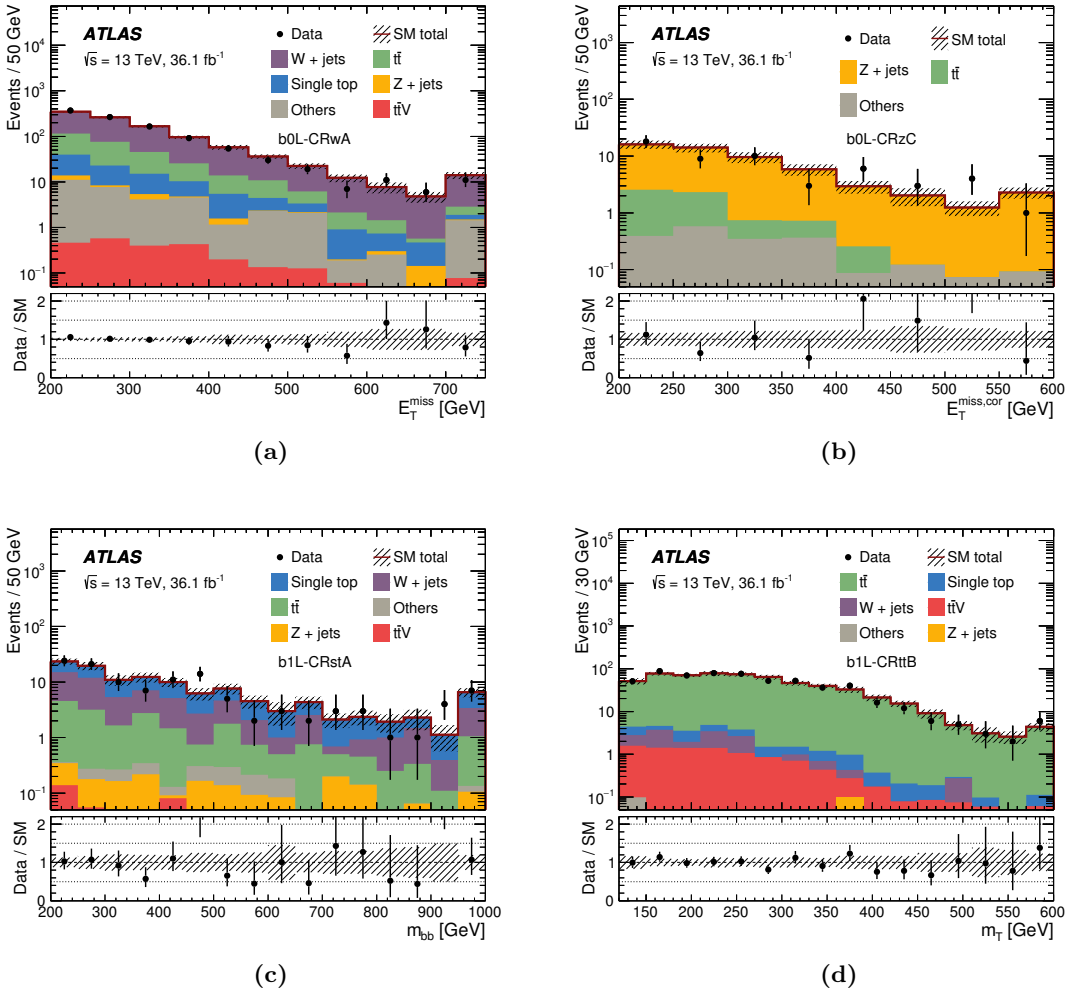


Figure 2. Example kinematic distributions in some of the control regions. (a) $E_{\mathrm{T}}^{\mathrm{miss}}$ in b0L-CRwA, (b) $E_{\mathrm{T}}^{\mathrm{miss,cor}}$ in b0L-CRzC, (c) m_{bb} in b1L-CRstA and (d) m_{T} in b1L-CRttB. In all distributions the MC normalization is rescaled using the results from the background-only fit, showing good agreement between data and the predicted SM shapes. The contributions from diboson, multijet and rare backgrounds are collectively called "Others". The shaded-grey band shows the detector-related systematic uncertainties and the statistical uncertainties of the MC samples as detailed in section 7 and the last bin includes overflow events.

7 Systematic uncertainties

Several sources of experimental and theoretical systematic uncertainty in the signal and background estimates are considered in these analyses. Their impact is reduced through the normalization of the dominant backgrounds in the control regions defined with kinematic selections resembling those of the corresponding signal region (see section 6). Experimental and theoretical uncertainties are included as nuisance parameters with Gaussian constraints in the likelihood fits, taking into account correlations between different regions. Uncertainties due to the numbers of events in the CRs are also introduced in the fit for each region. The dominant contributions are summarized in table 7.

JHEP11(2017)195

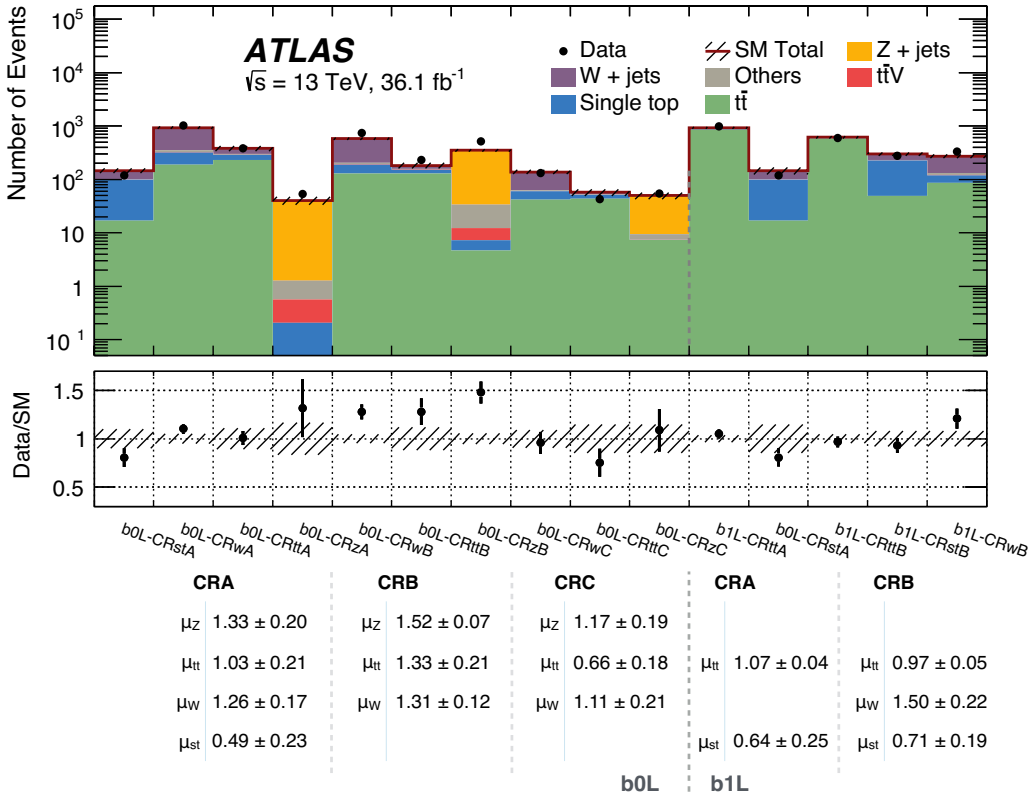


Figure 3. Data and MC predictions for all CRs associated with all b0L and b1L SRs before the likelihood fit, as well as the results obtained by the likelihood fit. In the top panel the normalization of the backgrounds is obtained from MC simulation and is the input value to the fit. The contributions from diboson, multijet and rare backgrounds are collectively called "Others". The panels at the bottom show the ratio of the observed events in each CR to the MC estimate, and the value of the normalization factors (μ) obtained for each of the backgrounds fitted. The uncertainty band around the MC prediction includes only the statistical uncertainty of the MC samples. The normalization factors μ are presented for each region and SM background process and take into account statistical and detector-related systematic uncertainties.

Source \ Region	b0L-SRAx	b0L-SRB	b0L-SRC	b1L-SRAx	b1L-SRB	b1L-SRA300-2j
Experimental uncertainty						
JES	2.3 – 3.4%	5.7%	4.3%	1.2 – 1.5%	0.9%	6.9%
JER	0.9 – 3.3%	3.5%	11%	5.3 – 8.6%	0.9%	4%
b-tagging	3.3 – 4.3%	7.5%	4.7%	6.1 – 6.3%	2%	6.6%
Theoretical modelling uncertainty						
Z+jets	9.6 – 12%	13%	11%	—	—	—
W+jets	3.4 – 5.2%	4.7%	7.6%	1.3 – 1.6%	8.6%	7.9%
Top production	2.2 – 3.1%	6%	3.6%	19%	13%	22%

Table 7. Summary of the dominant experimental and theoretical uncertainties for each signal region in zero-lepton and one-lepton channels. Uncertainties are quoted as relative to the total SM background predictions, with a range indicated for the three b0L-SRAs and the two b1L-SRAs. For theoretical modelling, uncertainties per dominant SM background process are quoted. The individual uncertainties can be correlated, and do not necessarily add in quadrature to the total background uncertainty.

JHEP11(2017)195

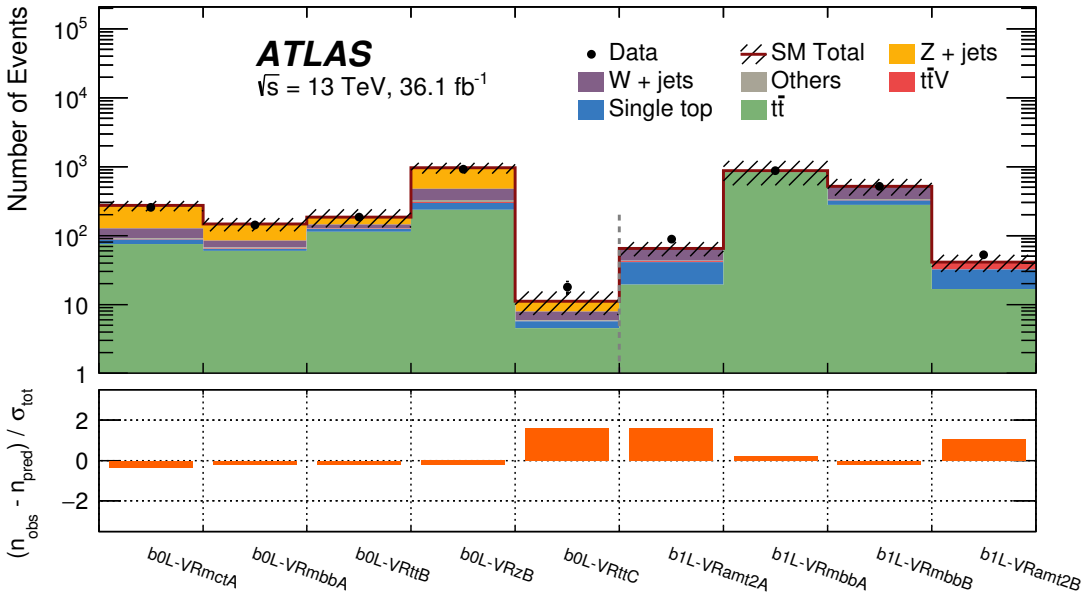


Figure 4. Results of the likelihood fit extrapolated to the VRs associated with the b0L and b1L analyses. The normalization of the backgrounds is obtained from the fit to the CRs. The upper panel shows the observed number of events and the predicted background yield. The contributions from diboson, multijet and rare backgrounds are collectively called "Others". All uncertainties defined in section 7 are included in the uncertainty band. The lower panel shows the pulls in each VR, where σ_{tot} is the error on the background estimation as a sum in quadrature of the systematic uncertainty and the statistical uncertainty on the estimate.

The dominant detector-related systematic effects are due to the uncertainties in the jet energy scale (JES) [59] and resolution (JER) [82], and in the b-tagging efficiency and mis-tagging rates. The latter are estimated by varying the η-, p_{T}- and flavour-dependent scale factors applied to each jet in the simulation within a range that reflects the systematic uncertainty in the measured tagging efficiency and mis-tag rates in 13 TeV data. The uncertainties associated with lepton and photon reconstruction and energy measurements are also considered but have a negligible impact on the final results. Lepton, photon and jet-related uncertainties are propagated to the $E_{\text{T}}^{\text{miss}}$ calculation, and additional uncertainties are included in the energy scale and resolution of the soft term.

Uncertainties in the modelling of the SM background processes from MC simulation and their theoretical cross-section uncertainties are also taken into account. The dominant uncertainty arises from Z+jets MC modelling for b0L-SRs and $t\bar{t}$ and single-top modelling (collectively referred to as "Top production" in table 7) for b1L-SRs. The Z+jets (as well as W+jets) modelling uncertainties are estimated by considering different merging (CKKW-L) and resummation scales using alternative samples, PDF variations from the NNPDF30NNLO replicas [46], as well as an envelope formed from seven-point scale variations of the renormalization and factorization scales. The various components are added in quadrature. A 40% uncertainty [83] is assigned to the heavy-flavour jet content in W+jets background, which is estimated from MC simulation in the one-lepton channel control re-

JHEP11(2017)195

gions. For b0L-SRA, b0L-SRC and b1L-SRB the uncertainty accounts for the different requirements on b-jets between the signal regions and the corresponding control regions.

Theoretical and modelling uncertainties of the top quark pair and single-top-quark (Wt) backgrounds are computed as the difference between the prediction from nominal samples and those from additional samples differing in generator or parameter settings. Hadronization and PS uncertainties are estimated using samples generated using Powheg-Box v2 and showered by Herwig++ v2.7.1 [84] with the UEEE5 [85] underlying-event tune. Uncertainties related to initial- and final-state radiation modelling, PS tune and (for $t\bar{t}$ only) choice of h_{damp} parameter in Powheg-Box v2 are estimated using alternative settings of the event generators. Finally, an alternative generator MadGraph5_aMC@NLO with showering by Herwig++ v2.7.1 is used to estimate the event generator uncertainties. One additional uncertainty stems from the modelling of the interference between the $t\bar{t}$ and Wt processes at NLO. Predictions from an inclusive $WWbb$ sample generated at LO using MadGraph5_aMC@NLO are compared with the sum of the $t\bar{t}$ and Wt predictions, and differences from the nominal predictions are taken as systematic uncertainties.

Uncertainties in backgrounds such as diboson and ttV are also estimated by comparisons of the nominal sample with alternative samples differing in generator or parameter settings (Powheg v2 with showering by Pythia v8.210 for dibosons; renormalization and factorization scale and A14 tune variations for ttV) and contribute less than 5% to the total uncertainty. The cross-sections used to normalize the MC yields to the highest order available are varied according to the scale uncertainty of the theoretical calculation. The cross-section uncertainties are 5% for W boson, Z boson and top quark pair production, 6% for dibosons, and 13% and 12% for ttW and ttZ, respectively. Finally, a conservative 100% systematic uncertainty associated to the multijet background estimate is considered and found to have a negligible effect.

For the SUSY signal processes, both the experimental and theoretical uncertainties in the expected signal yield are considered. Experimental uncertainties are found to be between 15% and 30% across the $\tilde{b}_1$–$\tilde{\chi}_1^0$ mass plane for exclusive $\tilde{b}_1 \to b\tilde{\chi}_1^0$ decays and between 10% and 25% for models where bottom squarks decay with a significant branching ratio as $\tilde{b}_1 \to t\tilde{\chi}_1^{\pm}$, assuming the one-lepton channel selection. In all SRs, they are largely dominated by the uncertainty in the b-tagging efficiency. Theoretical uncertainties in the NLO+NLL cross-section are calculated for each SUSY signal scenario and are dominated by the uncertainties in the renormalization and factorization scales, followed by the uncertainty in the PDF. They vary between 15% and 25% for bottom squark masses in the range between 400 GeV and 1100 GeV. Additional uncertainties in the acceptance and efficiency due to the modelling of initial-state radiation and scale variations in SUSY signal MC samples are also taken into account and contribute up to about 10%.

8 Results and interpretation

Tables 8 and 9 report the observed number of events and the SM prediction after the background-only fit for each signal region in the zero-lepton and one-lepton channels, respectively. The background-only fit results are compared to the pre-fit predictions based

JHEP11(2017)195

b0L- Signal Region	SRA350	SRA450	SRA550	SRB	SRC
Observed	81	24	10	45	7
Total background (fit)	70 ± 13	22 ± 5	7.2 ± 1.5	37 ± 7	5.5 ± 1.5
Z+jets	46 ± 12	13.6 ± 3.7	4.0 ± 1.2	20.0 ± 5.2	2.3 ± 0.8
$t\bar{t}$	2.0 ± 0.6	0.5 ± 0.2	0.16 ± 0.07	5.1 ± 2.7	0.8 ± 0.3
Single top	4.7 ± 3.4	1.2 ± 1.0	0.5 ± 0.3	2.6 ± 1.1	0.7 ± 0.3
W+jets	15 ± 5	5.0 ± 1.8	2.4 ± 1.0	5.5 ± 2.0	1.3 ± 0.8
Others	2.5 ± 1.7	1.4 ± 1.2	0.07 ± 0.03	4.0 ± 1.1	0.4 ± 0.1
Total background (MC exp.)	60.4	18.5	6.2	28	5.4
Z+jets	34.9	10.3	3.0	13.1	1.9
$t\bar{t}$	1.9	0.45	0.16	3.8	1.2
Single top	10	2.5	1.0	2.6	0.7
W+jets	11.6	4.0	1.9	4.2	1.2
Others	2.5	1.3	0.07	4.0	0.4

Table 8. Fit results in the b0L signal regions. The background normalization parameters are obtained from the fit in the control regions and are applied to the SRs. Smaller backgrounds such as diboson, ttV, multijet and rare processes are indicated as "Others". The individual uncertainties, including statistical, detector-related and theoretical systematic components, are symmetrized and can be correlated. They do not necessarily add in quadrature to the total systematic uncertainty.

on MC simulation. The largest background contribution in b0L-SRs arises from $Z \to \nu\bar{\nu}$ produced in association with b-quarks followed by W+jets production, whilst top quark and W+jets production dominates SM predictions for b1L-SRs. The results are also summarized in figure 5, where the pulls for each of the SRs are also presented. No significant excess above the expected Standard Model background yield is observed, although b1L-SRA300-2j presents a discrepancy between data and SM predictions of about 1.5σ.

Figure 6 shows the comparison between the observed data and the SM predictions for some relevant kinematic distributions for the b0L and b1L selections. For illustrative purposes, the distributions expected for scenarios with different bottom squark and neutralino masses depending on the SR considered are shown.

The results are translated into upper limits on contributions from physics beyond the SM (BSM) for each signal region. The CL_s method [86, 87] is used to derive the confidence level of the exclusion; signal models with a CL_s value below 0.05 are said to be excluded at 95% CL. The profile-likelihood-ratio test statistic is used to exclude the signal-plus-background hypothesis for specific signal models. S^{95}_{obs} (S^{95}_{exp}) is the observed (expected) upper limit at 95% CL on the number of events from BSM phenomena for each signal region. These limits, when normalized by the integrated luminosity of the data sample, may be interpreted as upper limits on the visible cross-section of BSM physics, σ_{vis}, defined as the product of the production cross-section, the acceptance and the selection efficiency of a BSM signal. Table 10 summarizes S^{95}_{obs}, S^{95}_{exp}, and σ_{vis} for all SRs, together with the p_0-values, which represent the probability of the SM background alone to fluctuate to the observed number of events or higher.

JHEP11(2017)195

b1L- Signal Region	SRA600	SRA750	SRB	SRA300-2j
Observed	21	13	69	12
Total background (fit)	24 ± 6	15 ± 4	53 ± 12	6.7 ± 2.3
$t\bar{t}$	10 ± 5	5.5 ± 2.7	16 ± 7	2.4 ± 1.3
Single top	7 ± 4	4.5 ± 2.8	10 ± 5	3.3 ± 2.0
W+jets	0.9 ± 0.5	0.6 ± 0.3	17 ± 8	0.4 ± 0.3
ttV	5.4 ± 0.6	4.0 ± 0.5	9 ± 1	0.6 ± 0.1
Others	0.07 ± 0.02	0.07 ± 0.03	1.8 ± 0.3	0.07 ± 0.02
Total background (MC exp.)	27	17	52	8.4
$t\bar{t}$	9	5.1	16	2.2
Single top	11	7.1	14	5.2
W+jets	0.9	0.6	11	0.4
ttV	5.4	4.0	9	0.6
Others	0.07	0.07	1.8	0.07

Table 9. Fit results in the b1L signal regions. The background normalization parameters are obtained from the background-only fit in the control regions and are applied to the SRs. Smaller backgrounds such as diboson, Z+jets, multijet and rare processes are indicated as "Others". The individual uncertainties, including detector-related and theoretical systematic components, are symmetrized and can be correlated. They do not necessarily add in quadrature to the total systematic uncertainty.

Signal channel	$\langle \epsilon A \sigma \rangle^{95}_{\text{obs}}$[fb]	S^{95}_{obs}	S^{95}_{exp}	p_0 (Z)
b0L-SRA350	1.06	38.2	$30.9^{+11.3}_{-8.4}$	0.28 (0.60)
b0L-SRA450	0.43	15.6	$13.9^{+5.6}_{-3.8}$	0.37 (0.34)
b0L-SRA550	0.30	10.7	$7.8^{+3.7}_{-1.6}$	0.20 (0.85)
b0L-SRB	0.72	26.1	$19.9^{+8.3}_{-5.4}$	0.23 (0.74)
b0L-SRC	0.24	8.7	$6.8^{+3.3}_{-1.3}$	0.30 (0.54)
b1L-SRA300-2j	0.39	14.1	$9.3^{+3.5}_{-3.1}$	0.08 (1.43)
b1L-SRA600	0.38	13.6	$14.8^{+5.4}_{-4.4}$	0.50 (0.00)
b1L-SRA750	0.27	9.9	$11.2^{+4.0}_{-2.3}$	0.50 (0.00)
b1L-SRB	1.12	40.3	$28.7^{+10.7}_{-8.2}$	0.21 (0.80)

Table 10. Left to right: 95% CL upper limits on the visible cross-section ($\langle \epsilon A \sigma \rangle^{95}_{\text{obs}}$) and on the number of signal events (S^{95}_{obs}). The third column (S^{95}_{exp}) shows the 95% CL upper limit on the number of signal events, given the expected number (and $\pm 1\sigma$ variations of the expected number) of background events. The last column reports the p_0-values and Z (the number of equivalent Gaussian standard deviations). The maximum allowed p_0-value is truncated at 0.5.

JHEP11(2017)195

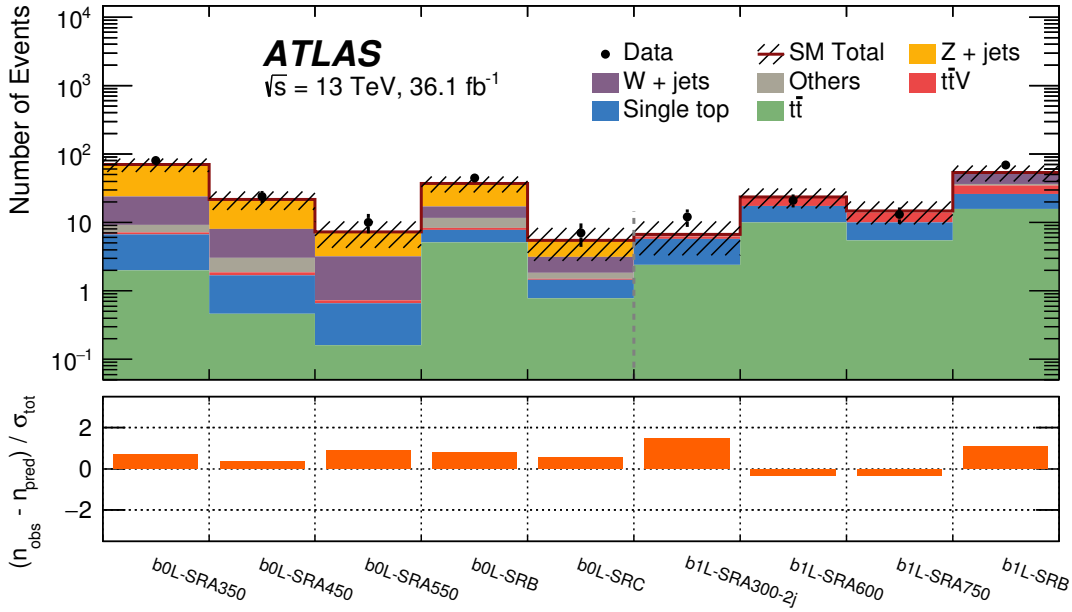


Figure 5. Results of the likelihood fit extrapolated to the SRs associated with the b0L and b1L analyses. The normalization of the backgrounds is obtained from the fit to the CRs. The upper panel shows the observed number of events and the predicted background yields. The contributions from diboson, multijet and rare backgrounds are collectively called "Others". All uncertainties defined in section 7 are included in the uncertainty band. The lower panel shows the pulls in each SR, where σ_{tot} is the error on the background estimation as a sum in quadrature of the systematic uncertainty and the statistical uncertainty on the estimate.

Exclusion limits are obtained assuming two types of SUSY particle mass hierarchy such that the lightest bottom squark decays either exclusively via $\tilde{b}_1 \to b\tilde{\chi}_1^0$ or into multiple channels, $\tilde{b}_1 \to b\tilde{\chi}_1^0$ and $\tilde{b}_1 \to t\tilde{\chi}_1^\pm$, assuming a 50% branching ratio and $\Delta m(\tilde{\chi}_1^\pm, \tilde{\chi}_1^0) \sim 1$ GeV. The first set of scenarios is targeted by the zero-lepton channel SRs only. For models with mixed decays, the expected limits from the SRs are compared and the observed limits are obtained by statistically combining the most sensitive zero-lepton SR with the most sensitive one-lepton SR. In all cases, the fit procedure takes into account correlations in the yield predictions between control and signal regions due to common background normalization parameters and systematic uncertainties. The experimental systematic uncertainties in the signal are taken into account for this calculation and are assumed to be fully correlated with those in the SM background.

For the exclusive $\tilde{b}_1 \to b\tilde{\chi}_1^0$ decay mode, at each point of the parameter space the SR with the best expected sensitivity is used. Sensitivity to scenarios with the largest mass difference between the $\tilde{b}_1$ and the $\tilde{\chi}_1^0$ is achieved with the most stringent m_{CT} threshold (b0L-SRA550). Sensitivity to scenarios with intermediate and small mass differences is obtained with the dedicated b0L-SRB and b0L-SRC selections, respectively. For the mixed-decays scenarios, a statistical combination is computed with the results of the zero-lepton and one-lepton channels as explained above. A combined fit is performed simultaneously on the control and signal regions of the two analyses. The best sensitivity to regions of the

JHEP11(2017)195

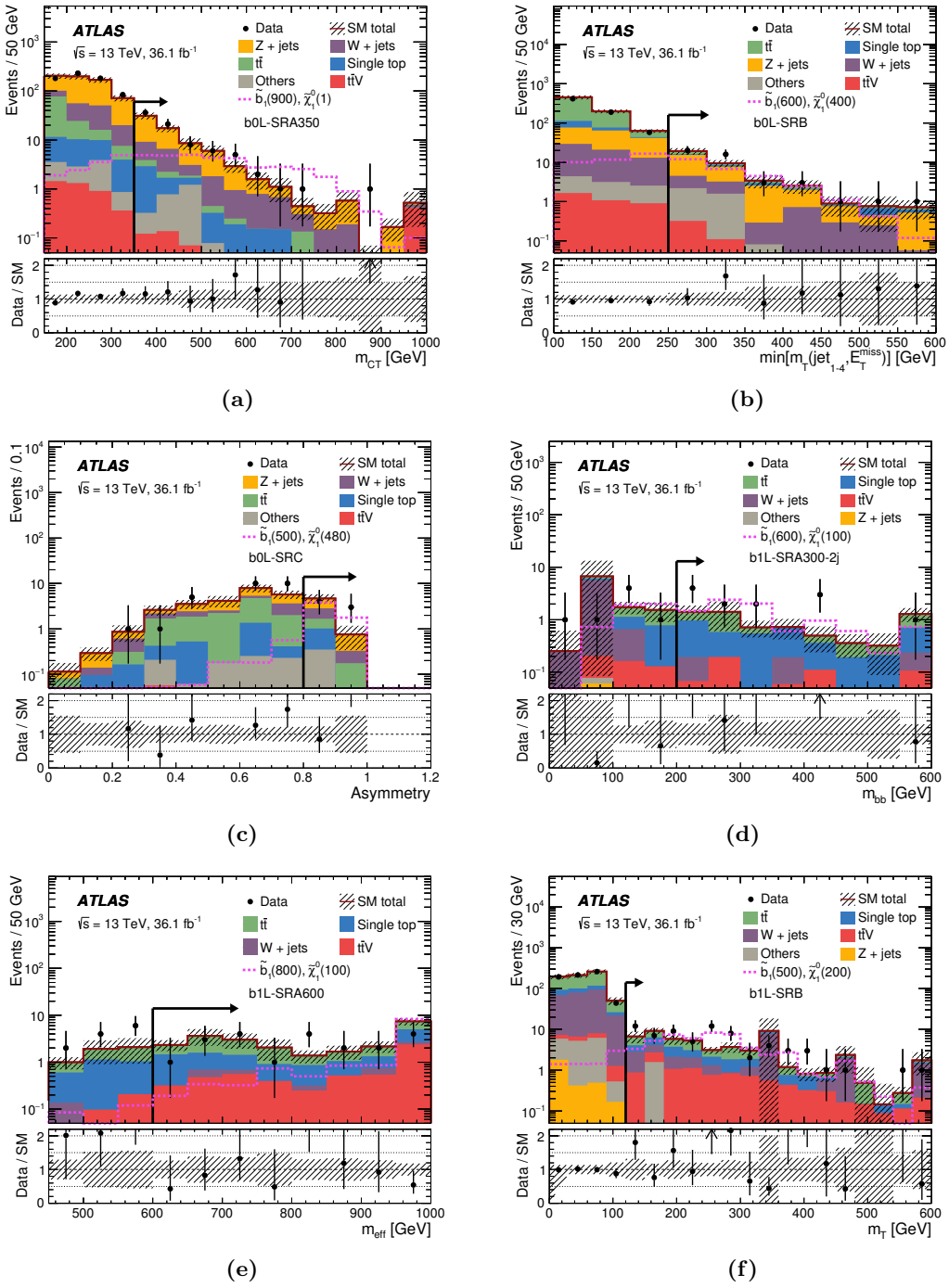
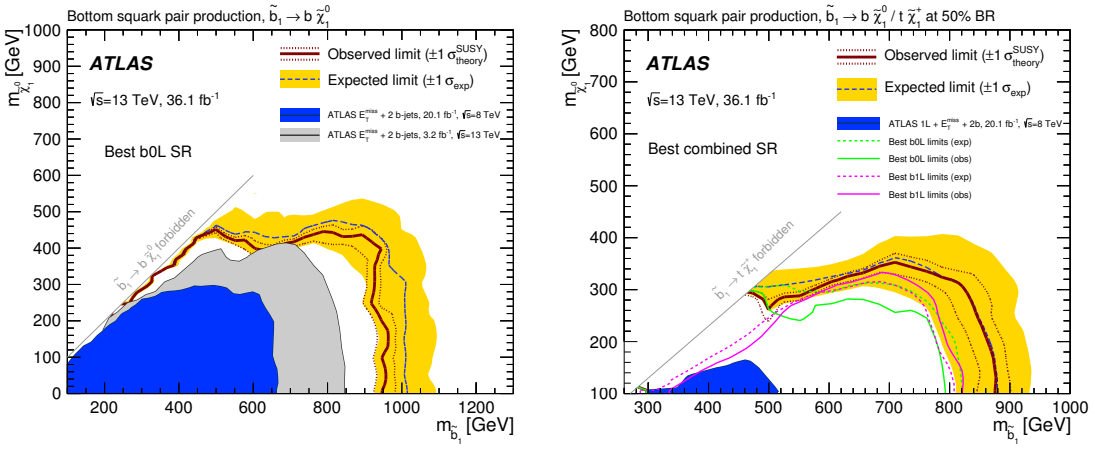


Figure 6. Distributions of (a) m_{CT} in b0L-SRA, (b) $\min[m_{\mathrm{T}}(\mathrm{jet}_{1-4}, E_{\mathrm{T}}^{\mathrm{miss}})]$ in b0L-SRB, (c) $\mathcal{A}$ in b0L-SRC, (d) m_{bb} in b1L-SRA300-2j, (e) m_{eff} in b1L-SRA, (f) m_{T} in b1L-SRB. All selection criteria are applied, except the selection on the variable that is displayed in each of the plots. The arrows indicate the final selection applied in the signal regions. The shaded-grey band shows the detector-related systematic uncertainties and the statistical uncertainties on the MC samples. The SM backgrounds are normalized to the values determined in the fit. The contributions from diboson, multijet and rare backgrounds are collectively called "Others". For illustration the distribution expected from selected signal models are overlaid. The last bin includes overflow events.

JHEP11(2017)195



(a) **(b)**

Figure 7. (a) Observed and expected exclusion contours at 95% CL, as well as $\pm1\sigma$ variation of the expected limit, in the $\tilde{b}_1$–$\tilde{\chi}_1^0$ mass plane. The SR with the best expected sensitivity is adopted for each point of the parameter space. The yellow band around the expected limit (dashed line) shows the impact of the experimental and SM background theoretical uncertainties. The dotted lines show the impact on the observed limit of the variation of the nominal signal cross-section by $\pm1\sigma$ of its theoretical uncertainties. (b) Same, for scenarios where multiple decay modes are considered for bottom squarks. The statistical combination of b0L-SRs and b1L-SRs is used in this case. In (b) differences between expected and observed contours around $m_{\tilde{b}_1} = 500$ GeV arise from the one σ level discrepancy between the data and the predicted SM background contributions in b0L-SRB and b1L-SRB.

$(\tilde{b}_1,\ \tilde{\chi}_1^0)$ mass plane close to the kinematic boundaries is obtained with the combination of the b0L-SR450 and b1L-SRB regions whilst stringent constraints on models with large mass differences are achieved with the results from the combination of zero-lepton and one-lepton SRs with the most stringent m_{CT} and m_{eff} thresholds, respectively.

Figures 7a and 7b show the observed (solid line) and expected (dashed line) exclusion contours at 95% CL in the $\tilde{b}_1$–$\tilde{\chi}_1^0$ mass plane for the two types of SUSY scenarios considered. Bottom squark masses up to 950 (860) GeV are excluded for $\tilde{\chi}_1^0$ masses below 420 (250) GeV in models with exclusive (mixed) decay modes. Multiple-decay bottom squark models are phenomenologically equivalent to models characterized by the pair production of top squarks decaying as $\tilde{t}_1 \to t\tilde{\chi}_1^0$ and $\tilde{t}_1 \to b\tilde{\chi}_1^{\pm}$, with the same assumptions for the branching ratios and $\Delta m(\tilde{\chi}_1^{\pm}, \tilde{\chi}_1^0)$. Hence the results can be interpreted as exclusion limits on top squark masses.

9 Conclusion

The results of a search for pair production of bottom and top squarks are reported. The analysis uses 36.1 fb^{-1} of pp collisions at $\sqrt{s} = 13$ TeV collected by the ATLAS experiment at the Large Hadron Collider in 2015 and 2016. Third-generation squarks are searched for in events containing large missing transverse momentum and jets, exactly two of which

JHEP11(2017)195

are identified as b-jets. Selections are defined with either no charged leptons (electrons and muons) in the final state, or one charged lepton. Zero-lepton channel signal regions target R-parity-conserving models in which the $\tilde{b}_1$ is the lightest squark and is assumed to decay exclusively via $\tilde{b}_1 \to b\tilde{\chi}_1^0$, where $\tilde{\chi}_1^0$ is the lightest neutralino. One-lepton channel signal regions target models where bottom or top squarks are produced and can decay into multiple channels, $\tilde{b}_1 \to b\tilde{\chi}_1^0$ and $\tilde{b}_1 \to t\tilde{\chi}_1^\pm$, or $\tilde{t}_1 \to t\tilde{\chi}_1^0$ and $\tilde{t}_1 \to b\tilde{\chi}_1^\pm$, where $\tilde{\chi}_1^\pm$ is the lightest chargino and the mass difference $m_{\tilde{\chi}_1^\pm} - m_{\tilde{\chi}_1^0}$ is set to 1 GeV. No significant excess above the expected Standard Model background is found and exclusion limits at 95% confidence level are placed on the visible cross-section and on the mass of the bottom (or top) squark. Bottom squark masses up to 950 GeV are excluded for $\tilde{\chi}_1^0$ masses below 420 GeV in models with exclusive decay modes. Bottom or top squark masses up to 860 GeV are excluded for $\tilde{\chi}_1^0$ masses below 250 GeV in models with mixed decay modes with equal branching ratios. The results significantly improve upon previous Run-1 and Run-2 searches at the ATLAS experiment and strengthen the constraints on bottom and top squark masses.

Acknowledgments

We thank CERN for the very successful operation of the LHC, as well as the support staff from our institutions without whom ATLAS could not be operated efficiently.

We acknowledge the support of ANPCyT, Argentina; YerPhI, Armenia; ARC, Australia; BMWFW and FWF, Austria; ANAS, Azerbaijan; SSTC, Belarus; CNPq and FAPESP, Brazil; NSERC, NRC and CFI, Canada; CERN; CONICYT, Chile; CAS, MOST and NSFC, China; COLCIENCIAS, Colombia; MSMT CR, MPO CR and VSC CR, Czech Republic; DNRF and DNSRC, Denmark; IN2P3-CNRS, CEA-DSM/IRFU, France; SRNSF, Georgia; BMBF, HGF, and MPG, Germany; GSRT, Greece; RGC, Hong Kong SAR, China; ISF, I-CORE and Benoziyo Center, Israel; INFN, Italy; MEXT and JSPS, Japan; CNRST, Morocco; NWO, Netherlands; RCN, Norway; MNiSW and NCN, Poland; FCT, Portugal; MNE/IFA, Romania; MES of Russia and NRC KI, Russian Federation; JINR; MESTD, Serbia; MSSR, Slovakia; ARRS and MIZŠ, Slovenia; DST/NRF, South Africa; MINECO, Spain; SRC and Wallenberg Foundation, Sweden; SERI, SNSF and Cantons of Bern and Geneva, Switzerland; MOST, Taiwan; TAEK, Turkey; STFC, United Kingdom; DOE and NSF, United States of America. In addition, individual groups and members have received support from BCKDF, the Canada Council, CANARIE, CRC, Compute Canada, FQRNT, and the Ontario Innovation Trust, Canada; EPLANET, ERC, ERDF, FP7, Horizon 2020 and Marie Skłodowska-Curie Actions, European Union; Investissements d'Avenir Labex and Idex, ANR, Région Auvergne and Fondation Partager le Savoir, France; DFG and AvH Foundation, Germany; Herakleitos, Thales and Aristeia programmes co-financed by EU-ESF and the Greek NSRF; BSF, GIF and Minerva, Israel; BRF, Norway; CERCA Programme Generalitat de Catalunya, Generalitat Valenciana, Spain; the Royal Society and Leverhulme Trust, United Kingdom.

The crucial computing support from all WLCG partners is acknowledged gratefully, in particular from CERN, the ATLAS Tier-1 facilities at TRIUMF (Canada), NDGF

JHEP11(2017)195

(Denmark, Norway, Sweden), CC-IN2P3 (France), KIT/GridKA (Germany), INFN-CNAF (Italy), NL-T1 (Netherlands), PIC (Spain), ASGC (Taiwan), RAL (U.K.) and BNL (U.S.A.), the Tier-2 facilities worldwide and large non-WLCG resource providers. Major contributors of computing resources are listed in ref. [88].

Open Access. This article is distributed under the terms of the Creative Commons Attribution License (CC-BY 4.0), which permits any use, distribution and reproduction in any medium, provided the original author(s) and source are credited.

References

[1] Yu. A. Golfand and E.P. Likhtman, *Extension of the algebra of Poincaré group generators and violation of p invariance*, *JETP Lett.* **13** (1971) 323 [INSPIRE].

[2] D.V. Volkov and V.P. Akulov, *Is the neutrino a goldstone particle?*, *Phys. Lett.* **46B** (1973) 109 [INSPIRE].

[3] J. Wess and B. Zumino, *Supergauge transformations in four-dimensions*, *Nucl. Phys.* **B 70** (1974) 39 [INSPIRE].

[4] J. Wess and B. Zumino, *Supergauge invariant extension of quantum electrodynamics*, *Nucl. Phys.* **B 78** (1974) 1 [INSPIRE].

[5] S. Ferrara and B. Zumino, *Supergauge invariant Yang-Mills theories*, *Nucl. Phys.* **B 79** (1974) 413 [INSPIRE].

[6] A. Salam and J.A. Strathdee, *Supersymmetry and nonabelian gauges*, *Phys. Lett.* **51B** (1974) 353 [INSPIRE].

[7] N. Sakai, *Naturalness in supersymmetric guts*, *Z. Phys.* **C 11** (1981) 153 [INSPIRE].

[8] S. Dimopoulos, S. Raby and F. Wilczek, *Supersymmetry and the scale of unification*, *Phys. Rev.* **D 24** (1981) 1681 [INSPIRE].

[9] L.E. Ibáñez and G.G. Ross, *Low-energy predictions in supersymmetric grand unified theories*, *Phys. Lett.* **105B** (1981) 439 [INSPIRE].

[10] S. Dimopoulos and H. Georgi, *Softly broken supersymmetry and* SU(5), *Nucl. Phys.* **B 193** (1981) 150 [INSPIRE].

[11] H. Goldberg, *Constraint on the photino mass from cosmology*, *Phys. Rev. Lett.* **50** (1983) 1419 [*Erratum ibid.* **103** (2009) 099905] [INSPIRE].

[12] J.R. Ellis, J.S. Hagelin, D.V. Nanopoulos, K.A. Olive and M. Srednicki, *Supersymmetric relics from the Big Bang*, *Nucl. Phys.* **B 238** (1984) 453 [INSPIRE].

[13] R. Barbieri and G.F. Giudice, *Upper bounds on supersymmetric particle masses*, *Nucl. Phys.* **B 306** (1988) 63 [INSPIRE].

[14] B. de Carlos and J.A. Casas, *One loop analysis of the electroweak breaking in supersymmetric models and the fine tuning problem*, *Phys. Lett.* **B 309** (1993) 320 [hep-ph/9303291] [INSPIRE].

[15] P. Fayet, *Supersymmetry and weak, electromagnetic and strong interactions*, *Phys. Lett.* **64B** (1976) 159 [INSPIRE].

[16] P. Fayet, *Spontaneously broken supersymmetric theories of weak, electromagnetic and strong interactions*, *Phys. Lett.* **69B** (1977) 489 [INSPIRE].

JHEP11(2017)195

[17] G.R. Farrar and P. Fayet, *Phenomenology of the production, decay and detection of new hadronic states associated with supersymmetry*, *Phys. Lett.* **76B** (1978) 575 [INSPIRE].

[18] ATLAS collaboration, *Search for bottom squark pair production in proton-proton collisions at $\sqrt{s} = 13$ TeV with the ATLAS detector*, *Eur. Phys. J.* **C 76** (2016) 547 [arXiv:1606.08772].

[19] CMS collaboration, *Search for the pair production of third-generation squarks with two-body decays to a bottom or charm quark and a neutralino in proton-proton collisions at $\sqrt{s} = 13$ TeV*, arXiv:1707.07274 [INSPIRE].

[20] ATLAS collaboration, *ATLAS Run 1 searches for direct pair production of third-generation squarks at the Large Hadron Collider*, *Eur. Phys. J.* **C 75** (2015) 510 [arXiv:1506.08616] [INSPIRE].

[21] ATLAS collaboration, *The ATLAS experiment at the CERN Large Hadron Collider*, 2008 *JINST* **3** S08003 [INSPIRE].

[22] ATLAS collaboration, *ATLAS insertable B-layer technical design report*, ATLAS-TDR-19 (2010).

[23] ATLAS collaboration, *Performance of the ATLAS Trigger System in 2015*, *Eur. Phys. J.* **C 77** (2017) 317 [arXiv:1611.09661] [INSPIRE].

[24] ATLAS collaboration, *Improved luminosity determination in pp collisions at $\sqrt{s} = 7$ TeV using the ATLAS detector at the LHC*, *Eur. Phys. J.* **C 73** (2013) 2518 [arXiv:1302.4393].

[25] ATLAS collaboration, *2015 start-up trigger menu and initial performance assessment of the ATLAS trigger using Run-2 data*, ATL-DAQ-PUB-2016-001 (2016).

[26] ATLAS collaboration, *The ATLAS simulation infrastructure*, *Eur. Phys. J.* **C 70** (2010) 823 [arXiv:1005.4568] [INSPIRE].

[27] GEANT4 collaboration, S. Agostinelli et al., *GEANT4 — a simulation toolkit*, *Nucl. Instrum. Meth.* **A 506** (2003) 250 [INSPIRE].

[28] ATLAS collaboration, *The simulation principle and performance of the ATLAS fast calorimeter simulation FastCaloSim*, ATL-PHYS-PUB-2010-013 (2010).

[29] J. Alwall et al., *The automated computation of tree-level and next-to-leading order differential cross sections and their matching to parton shower simulations*, *JHEP* **07** (2014) 079 [arXiv:1405.0301] [INSPIRE].

[30] T. Sjöstrand, S. Mrenna and P.Z. Skands, *A brief introduction to PYTHIA 8.1*, *Comput. Phys. Commun.* **178** (2008) 852 [arXiv:0710.3820] [INSPIRE].

[31] ATLAS collaboration, *ATLAS Pythia 8 tunes to 7 TeV data*, ATL-PHYS-PUB-2014-021 (2014).

[32] L. Lönnblad and S. Prestel, *Merging multi-leg NLO matrix elements with parton showers*, *JHEP* **03** (2013) 166 [arXiv:1211.7278] [INSPIRE].

[33] R.D. Ball et al., *Parton distributions with LHC data*, *Nucl. Phys.* **B 867** (2013) 244 [arXiv:1207.1303] [INSPIRE].

[34] W. Beenakker, M. Krämer, T. Plehn, M. Spira and P.M. Zerwas, *Stop production at hadron colliders*, *Nucl. Phys.* **B 515** (1998) 3 [hep-ph/9710451] [INSPIRE].

[35] W. Beenakker, S. Brensing, M. Krämer, A. Kulesza, E. Laenen and I. Niessen, *Supersymmetric top and bottom squark production at hadron colliders*, *JHEP* **08** (2010) 098 [arXiv:1006.4771] [INSPIRE].

JHEP11(2017)195

[36] W. Beenakker et al., *Squark and gluino hadroproduction*, *Int. J. Mod. Phys.* **A 26** (2011) 2637 [arXiv:1105.1110] [INSPIRE].

[37] C. Borschensky et al., *Squark and gluino production cross sections in pp collisions at* $\sqrt{s} = 13$, 14, 33 *and* 100 *TeV*, *Eur. Phys. J.* **C 74** (2014) 3174 [arXiv:1407.5066] [INSPIRE].

[38] S. Alioli, P. Nason, C. Oleari and E. Re, *A general framework for implementing NLO calculations in shower Monte Carlo programs: the POWHEG BOX*, *JHEP* **06** (2010) 043 [arXiv:1002.2581] [INSPIRE].

[39] H.-L. Lai et al., *New parton distributions for collider physics*, *Phys. Rev.* **D 82** (2010) 074024 [arXiv:1007.2241] [INSPIRE].

[40] T. Sjöstrand, S. Mrenna and P.Z. Skands, *PYTHIA 6.4 physics and manual*, *JHEP* **05** (2006) 026 [hep-ph/0603175] [INSPIRE].

[41] P.Z. Skands, *Tuning Monte Carlo generators: the Perugia tunes*, *Phys. Rev.* **D 82** (2010) 074018 [arXiv:1005.3457] [INSPIRE].

[42] M. Czakon and A. Mitov, *Top++: a program for the calculation of the top-pair cross-section at hadron colliders*, *Comput. Phys. Commun.* **185** (2014) 2930 [arXiv:1112.5675] [INSPIRE].

[43] N. Kidonakis, *Next-to-next-to-leading-order collinear and soft gluon corrections for t-channel single top quark production*, *Phys. Rev.* **D 83** (2011) 091503 [arXiv:1103.2792] [INSPIRE].

[44] N. Kidonakis, *NNLL resummation for s-channel single top quark production*, *Phys. Rev.* **D 81** (2010) 054028 [arXiv:1001.5034] [INSPIRE].

[45] N. Kidonakis, *Two-loop soft anomalous dimensions for single top quark associated production with a* W^- *or* H^-, *Phys. Rev.* **D 82** (2010) 054018 [arXiv:1005.4451] [INSPIRE].

[46] T. Gleisberg et al., *Event generation with SHERPA 1.1*, *JHEP* **02** (2009) 007 [arXiv:0811.4622] [INSPIRE].

[47] T. Gleisberg and S. Hoeche, *Comix, a new matrix element generator*, *JHEP* **12** (2008) 039 [arXiv:0808.3674] [INSPIRE].

[48] F. Cascioli, P. Maierhofer and S. Pozzorini, *Scattering amplitudes with open loops*, *Phys. Rev. Lett.* **108** (2012) 111601 [arXiv:1111.5206] [INSPIRE].

[49] S. Schumann and F. Krauss, *A parton shower algorithm based on Catani-Seymour dipole factorisation*, *JHEP* **03** (2008) 038 [arXiv:0709.1027] [INSPIRE].

[50] S. Höche, F. Krauss, M. Schönherr and F. Siegert, *QCD matrix elements + parton showers: The NLO case*, *JHEP* **04** (2013) 027 [arXiv:1207.5030] [INSPIRE].

[51] R. Gavin, Y. Li, F. Petriello and S. Quackenbush, *FEWZ 2.0: a code for hadronic Z production at next-to-next-to-leading order*, *Comput. Phys. Commun.* **182** (2011) 2388 [arXiv:1011.3540] [INSPIRE].

[52] D.J. Lange, *The EvtGen particle decay simulation package*, *Nucl. Instrum. Meth.* **A 462** (2001) 152 [INSPIRE].

[53] A.D. Martin, W.J. Stirling, R.S. Thorne and G. Watt, *Update of parton distributions at NNLO*, *Phys. Lett.* **B 652** (2007) 292 [arXiv:0706.0459] [INSPIRE].

[54] ATLAS collaboration, *Summary of ATLAS PYTHIA 8 tunes*, ATL-PHYS-PUB-2012-003 (2012).

[55] ATLAS collaboration, *Vertex reconstruction performance of the ATLAS detector at* $\sqrt{s} = 13$ *TeV*, ATL-PHYS-PUB-2015-026 (2015).

JHEP11(2017)195

[56] ATLAS collaboration, *Topological cell clustering in the ATLAS calorimeters and its performance in LHC Run 1*, *Eur. Phys. J.* **C 77** (2017) 490 [arXiv:1603.02934] [INSPIRE].

[57] M. Cacciari, G.P. Salam and G. Soyez, *The anti-k_t jet clustering algorithm*, *JHEP* **04** (2008) 063 [arXiv:0802.1189] [INSPIRE].

[58] M. Cacciari, G.P. Salam and G. Soyez, *FastJet user manual*, *Eur. Phys. J.* **C 72** (2012) 1896 [arXiv:1111.6097] [INSPIRE].

[59] ATLAS collaboration, *Jet energy scale measurements and their systematic uncertainties in proton-proton collisions at $\sqrt{s} = 13$ TeV with the ATLAS detector*, *Phys. Rev.* **D 96** (2017) 072002 [arXiv:1703.09665] [INSPIRE].

[60] ATLAS collaboration, *Selection of jets produced in 13 TeV proton-proton collisions with the ATLAS detector*, ATLAS-CONF-2015-029 (2015).

[61] ATLAS collaboration, *Performance of pile-up mitigation techniques for jets in pp collisions at $\sqrt{s} = 8$ TeV using the ATLAS detector*, *Eur. Phys. J.* **C 76** (2016) 581 [arXiv:1510.03823].

[62] ATLAS collaboration, *Jet calibration and systematic uncertainties for jets reconstructed in the ATLAS detector at $\sqrt{s} = 13$ TeV*, ATL-PHYS-PUB-2015-015 (2015).

[63] ATLAS collaboration, *Performance of b-jet identification in the ATLAS experiment*, 2016 *JINST* **11** P04008 [arXiv:1512.01094] [INSPIRE].

[64] ATLAS collaboration, *Optimisation of the ATLAS b-tagging performance for the 2016 LHC Run*, ATL-PHYS-PUB-2016-012 (2016).

[65] ATLAS collaboration, *Electron efficiency measurements with the ATLAS detector using 2012 LHC proton–proton collision data*, *Eur. Phys. J.* **C 77** (2017) 195 [arXiv:1612.01456] [INSPIRE].

[66] ATLAS collaboration, *Electron and photon energy calibration with the ATLAS detector using LHC Run 1 data*, *Eur. Phys. J.* **C 74** (2014) 3071 [arXiv:1407.5063] [INSPIRE].

[67] ATLAS collaboration, *Electron identification measurements in ATLAS using $\sqrt{s} = 13$ TeV data with 50 ns bunch spacing*, ATL-PHYS-PUB-2015-041 (2015).

[68] ATLAS collaboration, *Muon reconstruction performance of the ATLAS detector in proton–proton collision data at $\sqrt{s} = 13$ TeV*, *Eur. Phys. J.* **C 76** (2016) 292 [arXiv:1603.05598].

[69] ATLAS collaboration, *Measurement of the $t\bar{t}$ production cross-section using $e\mu$ events with b-tagged jets in pp collisions at $\sqrt{s} = 13$ TeV with the ATLAS detector*, *Phys. Lett.* **B 761** (2016) 136 [arXiv:1606.02699].

[70] ATLAS collaboration, *Performance of algorithms that reconstruct missing transverse momentum in $\sqrt{s} = 8$ TeV proton-proton collisions in the ATLAS detector*, *Eur. Phys. J.* **C 77** (2017) 241 [arXiv:1609.09324].

[71] ATLAS collaboration, *Jet energy measurement with the ATLAS detector in proton–proton collisions at $\sqrt{s} = 7$ TeV*, *Eur. Phys. J.* **C 73** (2013) 2304 [arXiv:1112.6426].

[72] ATLAS collaboration, *Measurement of the photon identification efficiencies with the ATLAS detector using LHC Run-1 data*, *Eur. Phys. J.* **C 76** (2016) 666 [arXiv:1606.01813] [INSPIRE].

[73] D.R. Tovey, *On measuring the masses of pair-produced semi-invisibly decaying particles at hadron colliders*, *JHEP* **04** (2008) 034 [arXiv:0802.2879] [INSPIRE].

JHEP11(2017)195

[74] ATLAS collaboration, *Search for direct third-generation squark pair production in final states with missing transverse momentum and two b-jets in $\sqrt{s} = 8$ TeV pp collisions with the ATLAS detector*, *JHEP* **10** (2013) 189 [arXiv:1308.2631].

[75] A.J. Barr, B. Gripaios and C.G. Lester, *Transverse masses and kinematic constraints: from the boundary to the crease*, *JHEP* **11** (2009) 096 [arXiv:0908.3779] [INSPIRE].

[76] P. Konar, K. Kong, K.T. Matchev and M. Park, *Dark matter particle spectroscopy at the LHC: generalizing M(T2) to asymmetric event topologies*, *JHEP* **04** (2010) 086 [arXiv:0911.4126] [INSPIRE].

[77] C.G. Lester and D.J. Summers, *Measuring masses of semiinvisibly decaying particles pair produced at hadron colliders*, *Phys. Lett.* **B 463** (1999) 99 [hep-ph/9906349] [INSPIRE].

[78] M. Baak et al., *HistFitter software framework for statistical data analysis*, *Eur. Phys. J.* **C 75** (2015) 153 [arXiv:1410.1280] [INSPIRE].

[79] ATLAS collaboration, *Search for squarks and gluinos with the ATLAS detector in final states with jets and missing transverse momentum using 4.7 fb^{-1} of $\sqrt{s} = 7$ TeV proton-proton collision data*, *Phys. Rev.* **D 87** (2013) 012008 [arXiv:1208.0949].

[80] ATLAS collaboration, *Search for squarks and gluinos in events with isolated leptons, jets and missing transverse momentum at $\sqrt{s} = 8$ TeV with the ATLAS detector*, *JHEP* **04** (2015) 116 [arXiv:1501.03555] [INSPIRE].

[81] ATLAS collaboration, *Studies on top-quark Monte Carlo modelling with Sherpa and MG5_aMC@NLO*, ATL-PHYS-PUB-2017-007 (2017).

[82] ATLAS collaboration, *Jet energy resolution in proton–proton collisions at $\sqrt{s} = 7$ TeV recorded in 2010 with the ATLAS detector*, *Eur. Phys. J.* **C 73** (2013) 2306 [arXiv:1210.6210].

[83] ATLAS collaboration, *Measurement of the cross section for the production of a W boson in association with b-jets in pp collisions at $\sqrt{s} = 7$ TeV with the ATLAS detector*, *Phys. Lett.* **B 707** (2012) 418 [arXiv:1109.1470].

[84] M. Bahr et al., *HERWIG++ physics and manual*, *Eur. Phys. J.* **C 58** (2008) 639 [arXiv:0803.0883] [INSPIRE].

[85] S. Gieseke, C. Rohr and A. Siodmok, *Colour reconnections in HERWIG++*, *Eur. Phys. J.* **C 72** (2012) 2225 [arXiv:1206.0041] [INSPIRE].

[86] T. Junk, *Confidence level computation for combining searches with small statistics*, *Nucl. Instrum. Meth.* **A 434** (1999) 435 [hep-ex/9902006] [INSPIRE].

[87] A.L. Read, *Presentation of search results: the CL(s) technique*, *J. Phys.* **G 28** (2002) 2693 [INSPIRE].

[88] ATLAS collaboration, *ATLAS computing acknowledgements 2016-2017*, ATL-GEN-PUB-2016-002 (2016).

JHEP11(2017)195

The ATLAS collaboration

M. Aaboud[137d], G. Aad[88], B. Abbott[115], O. Abdinov[12,*], B. Abeloos[119], S.H. Abidi[161], O.S. AbouZeid[139], N.L. Abraham[151], H. Abramowicz[155], H. Abreu[154], R. Abreu[118], Y. Abulaiti[148a,148b], B.S. Acharya[167a,167b,a], S. Adachi[157], L. Adamczyk[41a], J. Adelman[110], M. Adersberger[102], T. Adye[133], A.A. Affolder[139], Y. Afik[154], T. Agatonovic-Jovin[14], C. Agheorghiesei[28c], J.A. Aguilar-Saavedra[128a,128f], S.P. Ahlen[24], F. Ahmadov[68,b], G. Aielli[135a,135b], S. Akatsuka[71], H. Akerstedt[148a,148b], T.P.A. Åkesson[84], E. Akilli[52], A.V. Akimov[98], G.L. Alberghi[22a,22b], J. Albert[172], P. Albicocco[50], M.J. Alconada Verzini[74], S.C. Alderweireldt[108], M. Aleksa[32], I.N. Aleksandrov[68], C. Alexa[28b], G. Alexander[155], T. Alexopoulos[10], M. Alhroob[115], B. Ali[130], M. Aliev[76a,76b], G. Alimonti[94a], J. Alison[33], S.P. Alkire[38], B.M.M. Allbrooke[151], B.W. Allen[118], P.P. Allport[19], A. Aloisio[106a,106b], A. Alonso[39], F. Alonso[74], C. Alpigiani[140], A.A. Alshehri[56], M.I. Alstaty[88], B. Alvarez Gonzalez[32], D. Álvarez Piqueras[170], M.G. Alviggi[106a,106b], B.T. Amadio[16], Y. Amaral Coutinho[26a], C. Amelung[25], D. Amidei[92], S.P. Amor Dos Santos[128a,128c], S. Amoroso[32], G. Amundsen[25], C. Anastopoulos[141], L.S. Ancu[52], N. Andari[19], T. Andeen[11], C.F. Anders[60b], J.K. Anders[77], K.J. Anderson[33], A. Andreazza[94a,94b], V. Andrei[60a], S. Angelidakis[37], I. Angelozzi[109], A. Angerami[38], A.V. Anisenkov[111,c], N. Anjos[13], A. Annovi[126a,126b], C. Antel[60a], M. Antonelli[50], A. Antonov[100,*], D.J. Antrim[166], F. Anulli[134a], M. Aoki[69], L. Aperio Bella[32], G. Arabidze[93], Y. Arai[69], J.P. Araque[128a], V. Araujo Ferraz[26a], A.T.H. Arce[48], R.E. Ardell[80], F.A. Arduh[74], J-F. Arguin[97], S. Argyropoulos[66], M. Arik[20a], A.J. Armbruster[32], L.J. Armitage[79], O. Arnaez[161], H. Arnold[51], M. Arratia[30], O. Arslan[23], A. Artamonov[99,*], G. Artoni[122], S. Artz[86], S. Asai[157], N. Asbah[45], A. Ashkenazi[155], L. Asquith[151], K. Assamagan[27], R. Astalos[146a], M. Atkinson[169], N.B. Atlay[143], K. Augsten[130], G. Avolio[32], B. Axen[16], M.K. Ayoub[119], G. Azuelos[97,d], A.E. Baas[60a], M.J. Baca[19], H. Bachacou[138], K. Bachas[76a,76b], M. Backes[122], P. Bagnaia[134a,134b], M. Bahmani[42], H. Bahrasemani[144], J.T. Baines[133], M. Bajic[39], O.K. Baker[179], E.M. Baldin[111,c], P. Balek[175], F. Balli[138], W.K. Balunas[124], E. Banas[42], A. Bandyopadhyay[23], Sw. Banerjee[176,e], A.A.E. Bannoura[178], L. Barak[155], E.L. Barberio[91], D. Barberis[53a,53b], M. Barbero[88], T. Barillari[103], M-S Barisits[32], J.T. Barkeloo[118], T. Barklow[145], N. Barlow[30], S.L. Barnes[36c], B.M. Barnett[133], R.M. Barnett[16], Z. Barnovska-Blenessy[36a], A. Baroncelli[136a], G. Barone[25], A.J. Barr[122], L. Barranco Navarro[170], F. Barreiro[85], J. Barreiro Guimarães da Costa[35a], R. Bartoldus[145], A.E. Barton[75], P. Bartos[146a], A. Basalaev[125], A. Bassalat[119,f], R.L. Bates[56], S.J. Batista[161], J.R. Batley[30], M. Battaglia[139], M. Bauce[134a,134b], F. Bauer[138], H.S. Bawa[145,g], J.B. Beacham[113], M.D. Beattie[75], T. Beau[83], P.H. Beauchemin[165], P. Bechtle[23], H.P. Beck[18,h], H.C. Beck[57], K. Becker[122], M. Becker[86], C. Becot[112], A.J. Beddall[20e], A. Beddall[20b], V.A. Bednyakov[68], M. Bedognetti[109], C.P. Bee[150], T.A. Beermann[32], M. Begalli[26a], M. Begel[27], J.K. Behr[45], A.S. Bell[81], G. Bella[155], L. Bellagamba[22a], A. Bellerive[31], M. Bellomo[154], K. Belotskiy[100], O. Beltramello[32], N.L. Belyaev[100], O. Benary[155,*], D. Benchekroun[137a], M. Bender[102], K. Bendtz[148a,148b], N. Benekos[10], Y. Benhammou[155], E. Benhar Noccioli[179], J. Benitez[66], D.P. Benjamin[48], M. Benoit[52], J.R. Bensinger[25], S. Bentvelsen[109], L. Beresford[122], M. Beretta[50], D. Berge[109], E. Bergeaas Kuutmann[168], N. Berger[5], J. Beringer[16], S. Berlendis[58], N.R. Bernard[89], G. Bernardi[83], C. Bernius[145], F.U. Bernlochner[23], T. Berry[80], P. Berta[86], C. Bertella[35a], G. Bertoli[148a,148b], F. Bertolucci[126a,126b], I.A. Bertram[75], C. Bertsche[45], D. Bertsche[115], G.J. Besjes[39], O. Bessidskaia Bylund[148a,148b], M. Bessner[45], N. Besson[138], A. Bethani[87], S. Bethke[103], A.J. Bevan[79], J. Beyer[103], R.M. Bianchi[127], O. Biebel[102], D. Biedermann[17], R. Bielski[87], K. Bierwagen[86], N.V. Biesuz[126a,126b], M. Biglietti[136a], T.R.V. Billoud[97], H. Bilokon[50], M. Bindi[57], A. Bingul[20b], C. Bini[134a,134b], S. Biondi[22a,22b], T. Bisanz[57], C. Bittrich[47], D.M. Bjergaard[48], J.E. Black[145], K.M. Black[24], R.E. Blair[6], T. Blazek[146a], I. Bloch[45],

JHEP11(2017)195

C. Blocker[25], A. Blue[56], W. Blum[86,*], U. Blumenschein[79], S. Blunier[34a], G.J. Bobbink[109], V.S. Bobrovnikov[111,c], S.S. Bocchetta[84], A. Bocci[48], C. Bock[102], M. Boehler[51], D. Boerner[178], D. Bogavac[102], A.G. Bogdanchikov[111], C. Bohm[148a], V. Boisvert[80], P. Bokan[168,i], T. Bold[41a], A.S. Boldyrev[101], A.E. Bolz[60b], M. Bomben[83], M. Bona[79], M. Boonekamp[138], A. Borisov[132], G. Borissov[75], J. Bortfeldt[32], D. Bortoletto[122], V. Bortolotto[62a,62b,62c], D. Boscherini[22a], M. Bosman[13], J.D. Bossio Sola[29], J. Boudreau[127], J. Bouffard[2], E.V. Bouhova-Thacker[75], D. Boumediene[37], C. Bourdarios[119], S.K. Boutle[56], A. Boveia[113], J. Boyd[32], I.R. Boyko[68], A.J. Bozson[80], J. Bracinik[19], A. Brandt[8], G. Brandt[57], O. Brandt[60a], U. Bratzler[158], B. Brau[89], J.E. Brau[118], W.D. Breaden Madden[56], K. Brendlinger[45], A.J. Brennan[91], L. Brenner[109], R. Brenner[168], S. Bressler[175], D.L. Briglin[19], T.M. Bristow[49], D. Britton[56], D. Britzger[45], F.M. Brochu[30], I. Brock[23], R. Brock[93], G. Brooijmans[38], T. Brooks[80], W.K. Brooks[34b], J. Brosamer[16], E. Brost[110], J.H Broughton[19], P.A. Bruckman de Renstrom[42], D. Bruncko[146b], A. Bruni[22a], G. Bruni[22a], L.S. Bruni[109], S. Bruno[135a,135b], BH Brunt[30], M. Bruschi[22a], N. Bruscino[23], P. Bryant[33], L. Bryngemark[45], T. Buanes[15], Q. Buat[144], P. Buchholz[143], A.G. Buckley[56], I.A. Budagov[68], F. Buehrer[51], M.K. Bugge[121], O. Bulekov[100], D. Bullock[8], T.J. Burch[110], S. Burdin[77], C.D. Burgard[51], A.M. Burger[5], B. Burghgrave[110], K. Burka[42], S. Burke[133], I. Burmeister[46], J.T.P. Burr[122], E. Busato[37], D. Büscher[51], V. Büscher[86], P. Bussey[56], J.M. Butler[24], C.M. Buttar[56], J.M. Butterworth[81], P. Butti[32], W. Buttinger[27], A. Buzatu[153], A.R. Buzykaev[111,c], S. Cabrera Urbán[170], D. Caforio[130], V.M. Cairo[40a,40b], O. Cakir[4a], N. Calace[52], P. Calafiura[16], A. Calandri[88], G. Calderini[83], P. Calfayan[64], G. Callea[40a,40b], L.P. Caloba[26a], S. Calvente Lopez[85], D. Calvet[37], S. Calvet[37], T.P. Calvet[88], R. Camacho Toro[33], S. Camarda[32], P. Camarri[135a,135b], D. Cameron[121], R. Caminal Armadans[169], C. Camincher[58], S. Campana[32], M. Campanelli[81], A. Camplani[94a,94b], A. Campoverde[143], V. Canale[106a,106b], M. Cano Bret[36c], J. Cantero[116], T. Cao[155], M.D.M. Capeans Garrido[32], I. Caprini[28b], M. Caprini[28b], M. Capua[40a,40b], R.M. Carbone[38], R. Cardarelli[135a], F. Cardillo[51], I. Carli[131], T. Carli[32], G. Carlino[106a], B.T. Carlson[127], L. Carminati[94a,94b], R.M.D. Carney[148a,148b], S. Caron[108], E. Carquin[34b], S. Carrá[94a,94b], G.D. Carrillo-Montoya[32], D. Casadei[19], M.P. Casado[13,j], M. Casolino[13], D.W. Casper[166], R. Castelijn[109], V. Castillo Gimenez[170], N.F. Castro[128a,k], A. Catinaccio[32], J.R. Catmore[121], A. Cattai[32], J. Caudron[23], V. Cavaliere[169], E. Cavallaro[13], D. Cavalli[94a], M. Cavalli-Sforza[13], V. Cavasinni[126a,126b], E. Celebi[20d], F. Ceradini[136a,136b], L. Cerda Alberich[170], A.S. Cerqueira[26b], A. Cerri[151], L. Cerrito[135a,135b], F. Cerutti[16], A. Cervelli[18], S.A. Cetin[20d], A. Chafaq[137a], D. Chakraborty[110], S.K. Chan[59], W.S. Chan[109], Y.L. Chan[62a], P. Chang[169], J.D. Chapman[30], D.G. Charlton[19], C.C. Chau[31], C.A. Chavez Barajas[151], S. Che[113], S. Cheatham[167a,167c], A. Chegwidden[93], S. Chekanov[6], S.V. Chekulaev[163a], G.A. Chelkov[68,l], M.A. Chelstowska[32], C. Chen[36a], C. Chen[67], H. Chen[27], J. Chen[36a], S. Chen[35b], S. Chen[157], X. Chen[35c,m], Y. Chen[70], H.C. Cheng[92], H.J. Cheng[35a], A. Cheplakov[68], E. Cheremushkina[132], R. Cherkaoui El Moursli[137e], E. Cheu[7], K. Cheung[63], L. Chevalier[138], V. Chiarella[50], G. Chiarelli[126a,126b], G. Chiodini[76a], A.S. Chisholm[32], A. Chitan[28b], Y.H. Chiu[172], M.V. Chizhov[68], K. Choi[64], A.R. Chomont[37], S. Chouridou[156], Y.S. Chow[62a], V. Christodoulou[81], M.C. Chu[62a], J. Chudoba[129], A.J. Chuinard[90], J.J. Chwastowski[42], L. Chytka[117], A.K. Ciftci[4a], D. Cinca[46], V. Cindro[78], I.A. Cioara[23], C. Ciocca[22a,22b], A. Ciocio[16], F. Cirotto[106a,106b], Z.H. Citron[175], M. Citterio[94a], M. Ciubancan[28b], A. Clark[52], B.L. Clark[59], M.R. Clark[38], P.J. Clark[49], R.N. Clarke[16], C. Clement[148a,148b], Y. Coadou[88], M. Cobal[167a,167c], A. Coccaro[52], J. Cochran[67], L. Colasurdo[108], B. Cole[38], A.P. Colijn[109], J. Collot[58], T. Colombo[166], P. Conde Muiño[128a,128b], E. Coniavitis[51], S.H. Connell[147b], I.A. Connelly[87], S. Constantinescu[28b], G. Conti[32], F. Conventi[106a,n], M. Cooke[16], A.M. Cooper-Sarkar[122], F. Cormier[171], K.J.R. Cormier[161], M. Corradi[134a,134b],

JHEP11(2017)195

F. Corriveau[90,o], A. Cortes-Gonzalez[32], G. Cortiana[103], G. Costa[94a], M.J. Costa[170], D. Costanzo[141], G. Cottin[30], G. Cowan[80], B.E. Cox[87], K. Cranmer[112], S.J. Crawley[56], R.A. Creager[124], G. Cree[31], S. Crépé-Renaudin[58], F. Crescioli[83], W.A. Cribbs[148a,148b], M. Cristinziani[23], V. Croft[112], G. Crosetti[40a,40b], A. Cueto[85], T. Cuhadar Donszelmann[141], A.R. Cukierman[145], J. Cummings[179], M. Curatolo[50], J. Cúth[86], S. Czekierda[42], P. Czodrowski[32], G. D'amen[22a,22b], S. D'Auria[56], L. D'eramo[83], M. D'Onofrio[77], M.J. Da Cunha Sargedas De Sousa[128a,128b], C. Da Via[87], W. Dabrowski[41a], T. Dado[146a], T. Dai[92], O. Dale[15], F. Dallaire[97], C. Dallapiccola[89], M. Dam[39], J.R. Dandoy[124], M.F. Daneri[29], N.P. Dang[176], A.C. Daniells[19], N.S. Dann[87], M. Danninger[171], M. Dano Hoffmann[138], V. Dao[150], G. Darbo[53a], S. Darmora[8], J. Dassoulas[3], A. Dattagupta[118], T. Daubney[45], W. Davey[23], C. David[45], T. Davidek[131], D.R. Davis[48], P. Davison[81], E. Dawe[91], I. Dawson[141], K. De[8], R. de Asmundis[106a], A. De Benedetti[115], S. De Castro[22a,22b], S. De Cecco[83], N. De Groot[108], P. de Jong[109], H. De la Torre[93], F. De Lorenzi[67], A. De Maria[57], D. De Pedis[134a], A. De Salvo[134a], U. De Sanctis[135a,135b], A. De Santo[151], K. De Vasconcelos Corga[88], J.B. De Vivie De Regie[119], R. Debbe[27], C. Debenedetti[139], D.V. Dedovich[68], N. Dehghanian[3], I. Deigaard[109], M. Del Gaudio[40a,40b], J. Del Peso[85], D. Delgove[119], F. Deliot[138], C.M. Delitzsch[7], A. Dell'Acqua[32], L. Dell'Asta[24], M. Dell'Orso[126a,126b], M. Della Pietra[106a,106b], D. della Volpe[52], M. Delmastro[5], C. Delporte[119], P.A. Delsart[58], D.A. DeMarco[161], S. Demers[179], M. Demichev[68], A. Demilly[83], S.P. Denisov[132], D. Denysiuk[138], D. Derendarz[42], J.E. Derkaoui[137d], F. Derue[83], P. Dervan[77], K. Desch[23], C. Deterre[45], K. Dette[161], M.R. Devesa[29], P.O. Deviveiros[32], A. Dewhurst[133], S. Dhaliwal[25], F.A. Di Bello[52], A. Di Ciaccio[135a,135b], L. Di Ciaccio[5], W.K. Di Clemente[124], C. Di Donato[106a,106b], A. Di Girolamo[32], B. Di Girolamo[32], B. Di Micco[136a,136b], R. Di Nardo[32], K.F. Di Petrillo[59], A. Di Simone[51], R. Di Sipio[161], D. Di Valentino[31], C. Diaconu[88], M. Diamond[161], F.A. Dias[39], M.A. Diaz[34a], E.B. Diehl[92], J. Dietrich[17], S. Díez Cornell[45], A. Dimitrievska[14], J. Dingfelder[23], P. Dita[28b], S. Dita[28b], F. Dittus[32], F. Djama[88], T. Djobava[54b], J.I. Djuvsland[60a], M.A.B. do Vale[26c], D. Dobos[32], M. Dobre[28b], C. Doglioni[84], J. Dolejsi[131], Z. Dolezal[131], M. Donadelli[26d], S. Donati[126a,126b], P. Dondero[123a,123b], J. Donini[37], J. Dopke[133], A. Doria[106a], M.T. Dova[74], A.T. Doyle[56], E. Drechsler[57], M. Dris[10], Y. Du[36b], J. Duarte-Campderros[155], A. Dubreuil[52], E. Duchovni[175], G. Duckeck[102], A. Ducourthial[83], O.A. Ducu[97,p], D. Duda[109], A. Dudarev[32], A.Chr. Dudder[86], E.M. Duffield[16], L. Duflot[119], M. Dührssen[32], C. Dulsen[178], M. Dumancic[175], A.E. Dumitriu[28b], A.K. Duncan[56], M. Dunford[60a], H. Duran Yildiz[4a], M. Düren[55], A. Durglishvili[54b], D. Duschinger[47], B. Dutta[45], D. Duvnjak[1], M. Dyndal[45], B.S. Dziedzic[42], C. Eckardt[45], K.M. Ecker[103], R.C. Edgar[92], T. Eifert[32], G. Eigen[15], K. Einsweiler[16], T. Ekelof[168], M. El Kacimi[137c], R. El Kosseifi[88], V. Ellajosyula[88], M. Ellert[168], S. Elles[5], F. Ellinghaus[178], A.A. Elliot[172], N. Ellis[32], J. Elmsheuser[27], M. Elsing[32], D. Emeliyanov[133], Y. Enari[157], O.C. Endner[86], J.S. Ennis[173], J. Erdmann[46], A. Ereditato[18], M. Ernst[27], S. Errede[169], M. Escalier[119], C. Escobar[170], B. Esposito[50], O. Estrada Pastor[170], A.I. Etienvre[138], E. Etzion[155], H. Evans[64], A. Ezhilov[125], M. Ezzi[137e], F. Fabbri[22a,22b], L. Fabbri[22a,22b], V. Fabiani[108], G. Facini[81], R.M. Fakhrutdinov[132], S. Falciano[134a], R.J. Falla[81], J. Faltova[32], Y. Fang[35a], M. Fanti[94a,94b], A. Farbin[8], A. Farilla[136a], C. Farina[127], E.M. Farina[123a,123b], T. Farooque[93], S. Farrell[16], S.M. Farrington[173], P. Farthouat[32], F. Fassi[137e], P. Fassnacht[32], D. Fassouliotis[9], M. Faucci Giannelli[49], A. Favareto[53a,53b], W.J. Fawcett[122], L. Fayard[119], O.L. Fedin[125,q], W. Fedorko[171], S. Feigl[121], L. Feligioni[88], C. Feng[36b], E.J. Feng[32], H. Feng[92], M.J. Fenton[56], A.B. Fenyuk[132], L. Feremenga[8], P. Fernandez Martinez[170], S. Fernandez Perez[13], J. Ferrando[45], A. Ferrari[168], P. Ferrari[109], R. Ferrari[123a], D.E. Ferreira de Lima[60b], A. Ferrer[170], D. Ferrere[52], C. Ferretti[92], F. Fiedler[86], A. Filipčič[78], M. Filipuzzi[45], F. Filthaut[108],

JHEP11(2017)195

M. Fincke-Keeler[172], K.D. Finelli[152], M.C.N. Fiolhais[128a,128c,r], L. Fiorini[170], A. Fischer[2], C. Fischer[13], J. Fischer[178], W.C. Fisher[93], N. Flaschel[45], I. Fleck[143], P. Fleischmann[92], R.R.M. Fletcher[124], T. Flick[178], B.M. Flierl[102], L.R. Flores Castillo[62a], M.J. Flowerdew[103], G.T. Forcolin[87], A. Formica[138], F.A. Förster[13], A. Forti[87], A.G. Foster[19], D. Fournier[119], H. Fox[75], S. Fracchia[141], P. Francavilla[83], M. Franchini[22a,22b], S. Franchino[60a], D. Francis[32], L. Franconi[121], M. Franklin[59], M. Frate[166], M. Fraternali[123a,123b], D. Freeborn[81], S.M. Fressard-Batraneanu[32], B. Freund[97], D. Froidevaux[32], J.A. Frost[122], C. Fukunaga[158], T. Fusayasu[104], J. Fuster[170], C. Gabaldon[58], O. Gabizon[154], A. Gabrielli[22a,22b], A. Gabrielli[16], G.P. Gach[41a], S. Gadatsch[32], S. Gadomski[80], G. Gagliardi[53a,53b], L.G. Gagnon[97], C. Galea[108], B. Galhardo[128a,128c], E.J. Gallas[122], B.J. Gallop[133], P. Gallus[130], G. Galster[39], K.K. Gan[113], S. Ganguly[37], Y. Gao[77], Y.S. Gao[145,g], F.M. Garay Walls[34a], C. García[170], J.E. García Navarro[170], J.A. García Pascual[35a], M. Garcia-Sciveres[16], R.W. Gardner[33], N. Garelli[145], V. Garonne[121], A. Gascon Bravo[45], K. Gasnikova[45], C. Gatti[50], A. Gaudiello[53a,53b], G. Gaudio[123a], I.L. Gavrilenko[98], C. Gay[171], G. Gaycken[23], E.N. Gazis[10], C.N.P. Gee[133], J. Geisen[57], M. Geisen[86], M.P. Geisler[60a], K. Gellerstedt[148a,148b], C. Gemme[53a], M.H. Genest[58], C. Geng[92], S. Gentile[134a,134b], C. Gentsos[156], S. George[80], D. Gerbaudo[13], A. Gershon[155], G. Geßner[46], S. Ghasemi[143], M. Ghneimat[23], B. Giacobbe[22a], S. Giagu[134a,134b], N. Giangiacomi[22a,22b], P. Giannetti[126a,126b], S.M. Gibson[80], M. Gignac[171], M. Gilchriese[16], D. Gillberg[31], G. Gilles[178], D.M. Gingrich[3,d], M.P. Giordani[167a,167c], F.M. Giorgi[22a], P.F. Giraud[138], P. Giromini[59], G. Giugliarelli[167a,167c], D. Giugni[94a], F. Giuli[122], C. Giuliani[103], M. Giulini[60b], B.K. Gjelsten[121], S. Gkaitatzis[156], I. Gkialas[9,s], E.L. Gkougkousis[13], P. Gkountoumis[10], L.K. Gladilin[101], C. Glasman[85], J. Glatzer[13], P.C.F. Glaysher[45], A. Glazov[45], M. Goblirsch-Kolb[25], J. Godlewski[42], S. Goldfarb[91], T. Golling[52], D. Golubkov[132], A. Gomes[128a,128b,128d], R. Gonçalo[128a], R. Goncalves Gama[26a], J. Goncalves Pinto Firmino Da Costa[138], G. Gonella[51], L. Gonella[19], A. Gongadze[68], S. González de la Hoz[170], S. Gonzalez-Sevilla[52], L. Goossens[32], P.A. Gorbounov[99], H.A. Gordon[27], I. Gorelov[107], B. Gorini[32], E. Gorini[76a,76b], A. Gorišek[78], A.T. Goshaw[48], C. Gössling[46], M.I. Gostkin[68], C.A. Gottardo[23], C.R. Goudet[119], D. Goujdami[137c], A.G. Goussiou[140], N. Govender[147b,t], E. Gozani[154], L. Graber[57], I. Grabowska-Bold[41a], P.O.J. Gradin[168], J. Gramling[166], E. Gramstad[121], S. Grancagnolo[17], V. Gratchev[125], P.M. Gravila[28f], C. Gray[56], H.M. Gray[16], Z.D. Greenwood[82,u], C. Grefe[23], K. Gregersen[81], I.M. Gregor[45], P. Grenier[145], K. Grevtsov[5], J. Griffiths[8], A.A. Grillo[139], K. Grimm[75], S. Grinstein[13,v], Ph. Gris[37], J.-F. Grivaz[119], S. Groh[86], E. Gross[175], J. Grosse-Knetter[57], G.C. Grossi[82], Z.J. Grout[81], A. Grummer[107], L. Guan[92], W. Guan[176], J. Guenther[65], F. Guescini[163a], D. Guest[166], O. Gueta[155], B. Gui[113], E. Guido[53a,53b], T. Guillemin[5], S. Guindon[32], U. Gul[56], C. Gumpert[32], J. Guo[36c], W. Guo[92], Y. Guo[36a], R. Gupta[43], S. Gupta[122], G. Gustavino[115], B.J. Gutelman[154], P. Gutierrez[115], N.G. Gutierrez Ortiz[81], C. Gutschow[81], C. Guyot[138], M.P. Guzik[41a], C. Gwenlan[122], C.B. Gwilliam[77], A. Haas[112], C. Haber[16], H.K. Hadavand[8], N. Haddad[137e], A. Hadef[88], S. Hageböck[23], M. Hagihara[164], H. Hakobyan[180,*], M. Haleem[45], J. Haley[116], G. Halladjian[93], G.D. Hallewell[88], K. Hamacher[178], P. Hamal[117], K. Hamano[172], A. Hamilton[147a], G.N. Hamity[141], P.G. Hamnett[45], L. Han[36a], S. Han[35a], K. Hanagaki[69,w], K. Hanawa[157], M. Hance[139], B. Haney[124], P. Hanke[60a], J.B. Hansen[39], J.D. Hansen[39], M.C. Hansen[23], P.H. Hansen[39], K. Hara[164], A.S. Hard[176], T. Harenberg[178], F. Hariri[119], S. Harkusha[95], P.F. Harrison[173], N.M. Hartmann[102], Y. Hasegawa[142], A. Hasib[49], S. Hassani[138], S. Haug[18], R. Hauser[93], L. Hauswald[47], L.B. Havener[38], M. Havranek[130], C.M. Hawkes[19], R.J. Hawkings[32], D. Hayakawa[159], D. Hayden[93], C.P. Hays[122], J.M. Hays[79], H.S. Hayward[77], S.J. Haywood[133], S.J. Head[19], T. Heck[86], V. Hedberg[84], L. Heelan[8], S. Heer[23], K.K. Heidegger[51], S. Heim[45], T. Heim[16], B. Heinemann[45,x], J.J. Heinrich[102],

JHEP11(2017)195

L. Heinrich[112], C. Heinz[55], J. Hejbal[129], L. Helary[32], A. Held[171], S. Hellman[148a,148b], C. Helsens[32], R.C.W. Henderson[75], Y. Heng[176], S. Henkelmann[171], A.M. Henriques Correia[32], S. Henrot-Versille[119], G.H. Herbert[17], H. Herde[25], V. Herget[177], Y. Hernández Jiménez[147c], H. Herr[86], G. Herten[51], R. Hertenberger[102], L. Hervas[32], T.C. Herwig[124], G.G. Hesketh[81], N.P. Hessey[163a], J.W. Hetherly[43], S. Higashino[69], E. Higón-Rodriguez[170], K. Hildebrand[33], E. Hill[172], J.C. Hill[30], K.H. Hiller[45], S.J. Hillier[19], M. Hils[47], I. Hinchliffe[16], M. Hirose[51], D. Hirschbuehl[178], B. Hiti[78], O. Hladik[129], X. Hoad[49], J. Hobbs[150], N. Hod[163a], M.C. Hodgkinson[141], P. Hodgson[141], A. Hoecker[32], M.R. Hoeferkamp[107], F. Hoenig[102], D. Hohn[23], T.R. Holmes[33], M. Homann[46], S. Honda[164], T. Honda[69], T.M. Hong[127], B.H. Hooberman[169], W.H. Hopkins[118], Y. Horii[105], A.J. Horton[144], J-Y. Hostachy[58], A. Hostiuc[140], S. Hou[153], A. Hoummada[137a], J. Howarth[87], J. Hoya[74], M. Hrabovsky[117], J. Hrdinka[32], I. Hristova[17], J. Hrivnac[119], T. Hryn'ova[5], A. Hrynevich[96], P.J. Hsu[63], S.-C. Hsu[140], Q. Hu[36a], S. Hu[36c], Y. Huang[35a], Z. Hubacek[130], F. Hubaut[88], F. Huegging[23], T.B. Huffman[122], E.W. Hughes[38], G. Hughes[75], M. Huhtinen[32], P. Huo[150], N. Huseynov[68,b], J. Huston[93], J. Huth[59], G. Iacobucci[52], G. Iakovidis[27], I. Ibragimov[143], L. Iconomidou-Fayard[119], Z. Idrissi[137e], P. Iengo[32], O. Igonkina[109,y], T. Iizawa[174], Y. Ikegami[69], M. Ikeno[69], Y. Ilchenko[11,z], D. Iliadis[156], N. Ilic[145], G. Introzzi[123a,123b], P. Ioannou[9,*], M. Iodice[136a], K. Iordanidou[38], V. Ippolito[59], M.F. Isacson[168], N. Ishijima[120], M. Ishino[157], M. Ishitsuka[159], C. Issever[122], S. Istin[20a], F. Ito[164], J.M. Iturbe Ponce[62a], R. Iuppa[162a,162b], H. Iwasaki[69], J.M. Izen[44], V. Izzo[106a], S. Jabbar[3], P. Jackson[1], R.M. Jacobs[23], V. Jain[2], K.B. Jakobi[86], K. Jakobs[51], S. Jakobsen[65], T. Jakoubek[129], D.O. Jamin[116], D.K. Jana[82], R. Jansky[52], J. Janssen[23], M. Janus[57], P.A. Janus[41a], G. Jarlskog[84], N. Javadov[68,b], T. Javůrek[51], M. Javurkova[51], F. Jeanneau[138], L. Jeanty[16], J. Jejelava[54a,aa], A. Jelinskas[173], P. Jenni[51,ab], C. Jeske[173], S. Jézéquel[5], H. Ji[176], J. Jia[150], H. Jiang[67], Y. Jiang[36a], Z. Jiang[145], S. Jiggins[81], J. Jimenez Pena[170], S. Jin[35a], A. Jinaru[28b], O. Jinnouchi[159], H. Jivan[147c], P. Johansson[141], K.A. Johns[7], C.A. Johnson[64], W.J. Johnson[140], K. Jon-And[148a,148b], R.W.L. Jones[75], S.D. Jones[151], S. Jones[7], T.J. Jones[77], J. Jongmanns[60a], P.M. Jorge[128a,128b], J. Jovicevic[163a], X. Ju[176], A. Juste Rozas[13,v], M.K. Köhler[175], A. Kaczmarska[42], M. Kado[119], H. Kagan[113], M. Kagan[145], S.J. Kahn[88], T. Kaji[174], E. Kajomovitz[48], C.W. Kalderon[84], A. Kaluza[86], S. Kama[43], A. Kamenshchikov[132], N. Kanaya[157], L. Kanjir[78], V.A. Kantserov[100], J. Kanzaki[69], B. Kaplan[112], L.S. Kaplan[176], D. Kar[147c], K. Karakostas[10], N. Karastathis[10], M.J. Kareem[57], E. Karentzos[10], S.N. Karpov[68], Z.M. Karpova[68], K. Karthik[112], V. Kartvelishvili[75], A.N. Karyukhin[132], K. Kasahara[164], L. Kashif[176], R.D. Kass[113], A. Kastanas[149], Y. Kataoka[157], C. Kato[157], A. Katre[52], J. Katzy[45], K. Kawade[70], K. Kawagoe[73], T. Kawamoto[157], G. Kawamura[57], E.F. Kay[77], V.F. Kazanin[111,c], R. Keeler[172], R. Kehoe[43], J.S. Keller[31], E. Kellermann[84], J.J. Kempster[80], J Kendrick[19], H. Keoshkerian[161], O. Kepka[129], B.P. Kerševan[78], S. Kersten[178], R.A. Keyes[90], M. Khader[169], F. Khalil-zada[12], A. Khanov[116], A.G. Kharlamov[111,c], T. Kharlamova[111,c], A. Khodinov[160], T.J. Khoo[52], V. Khovanskiy[99,*], E. Khramov[68], J. Khubua[54b,ac], S. Kido[70], C.R. Kilby[80], H.Y. Kim[8], S.H. Kim[164], Y.K. Kim[33], N. Kimura[156], O.M. Kind[17], B.T. King[77], D. Kirchmeier[47], J. Kirk[133], A.E. Kiryunin[103], T. Kishimoto[157], D. Kisielewska[41a], V. Kitali[45], O. Kivernyk[5], E. Kladiva[146b], T. Klapdor-Kleingrothaus[51], M.H. Klein[92], M. Klein[77], U. Klein[77], K. Kleinknecht[86], P. Klimek[110], A. Klimentov[27], R. Klingenberg[46], T. Klingl[23], T. Klioutchnikova[32], E.-E. Kluge[60a], P. Kluit[109], S. Kluth[103], E. Kneringer[65], E.B.F.G. Knoops[88], A. Knue[103], A. Kobayashi[157], D. Kobayashi[159], T. Kobayashi[157], M. Kobel[47], M. Kocian[145], P. Kodys[131], T. Koffas[31], E. Koffeman[109], N.M. Köhler[103], T. Koi[145], M. Kolb[60b], I. Koletsou[5], A.A. Komar[98,*], T. Kondo[69], N. Kondrashova[36c], K. Köneke[51], A.C. König[108], T. Kono[69,ad], R. Konoplich[112,ae], N. Konstantinidis[81], R. Kopeliansky[64],

JHEP11(2017)195

S. Koperny[41a], A.K. Kopp[51], K. Korcyl[42], K. Kordas[156], A. Korn[81], A.A. Korol[111,c], I. Korolkov[13], E.V. Korolkova[141], O. Kortner[103], S. Kortner[103], T. Kosek[131], V.V. Kostyukhin[23], A. Kotwal[48], A. Koulouris[10], A. Kourkoumeli-Charalampidi[123a,123b], C. Kourkoumelis[9], E. Kourlitis[141], V. Kouskoura[27], A.B. Kowalewska[42], R. Kowalewski[172], T.Z. Kowalski[41a], C. Kozakai[157], W. Kozanecki[138], A.S. Kozhin[132], V.A. Kramarenko[101], G. Kramberger[78], D. Krasnopevtsev[100], M.W. Krasny[83], A. Krasznahorkay[32], D. Krauss[103], J.A. Kremer[41a], J. Kretzschmar[77], K. Kreutzfeldt[55], P. Krieger[161], K. Krizka[16], K. Kroeninger[46], H. Kroha[103], J. Kroll[129], J. Kroll[124], J. Kroseberg[23], J. Krstic[14], U. Kruchonak[68], H. Krüger[23], N. Krumnack[67], M.C. Kruse[48], T. Kubota[91], H. Kucuk[81], S. Kuday[4b], J.T. Kuechler[178], S. Kuehn[32], A. Kugel[60a], F. Kuger[177], T. Kuhl[45], V. Kukhtin[68], R. Kukla[88], Y. Kulchitsky[95], S. Kuleshov[34b], Y.P. Kulinich[169], M. Kuna[134a,134b], T. Kunigo[71], A. Kupco[129], T. Kupfer[46], O. Kuprash[155], H. Kurashige[70], L.L. Kurchaninov[163a], Y.A. Kurochkin[95], M.G. Kurth[35a], V. Kus[129], E.S. Kuwertz[172], M. Kuze[159], J. Kvita[117], T. Kwan[172], D. Kyriazopoulos[141], A. La Rosa[103], J.L. La Rosa Navarro[26d], L. La Rotonda[40a,40b], F. La Ruffa[40a,40b], C. Lacasta[170], F. Lacava[134a,134b], J. Lacey[45], D.P.J. Lack[87], H. Lacker[17], D. Lacour[83], E. Ladygin[68], R. Lafaye[5], B. Laforge[83], T. Lagouri[179], S. Lai[57], S. Lammers[64], W. Lampl[7], E. Lançon[27], U. Landgraf[51], M.P.J. Landon[79], M.C. Lanfermann[52], V.S. Lang[45], J.C. Lange[13], R.J. Langenberg[32], A.J. Lankford[166], F. Lanni[27], K. Lantzsch[23], A. Lanza[123a], A. Lapertosa[53a,53b], S. Laplace[83], J.F. Laporte[138], T. Lari[94a], F. Lasagni Manghi[22a,22b], M. Lassnig[32], T.S. Lau[62a], P. Laurelli[50], W. Lavrijsen[16], A.T. Law[139], P. Laycock[77], T. Lazovich[59], M. Lazzaroni[94a,94b], B. Le[91], O. Le Dortz[83], E. Le Guirriec[88], E.P. Le Quilleuc[138], M. LeBlanc[172], T. LeCompte[6], F. Ledroit-Guillon[58], C.A. Lee[27], G.R. Lee[133,af], S.C. Lee[153], L. Lee[59], B. Lefebvre[90], G. Lefebvre[83], M. Lefebvre[172], F. Legger[102], C. Leggett[16], G. Lehmann Miotto[32], X. Lei[7], W.A. Leight[45], M.A.L. Leite[26d], R. Leitner[131], D. Lellouch[175], B. Lemmer[57], K.J.C. Leney[81], T. Lenz[23], B. Lenzi[32], R. Leone[7], S. Leone[126a,126b], C. Leonidopoulos[49], G. Lerner[151], C. Leroy[97], A.A.J. Lesage[138], C.G. Lester[30], M. Levchenko[125], J. Levêque[5], D. Levin[92], L.J. Levinson[175], M. Levy[19], D. Lewis[79], B. Li[36a,ag], Changqiao Li[36a], H. Li[150], L. Li[36c], Q. Li[35a], Q. Li[36a], S. Li[48], X. Li[36c], Y. Li[143], Z. Liang[35a], B. Liberti[135a], A. Liblong[161], K. Lie[62c], J. Liebal[23], W. Liebig[15], A. Limosani[152], S.C. Lin[182], T.H. Lin[86], R.A. Linck[64], B.E. Lindquist[150], A.E. Lionti[52], E. Lipeles[124], A. Lipniacka[15], M. Lisovyi[60b], T.M. Liss[169,ah], A. Lister[171], A.M. Litke[139], B. Liu[67], H. Liu[92], H. Liu[27], J.K.K. Liu[122], J. Liu[36b], J.B. Liu[36a], K. Liu[88], L. Liu[169], M. Liu[36a], Y.L. Liu[36a], Y. Liu[36a], M. Livan[123a,123b], A. Lleres[58], J. Llorente Merino[35a], S.L. Lloyd[79], C.Y. Lo[62b], F. Lo Sterzo[153], E.M. Lobodzinska[45], P. Loch[7], F.K. Loebinger[87], A. Loesle[51], K.M. Loew[25], A. Loginov[179,*], T. Lohse[17], K. Lohwasser[141], M. Lokajicek[129], B.A. Long[24], J.D. Long[169], R.E. Long[75], L. Longo[76a,76b], K.A. Looper[113], J.A. Lopez[34b], D. Lopez Mateos[59], I. Lopez Paz[13], A. Lopez Solis[83], J. Lorenz[102], N. Lorenzo Martinez[5], M. Losada[21], P.J. Lösel[102], X. Lou[35a], A. Lounis[119], J. Love[6], P.A. Love[75], H. Lu[62a], N. Lu[92], Y.J. Lu[63], H.J. Lubatti[140], C. Luci[134a,134b], A. Lucotte[58], C. Luedtke[51], F. Luehring[64], W. Lukas[65], L. Luminari[134a], O. Lundberg[148a,148b], B. Lund-Jensen[149], M.S. Lutz[89], P.M. Luzi[83], D. Lynn[27], R. Lysak[129], E. Lytken[84], F. Lyu[35a], V. Lyubushkin[68], H. Ma[27], L.L. Ma[36b], Y. Ma[36b], G. Maccarrone[50], A. Macchiolo[103], C.M. Macdonald[141], B. Maček[78], J. Machado Miguens[124,128b], D. Madaffari[170], R. Madar[37], W.F. Mader[47], A. Madsen[45], J. Maeda[70], S. Maeland[15], T. Maeno[27], A.S. Maevskiy[101], V. Magerl[51], J. Mahlstedt[109], C. Maiani[119], C. Maidantchik[26a], A.A. Maier[103], T. Maier[102], A. Maio[128a,128b,128d], O. Majersky[146a], S. Majewski[118], Y. Makida[69], N. Makovec[119], B. Malaescu[83], Pa. Malecki[42], V.P. Maleev[125], F. Malek[58], U. Mallik[66], D. Malon[6], C. Malone[30], S. Maltezos[10], S. Malyukov[32], J. Mamuzic[170], G. Mancini[50], I. Mandić[78], J. Maneira[128a,128b], L. Manhaes de Andrade Filho[26b], J. Manjarres Ramos[47], K.H. Mankinen[84], A. Mann[102], A. Manousos[32], B. Mansoulie[138],

JHEP11(2017)195

J.D. Mansour[35a], R. Mantifel[90], M. Mantoani[57], S. Manzoni[94a,94b], L. Mapelli[32], G. Marceca[29], L. March[52], L. Marchese[122], G. Marchiori[83], M. Marcisovsky[129], C.A. Marin Tobon[32], M. Marjanovic[37], D.E. Marley[92], F. Marroquim[26a], S.P. Marsden[87], Z. Marshall[16], M.U.F Martensson[168], S. Marti-Garcia[170], C.B. Martin[113], T.A. Martin[173], V.J. Martin[49], B. Martin dit Latour[15], M. Martinez[13,v], V.I. Martinez Outschoorn[169], S. Martin-Haugh[133], V.S. Martoiu[28b], A.C. Martyniuk[81], A. Marzin[32], L. Masetti[86], T. Mashimo[157], R. Mashinistov[98], J. Masik[87], A.L. Maslennikov[111,c], L. Massa[135a,135b], P. Mastrandrea[5], A. Mastroberardino[40a,40b], T. Masubuchi[157], P. Mättig[178], J. Maurer[28b], S.J. Maxfield[77], D.A. Maximov[111,c], R. Mazini[153], I. Maznas[156], S.M. Mazza[94a,94b], N.C. Mc Fadden[107], G. Mc Goldrick[161], S.P. Mc Kee[92], A. McCarn[92], R.L. McCarthy[150], T.G. McCarthy[103], L.I. McClymont[81], E.F. McDonald[91], J.A. Mcfayden[32], G. Mchedlidze[57], S.J. McMahon[133], P.C. McNamara[91], C.J. McNicol[173], R.A. McPherson[172,o], S. Meehan[140], T.J. Megy[51], S. Mehlhase[102], A. Mehta[77], T. Meideck[58], K. Meier[60a], B. Meirose[44], D. Melini[170,ai], B.R. Mellado Garcia[147c], J.D. Mellenthin[57], M. Melo[146a], F. Meloni[18], A. Melzer[23], S.B. Menary[87], L. Meng[77], X.T. Meng[92], A. Mengarelli[22a,22b], S. Menke[103], E. Meoni[40a,40b], S. Mergelmeyer[17], C. Merlassino[18], P. Mermod[52], L. Merola[106a,106b], C. Meroni[94a], F.S. Merritt[33], A. Messina[134a,134b], J. Metcalfe[6], A.S. Mete[166], C. Meyer[124], J-P. Meyer[138], J. Meyer[109], H. Meyer Zu Theenhausen[60a], F. Miano[151], R.P. Middleton[133], S. Miglioranzi[53a,53b], L. Mijović[49], G. Mikenberg[175], M. Mikestikova[129], M. Mikuž[78], M. Milesi[91], A. Milic[161], D.A. Millar[79], D.W. Miller[33], C. Mills[49], A. Milov[175], D.A. Milstead[148a,148b], A.A. Minaenko[132], Y. Minami[157], I.A. Minashvili[54b], A.I. Mincer[112], B. Mindur[41a], M. Mineev[68], Y. Minegishi[157], Y. Ming[176], L.M. Mir[13], K.P. Mistry[124], T. Mitani[174], J. Mitrevski[102], V.A. Mitsou[170], A. Miucci[18], P.S. Miyagawa[141], A. Mizukami[69], J.U. Mjörnmark[84], T. Mkrtchyan[180], M. Mlynarikova[131], T. Moa[148a,148b], K. Mochizuki[97], P. Mogg[51], S. Mohapatra[38], S. Molander[148a,148b], R. Moles-Valls[23], M.C. Mondragon[93], K. Mönig[45], J. Monk[39], E. Monnier[88], A. Montalbano[150], J. Montejo Berlingen[32], F. Monticelli[74], S. Monzani[94a,94b], R.W. Moore[3], N. Morange[119], D. Moreno[21], M. Moreno Llácer[32], P. Morettini[53a], S. Morgenstern[32], D. Mori[144], T. Mori[157], M. Morii[59], M. Morinaga[174], V. Morisbak[121], A.K. Morley[32], G. Mornacchi[32], J.D. Morris[79], L. Morvaj[150], P. Moschovakos[10], M. Mosidze[54b], H.J. Moss[141], J. Moss[145,aj], K. Motohashi[159], R. Mount[145], E. Mountricha[27], E.J.W. Moyse[89], S. Muanza[88], F. Mueller[103], J. Mueller[127], R.S.P. Mueller[102], D. Muenstermann[75], P. Mullen[56], G.A. Mullier[18], F.J. Munoz Sanchez[87], W.J. Murray[173,133], H. Musheghyan[32], M. Muškinja[78], A.G. Myagkov[132,ak], M. Myska[130], B.P. Nachman[16], O. Nackenhorst[52], K. Nagai[122], R. Nagai[69,ad], K. Nagano[69], Y. Nagasaka[61], K. Nagata[164], M. Nagel[51], E. Nagy[88], A.M. Nairz[32], Y. Nakahama[105], K. Nakamura[69], T. Nakamura[157], I. Nakano[114], R.F. Naranjo Garcia[45], R. Narayan[11], D.I. Narrias Villar[60a], I. Naryshkin[125], T. Naumann[45], G. Navarro[21], R. Nayyar[7], H.A. Neal[92], P.Yu. Nechaeva[98], T.J. Neep[138], A. Negri[123a,123b], M. Negrini[22a], S. Nektarijevic[108], C. Nellist[119], A. Nelson[166], M.E. Nelson[122], S. Nemecek[129], P. Nemethy[112], M. Nessi[32,al], M.S. Neubauer[169], M. Neumann[178], P.R. Newman[19], T.Y. Ng[62c], T. Nguyen Manh[97], R.B. Nickerson[122], R. Nicolaidou[138], J. Nielsen[139], V. Nikolaenko[132,ak], I. Nikolic-Audit[83], K. Nikolopoulos[19], J.K. Nilsen[121], P. Nilsson[27], Y. Ninomiya[157], A. Nisati[134a], N. Nishu[36c], R. Nisius[103], I. Nitsche[46], T. Nitta[174], T. Nobe[157], Y. Noguchi[71], M. Nomachi[120], I. Nomidis[31], M.A. Nomura[27], T. Nooney[79], M. Nordberg[32], N. Norjoharuddeen[122], O. Novgorodova[47], M. Nozaki[69], L. Nozka[117], K. Ntekas[166], E. Nurse[81], F. Nuti[91], K. O'connor[25], D.C. O'Neil[144], A.A. O'Rourke[45], V. O'Shea[56], F.G. Oakham[31,d], H. Oberlack[103], T. Obermann[23], J. Ocariz[83], A. Ochi[70], I. Ochoa[38], J.P. Ochoa-Ricoux[34a], S. Oda[73], S. Odaka[69], A. Oh[87], S.H. Oh[48], C.C. Ohm[16], H. Ohman[168], H. Oide[53a,53b], H. Okawa[164], Y. Okumura[157], T. Okuyama[69], A. Olariu[28b], L.F. Oleiro Seabra[128a], S.A. Olivares Pino[34a], D. Oliveira Damazio[27], A. Olszewski[42],

JHEP11(2017)195

J. Olszowska[42], A. Onofre[128a,128e], K. Onogi[105], P.U.E. Onyisi[11,z], H. Oppen[121], M.J. Oreglia[33], Y. Oren[155], D. Orestano[136a,136b], N. Orlando[62b], R.S. Orr[161], B. Osculati[53a,53b,*], R. Ospanov[36a], G. Otero y Garzon[29], H. Otono[73], M. Ouchrif[137d], F. Ould-Saada[121], A. Ouraou[138], K.P. Oussoren[109], Q. Ouyang[35a], M. Owen[56], R.E. Owen[19], V.E. Ozcan[20a], N. Ozturk[8], K. Pachal[144], A. Pacheco Pages[13], L. Pacheco Rodriguez[138], C. Padilla Aranda[13], S. Pagan Griso[16], M. Paganini[179], F. Paige[27], G. Palacino[64], S. Palazzo[40a,40b], S. Palestini[32], M. Palka[41b], D. Pallin[37], E.St. Panagiotopoulou[10], I. Panagoulias[10], C.E. Pandini[126a,126b], J.G. Panduro Vazquez[80], P. Pani[32], S. Panitkin[27], D. Pantea[28b], L. Paolozzi[52], Th.D. Papadopoulou[10], K. Papageorgiou[9,s], A. Paramonov[6], D. Paredes Hernandez[179], A.J. Parker[75], M.A. Parker[30], K.A. Parker[45], F. Parodi[53a,53b], J.A. Parsons[38], U. Parzefall[51], V.R. Pascuzzi[161], J.M. Pasner[139], E. Pasqualucci[134a], S. Passaggio[53a], Fr. Pastore[80], S. Pataraia[86], J.R. Pater[87], T. Pauly[32], B. Pearson[103], S. Pedraza Lopez[170], R. Pedro[128a,128b], S.V. Peleganchuk[111,c], O. Penc[129], C. Peng[35a], H. Peng[36a], J. Penwell[64], B.S. Peralva[26b], M.M. Perego[138], D.V. Perepelitsa[27], F. Peri[17], L. Perini[94a,94b], H. Pernegger[32], S. Perrella[106a,106b], R. Peschke[45], V.D. Peshekhonov[68,*], K. Peters[45], R.F.Y. Peters[87], B.A. Petersen[32], T.C. Petersen[39], E. Petit[58], A. Petridis[1], C. Petridou[156], P. Petroff[119], E. Petrolo[134a], M. Petrov[122], F. Petrucci[136a,136b], N.E. Pettersson[89], A. Peyaud[138], R. Pezoa[34b], F.H. Phillips[93], P.W. Phillips[133], G. Piacquadio[150], E. Pianori[173], A. Picazio[89], E. Piccaro[79], M.A. Pickering[122], R. Piegaia[29], J.E. Pilcher[33], A.D. Pilkington[87], A.W.J. Pin[87], M. Pinamonti[135a,135b], J.L. Pinfold[3], H. Pirumov[45], M. Pitt[175], L. Plazak[146a], M.-A. Pleier[27], V. Pleskot[86], E. Plotnikova[68], D. Pluth[67], P. Podberezko[111], R. Poettgen[84], R. Poggi[123a,123b], L. Poggioli[119], I. Pogrebnyak[93], D. Pohl[23], G. Polesello[123a], A. Poley[45], A. Policicchio[40a,40b], R. Polifka[32], A. Polini[22a], C.S. Pollard[56], V. Polychronakos[27], K. Pommès[32], D. Ponomarenko[100], L. Pontecorvo[134a], G.A. Popeneciu[28d], D.M. Portillo Quintero[83], S. Pospisil[130], K. Potamianos[16], I.N. Potrap[68], C.J. Potter[30], H. Potti[11], T. Poulsen[84], J. Poveda[32], M.E. Pozo Astigarraga[32], P. Pralavorio[88], A. Pranko[16], S. Prell[67], D. Price[87], M. Primavera[76a], S. Prince[90], N. Proklova[100], K. Prokofiev[62c], F. Prokoshin[34b], S. Protopopescu[27], J. Proudfoot[6], M. Przybycien[41a], A. Puri[169], P. Puzo[119], J. Qian[92], G. Qin[56], Y. Qin[87], A. Quadt[57], M. Queitsch-Maitland[45], D. Quilty[56], S. Raddum[121], V. Radeka[27], V. Radescu[122], S.K. Radhakrishnan[150], P. Radloff[118], P. Rados[91], F. Ragusa[94a,94b], G. Rahal[181], J.A. Raine[87], S. Rajagopalan[27], C. Rangel-Smith[168], T. Rashid[119], S. Raspopov[5], M.G. Ratti[94a,94b], D.M. Rauch[45], F. Rauscher[102], S. Rave[86], I. Ravinovich[175], J.H. Rawling[87], M. Raymond[32], A.L. Read[121], N.P. Readioff[58], M. Reale[76a,76b], D.M. Rebuzzi[123a,123b], A. Redelbach[177], G. Redlinger[27], R. Reece[139], R.G. Reed[147c], K. Reeves[44], L. Rehnisch[17], J. Reichert[124], A. Reiss[86], C. Rembser[32], H. Ren[35a], M. Rescigno[134a], S. Resconi[94a], E.D. Resseguie[124], S. Rettie[171], E. Reynolds[19], O.L. Rezanova[111,c], P. Reznicek[131], R. Rezvani[97], R. Richter[103], S. Richter[81], E. Richter-Was[41b], O. Ricken[23], M. Ridel[83], P. Rieck[103], C.J. Riegel[178], J. Rieger[57], O. Rifki[115], M. Rijssenbeek[150], A. Rimoldi[123a,123b], M. Rimoldi[18], L. Rinaldi[22a], G. Ripellino[149], B. Ristić[32], E. Ritsch[32], I. Riu[13], F. Rizatdinova[116], E. Rizvi[79], C. Rizzi[13], R.T. Roberts[87], S.H. Robertson[90,o], A. Robichaud-Veronneau[90], D. Robinson[30], J.E.M. Robinson[45], A. Robson[56], E. Rocco[86], C. Roda[126a,126b], Y. Rodina[88,am], S. Rodriguez Bosca[170], A. Rodriguez Perez[13], D. Rodriguez Rodriguez[170], S. Roe[32], C.S. Rogan[59], O. Røhne[121], J. Roloff[59], A. Romaniouk[100], M. Romano[22a,22b], S.M. Romano Saez[37], E. Romero Adam[170], N. Rompotis[77], M. Ronzani[51], L. Roos[83], S. Rosati[134a], K. Rosbach[51], P. Rose[139], N.-A. Rosien[57], E. Rossi[106a,106b], L.P. Rossi[53a], J.H.N. Rosten[30], R. Rosten[140], M. Rotaru[28b], J. Rothberg[140], D. Rousseau[119], A. Rozanov[88], Y. Rozen[154], X. Ruan[147c], F. Rubbo[145], F. Rühr[51], A. Ruiz-Martinez[31], Z. Rurikova[51], N.A. Rusakovich[68],

JHEP11(2017)195

H.L. Russell[90], J.P. Rutherfoord[7], N. Ruthmann[32], Y.F. Ryabov[125], M. Rybar[169], G. Rybkin[119], S. Ryu[6], A. Ryzhov[132], G.F. Rzehorz[57], A.F. Saavedra[152], G. Sabato[109], S. Sacerdoti[29], H.F-W. Sadrozinski[139], R. Sadykov[68], F. Safai Tehrani[134a], P. Saha[110], M. Sahinsoy[60a], M. Saimpert[45], M. Saito[157], T. Saito[157], H. Sakamoto[157], Y. Sakurai[174], G. Salamanna[136a,136b], J.E. Salazar Loyola[34b], D. Salek[109], P.H. Sales De Bruin[168], D. Salihagic[103], A. Salnikov[145], J. Salt[170], D. Salvatore[40a,40b], F. Salvatore[151], A. Salvucci[62a,62b,62c], A. Salzburger[32], D. Sammel[51], D. Sampsonidis[156], D. Sampsonidou[156], J. Sánchez[170], V. Sanchez Martinez[170], A. Sanchez Pineda[167a,167c], H. Sandaker[121], R.L. Sandbach[79], C.O. Sander[45], M. Sandhoff[178], C. Sandoval[21], D.P.C. Sankey[133], M. Sannino[53a,53b], Y. Sano[105], A. Sansoni[50], C. Santoni[37], H. Santos[128a], I. Santoyo Castillo[151], A. Sapronov[68], J.G. Saraiva[128a,128d], B. Sarrazin[23], O. Sasaki[69], K. Sato[164], E. Sauvan[5], G. Savage[80], P. Savard[161,d], N. Savic[103], C. Sawyer[133], L. Sawyer[82,u], J. Saxon[33], C. Sbarra[22a], A. Sbrizzi[22a,22b], T. Scanlon[81], D.A. Scannicchio[166], J. Schaarschmidt[140], P. Schacht[103], B.M. Schachtner[102], D. Schaefer[32], L. Schaefer[124], R. Schaefer[45], J. Schaeffer[86], S. Schaepe[23], S. Schaetzel[60b], U. Schäfer[86], A.C. Schaffer[119], D. Schaile[102], R.D. Schamberger[150], V.A. Schegelsky[125], D. Scheirich[131], M. Schernau[166], C. Schiavi[53a,53b], S. Schier[139], L.K. Schildgen[23], C. Schillo[51], M. Schioppa[40a,40b], S. Schlenker[32], K.R. Schmidt-Sommerfeld[103], K. Schmieden[32], C. Schmitt[86], S. Schmitt[45], S. Schmitz[86], U. Schnoor[51], L. Schoeffel[138], A. Schoening[60b], B.D. Schoenrock[93], E. Schopf[23], M. Schott[86], J.F.P. Schouwenberg[108], J. Schovancova[32], S. Schramm[52], N. Schuh[86], A. Schulte[86], M.J. Schultens[23], H.-C. Schultz-Coulon[60a], H. Schulz[17], M. Schumacher[51], B.A. Schumm[139], Ph. Schune[138], A. Schwartzman[145], T.A. Schwarz[92], H. Schweiger[87], Ph. Schwemling[138], R. Schwienhorst[93], J. Schwindling[138], A. Sciandra[23], G. Sciolla[25], M. Scornajenghi[40a,40b], F. Scuri[126a,126b], F. Scutti[91], J. Searcy[92], P. Seema[23], S.C. Seidel[107], A. Seiden[139], J.M. Seixas[26a], G. Sekhniaidze[106a], K. Sekhon[92], S.J. Sekula[43], N. Semprini-Cesari[22a,22b], S. Senkin[37], C. Serfon[121], L. Serin[119], L. Serkin[167a,167b], M. Sessa[136a,136b], R. Seuster[172], H. Severini[115], T. Sfiligoj[78], F. Sforza[165], A. Sfyrla[52], E. Shabalina[57], N.W. Shaikh[148a,148b], L.Y. Shan[35a], R. Shang[169], J.T. Shank[24], M. Shapiro[16], P.B. Shatalov[99], K. Shaw[167a,167b], S.M. Shaw[87], A. Shcherbakova[148a,148b], C.Y. Shehu[151], Y. Shen[115], N. Sherafati[31], P. Sherwood[81], L. Shi[153,an], S. Shimizu[70], C.O. Shimmin[179], M. Shimojima[104], I.P.J. Shipsey[122], S. Shirabe[73], M. Shiyakova[68,ao], J. Shlomi[175], A. Shmeleva[98], D. Shoaleh Saadi[97], M.J. Shochet[33], S. Shojaii[94a,94b], D.R. Shope[115], S. Shrestha[113], E. Shulga[100], M.A. Shupe[7], P. Sicho[129], A.M. Sickles[169], P.E. Sidebo[149], E. Sideras Haddad[147c], O. Sidiropoulou[177], A. Sidoti[22a,22b], F. Siegert[47], Dj. Sijacki[14], J. Silva[128a,128d], S.B. Silverstein[148a], V. Simak[130], Lj. Simic[14], S. Simion[119], E. Simioni[86], B. Simmons[81], M. Simon[86], P. Sinervo[161], N.B. Sinev[118], M. Sioli[22a,22b], G. Siragusa[177], I. Siral[92], S.Yu. Sivoklokov[101], J. Sjölin[148a,148b], M.B. Skinner[75], P. Skubic[115], M. Slater[19], T. Slavicek[130], M. Slawinska[42], K. Sliwa[165], R. Slovak[131], V. Smakhtin[175], B.H. Smart[5], J. Smiesko[146a], N. Smirnov[100], S.Yu. Smirnov[100], Y. Smirnov[100], L.N. Smirnova[101,ap], O. Smirnova[84], J.W. Smith[57], M.N.K. Smith[38], R.W. Smith[38], M. Smizanska[75], K. Smolek[130], A.A. Snesarev[98], I.M. Snyder[118], S. Snyder[27], R. Sobie[172,o], F. Socher[47], A. Soffer[155], A. Søgaard[49], D.A. Soh[153], G. Sokhrannyi[78], C.A. Solans Sanchez[32], M. Solar[130], E.Yu. Soldatov[100], U. Soldevila[170], A.A. Solodkov[132], A. Soloshenko[68], O.V. Solovyanov[132], V. Solovyev[125], P. Sommer[51], H. Son[165], A. Sopczak[130], D. Sosa[60b], C.L. Sotiropoulou[126a,126b], R. Soualah[167a,167c], A.M. Soukharev[111,c], D. South[45], B.C. Sowden[80], S. Spagnolo[76a,76b], M. Spalla[126a,126b], M. Spangenberg[173], F. Spanò[80], D. Sperlich[17], F. Spettel[103], T.M. Spieker[60a], R. Spighi[22a], G. Spigo[32], L.A. Spiller[91], M. Spousta[131], R.D. St. Denis[56,*], A. Stabile[94a], R. Stamen[60a], S. Stamm[17], E. Stanecka[42], R.W. Stanek[6], C. Stanescu[136a], M.M. Stanitzki[45], B.S. Stapf[109], S. Stapnes[121], E.A. Starchenko[132], G.H. Stark[33], J. Stark[58], S.H Stark[39], P. Staroba[129], P. Starovoitov[60a], S. Stärz[32], R. Staszewski[42], M. Stegler[45], P. Steinberg[27], B. Stelzer[144],

JHEP11(2017)195

H.J. Stelzer[32], O. Stelzer-Chilton[163a], H. Stenzel[55], G.A. Stewart[56], M.C. Stockton[118], M. Stoebe[90], G. Stoicea[28b], P. Stolte[57], S. Stonjek[103], A.R. Stradling[8], A. Straessner[47], M.E. Stramaglia[18], J. Strandberg[149], S. Strandberg[148a,148b], M. Strauss[115], P. Strizenec[146b], R. Ströhmer[177], D.M. Strom[118], R. Stroynowski[43], A. Strubig[49], S.A. Stucci[27], B. Stugu[15], N.A. Styles[45], D. Su[145], J. Su[127], S. Suchek[60a], Y. Sugaya[120], M. Suk[130], V.V. Sulin[98], DMS Sultan[162a,162b], S. Sultansoy[4c], T. Sumida[71], S. Sun[59], X. Sun[3], K. Suruliz[151], C.J.E. Suster[152], M.R. Sutton[151], S. Suzuki[69], M. Svatos[129], M. Swiatlowski[33], S.P. Swift[2], I. Sykora[146a], T. Sykora[131], D. Ta[51], K. Tackmann[45], J. Taenzer[155], A. Taffard[166], R. Tafirout[163a], E. Tahirovic[79], N. Taiblum[155], H. Takai[27], R. Takashima[72], E.H. Takasugi[103], T. Takeshita[142], Y. Takubo[69], M. Talby[88], A.A. Talyshev[111,c], J. Tanaka[157], M. Tanaka[159], R. Tanaka[119], S. Tanaka[69], R. Tanioka[70], B.B. Tannenwald[113], S. Tapia Araya[34b], S. Tapprogge[86], S. Tarem[154], G.F. Tartarelli[94a], P. Tas[131], M. Tasevsky[129], T. Tashiro[71], E. Tassi[40a,40b], A. Tavares Delgado[128a,128b], Y. Tayalati[137e], A.C. Taylor[107], A.J. Taylor[49], G.N. Taylor[91], P.T.E. Taylor[91], W. Taylor[163b], P. Teixeira-Dias[80], D. Temple[144], H. Ten Kate[32], P.K. Teng[153], J.J. Teoh[120], F. Tepel[178], S. Terada[69], K. Terashi[157], J. Terron[85], S. Terzo[13], M. Testa[50], R.J. Teuscher[161,o], T. Theveneaux-Pelzer[88], F. Thiele[39], J.P. Thomas[19], J. Thomas-Wilsker[80], P.D. Thompson[19], A.S. Thompson[56], L.A. Thomsen[179], E. Thomson[124], M.J. Tibbetts[16], R.E. Ticse Torres[88], V.O. Tikhomirov[98,aq], Yu.A. Tikhonov[111,c], S. Timoshenko[100], P. Tipton[179], S. Tisserant[88], K. Todome[159], S. Todorova-Nova[5], S. Todt[47], J. Tojo[73], S. Tokár[146a], K. Tokushuku[69], E. Tolley[59], L. Tomlinson[87], M. Tomoto[105], L. Tompkins[145,ar], K. Toms[107], B. Tong[59], P. Tornambe[51], E. Torrence[118], H. Torres[47], E. Torró Pastor[140], J. Toth[88,as], F. Touchard[88], D.R. Tovey[141], C.J. Treado[112], T. Trefzger[177], F. Tresoldi[151], A. Tricoli[27], I.M. Trigger[163a], S. Trincaz-Duvoid[83], M.F. Tripiana[13], W. Trischuk[161], B. Trocmé[58], A. Trofymov[45], C. Troncon[94a], M. Trottier-McDonald[16], M. Trovatelli[172], L. Truong[147b], M. Trzebinski[42], A. Trzupek[42], K.W. Tsang[62a], J.C-L. Tseng[122], P.V. Tsiareshka[95], G. Tsipolitis[10], N. Tsirintanis[9], S. Tsiskaridze[13], V. Tsiskaridze[51], E.G. Tskhadadze[54a], K.M. Tsui[62a], I.I. Tsukerman[99], V. Tsulaia[16], S. Tsuno[69], D. Tsybychev[150], Y. Tu[62b], A. Tudorache[28b], V. Tudorache[28b], T.T. Tulbure[28a], A.N. Tuna[59], S.A. Tupputi[22a,22b], S. Turchikhin[68], D. Turgeman[175], I. Turk Cakir[4b,at], R. Turra[94a], P.M. Tuts[38], G. Ucchielli[22a,22b], I. Ueda[69], M. Ughetto[148a,148b], F. Ukegawa[164], G. Unal[32], A. Undrus[27], G. Unel[166], F.C. Ungaro[91], Y. Unno[69], C. Unverdorben[102], J. Urban[146b], P. Urquijo[91], P. Urrejola[86], G. Usai[8], J. Usui[69], L. Vacavant[88], V. Vacek[130], B. Vachon[90], K.O.H. Vadla[121], A. Vaidya[81], C. Valderanis[102], E. Valdes Santurio[148a,148b], M. Valente[52], S. Valentinetti[22a,22b], A. Valero[170], L. Valéry[13], S. Valkar[131], A. Vallier[5], J.A. Valls Ferrer[170], W. Van Den Wollenberg[109], H. van der Graaf[109], P. van Gemmeren[6], J. Van Nieuwkoop[144], I. van Vulpen[109], M.C. van Woerden[109], M. Vanadia[135a,135b], W. Vandelli[32], A. Vaniachine[160], P. Vankov[109], G. Vardanyan[180], R. Vari[134a], E.W. Varnes[7], C. Varni[53a,53b], T. Varol[43], D. Varouchas[119], A. Vartapetian[8], K.E. Varvell[152], J.G. Vasquez[179], G.A. Vasquez[34b], F. Vazeille[37], D. Vazquez Furelos[13], T. Vazquez Schroeder[90], J. Veatch[57], V. Veeraraghavan[7], L.M. Veloce[161], F. Veloso[128a,128c], S. Veneziano[134a], A. Ventura[76a,76b], M. Venturi[172], N. Venturi[32], A. Venturini[25], V. Vercesi[123a], M. Verducci[136a,136b], W. Verkerke[109], A.T. Vermeulen[109], J.C. Vermeulen[109], M.C. Vetterli[144,d], N. Viaux Maira[34b], O. Viazlo[84], I. Vichou[169,*], T. Vickey[141], O.E. Vickey Boeriu[141], G.H.A. Viehhauser[122], S. Viel[16], L. Vigani[122], M. Villa[22a,22b], M. Villaplana Perez[94a,94b], E. Vilucchi[50], M.G. Vincter[31], V.B. Vinogradov[68], A. Vishwakarma[45], C. Vittori[22a,22b], I. Vivarelli[151], S. Vlachos[10], M. Vogel[178], P. Vokac[130], G. Volpi[13], H. von der Schmitt[103], E. von Toerne[23], V. Vorobel[131], K. Vorobev[100], M. Vos[170], R. Voss[32], J.H. Vossebeld[77], N. Vranjes[14], M. Vranjes Milosavljevic[14], V. Vrba[130], M. Vreeswijk[109], R. Vuillermet[32], I. Vukotic[33], P. Wagner[23], W. Wagner[178], J. Wagner-Kuhr[102], H. Wahlberg[74], S. Wahrmund[47],

JHEP11(2017)195

J. Walder[75], R. Walker[102], W. Walkowiak[143], V. Wallangen[148a,148b], C. Wang[35b], C. Wang[36b,au], F. Wang[176], H. Wang[16], H. Wang[3], J. Wang[45], J. Wang[152], Q. Wang[115], R. Wang[6], S.M. Wang[153], T. Wang[38], W. Wang[153,av], W. Wang[36a,aw], Z. Wang[36c], C. Wanotayaroj[118], A. Warburton[90], C.P. Ward[30], D.R. Wardrope[81], A. Washbrook[49], P.M. Watkins[19], A.T. Watson[19], M.F. Watson[19], G. Watts[140], S. Watts[87], B.M. Waugh[81], A.F. Webb[11], S. Webb[86], M.S. Weber[18], S.W. Weber[177], S.A. Weber[31], J.S. Webster[6], A.R. Weidberg[122], B. Weinert[64], J. Weingarten[57], M. Weirich[86], C. Weiser[51], H. Weits[109], P.S. Wells[32], T. Wenaus[27], T. Wengler[32], S. Wenig[32], N. Wermes[23], M.D. Werner[67], P. Werner[32], M. Wessels[60a], T.D. Weston[18], K. Whalen[118], N.L. Whallon[140], A.M. Wharton[75], A.S. White[92], A. White[8], M.J. White[1], R. White[34b], D. Whiteson[166], B.W. Whitmore[75], F.J. Wickens[133], W. Wiedenmann[176], M. Wielers[133], C. Wiglesworth[39], L.A.M. Wiik-Fuchs[51], A. Wildauer[103], F. Wilk[87], H.G. Wilkens[32], H.H. Williams[124], S. Williams[109], C. Willis[93], S. Willocq[89], J.A. Wilson[19], I. Wingerter-Seez[5], E. Winkels[151], F. Winklmeier[118], O.J. Winston[151], B.T. Winter[23], M. Wittgen[145], M. Wobisch[82,u], T.M.H. Wolf[109], R. Wolff[88], M.W. Wolter[42], H. Wolters[128a,128c], V.W.S. Wong[171], S.D. Worm[19], B.K. Wosiek[42], J. Wotschack[32], K.W. Wozniak[42], M. Wu[33], S.L. Wu[176], X. Wu[52], Y. Wu[92], T.R. Wyatt[87], B.M. Wynne[49], S. Xella[39], Z. Xi[92], L. Xia[35c], D. Xu[35a], L. Xu[27], T. Xu[138], B. Yabsley[152], S. Yacoob[147a], D. Yamaguchi[159], Y. Yamaguchi[159], A. Yamamoto[69], S. Yamamoto[157], T. Yamanaka[157], F. Yamane[70], M. Yamatani[157], Y. Yamazaki[70], Z. Yan[24], H. Yang[36c], H. Yang[16], Y. Yang[153], Z. Yang[15], W-M. Yao[16], Y.C. Yap[83], Y. Yasu[69], E. Yatsenko[5], K.H. Yau Wong[23], J. Ye[43], S. Ye[27], I. Yeletskikh[68], E. Yigitbasi[24], E. Yildirim[86], K. Yorita[174], K. Yoshihara[124], C. Young[145], C.J.S. Young[32], J. Yu[8], J. Yu[67], S.P.Y. Yuen[23], I. Yusuff[30,ax], B. Zabinski[42], G. Zacharis[10], R. Zaidan[13], A.M. Zaitsev[132,ak], N. Zakharchuk[45], J. Zalieckas[15], A. Zaman[150], S. Zambito[59], D. Zanzi[91], C. Zeitnitz[178], G. Zemaityte[122], A. Zemla[41a], J.C. Zeng[169], Q. Zeng[145], O. Zenin[132], T. Ženiš[146a], D. Zerwas[119], D. Zhang[92], F. Zhang[176], G. Zhang[36a,aw], H. Zhang[119], J. Zhang[6], L. Zhang[51], L. Zhang[36a], M. Zhang[169], P. Zhang[35b], R. Zhang[23], R. Zhang[36a,au], X. Zhang[36b], Y. Zhang[35a], Z. Zhang[119], X. Zhao[43], Y. Zhao[36b,ay], Z. Zhao[36a], A. Zhemchugov[68], B. Zhou[92], C. Zhou[176], L. Zhou[43], M. Zhou[35a], M. Zhou[150], N. Zhou[35c], C.G. Zhu[36b], H. Zhu[35a], J. Zhu[92], Y. Zhu[36a], X. Zhuang[35a], K. Zhukov[98], A. Zibell[177], D. Zieminska[64], N.I. Zimine[68], C. Zimmermann[86], S. Zimmermann[51], Z. Zinonos[103], M. Zinser[86], M. Ziolkowski[143], L. Živković[14], G. Zobernig[176], A. Zoccoli[22a,22b], R. Zou[33], M. zur Nedden[17], L. Zwalinski[32]

[1] Department of Physics, University of Adelaide, Adelaide, Australia
[2] Physics Department, SUNY Albany, Albany NY, United States of America
[3] Department of Physics, University of Alberta, Edmonton AB, Canada
[4] [(a)] Department of Physics, Ankara University, Ankara; [(b)] Istanbul Aydin University, Istanbul; [(c)] Division of Physics, TOBB University of Economics and Technology, Ankara, Turkey
[5] LAPP, CNRS/IN2P3 and Université Savoie Mont Blanc, Annecy-le-Vieux, France
[6] High Energy Physics Division, Argonne National Laboratory, Argonne IL, United States of America
[7] Department of Physics, University of Arizona, Tucson AZ, United States of America
[8] Department of Physics, The University of Texas at Arlington, Arlington TX, United States of America
[9] Physics Department, National and Kapodistrian University of Athens, Athens, Greece
[10] Physics Department, National Technical University of Athens, Zografou, Greece
[11] Department of Physics, The University of Texas at Austin, Austin TX, United States of America
[12] Institute of Physics, Azerbaijan Academy of Sciences, Baku, Azerbaijan
[13] Institut de Física d'Altes Energies (IFAE), The Barcelona Institute of Science and Technology, Barcelona, Spain
[14] Institute of Physics, University of Belgrade, Belgrade, Serbia
[15] Department for Physics and Technology, University of Bergen, Bergen, Norway

JHEP11(2017)195

[16] Physics Division, Lawrence Berkeley National Laboratory and University of California, Berkeley CA, United States of America
[17] Department of Physics, Humboldt University, Berlin, Germany
[18] Albert Einstein Center for Fundamental Physics and Laboratory for High Energy Physics, University of Bern, Bern, Switzerland
[19] School of Physics and Astronomy, University of Birmingham, Birmingham, United Kingdom
[20] [(a)] Department of Physics, Bogazici University, Istanbul; [(b)] Department of Physics Engineering, Gaziantep University, Gaziantep; [(d)] Istanbul Bilgi University, Faculty of Engineering and Natural Sciences, Istanbul; [(e)] Bahcesehir University, Faculty of Engineering and Natural Sciences, Istanbul, Turkey
[21] Centro de Investigaciones, Universidad Antonio Narino, Bogota, Colombia
[22] [(a)] INFN Sezione di Bologna; [(b)] Dipartimento di Fisica e Astronomia, Università di Bologna, Bologna, Italy
[23] Physikalisches Institut, University of Bonn, Bonn, Germany
[24] Department of Physics, Boston University, Boston MA, United States of America
[25] Department of Physics, Brandeis University, Waltham MA, United States of America
[26] [(a)] Universidade Federal do Rio De Janeiro COPPE/EE/IF, Rio de Janeiro; [(b)] Electrical Circuits Department, Federal University of Juiz de Fora (UFJF), Juiz de Fora; [(c)] Federal University of Sao Joao del Rei (UFSJ), Sao Joao del Rei; [(d)] Instituto de Fisica, Universidade de Sao Paulo, Sao Paulo, Brazil
[27] Physics Department, Brookhaven National Laboratory, Upton NY, United States of America
[28] [(a)] Transilvania University of Brasov, Brasov; [(b)] Horia Hulubei National Institute of Physics and Nuclear Engineering, Bucharest; [(c)] Department of Physics, Alexandru Ioan Cuza University of Iasi, Iasi; [(d)] National Institute for Research and Development of Isotopic and Molecular Technologies, Physics Department, Cluj Napoca; [(e)] University Politehnica Bucharest, Bucharest; [(f)] West University in Timisoara, Timisoara, Romania
[29] Departamento de Física, Universidad de Buenos Aires, Buenos Aires, Argentina
[30] Cavendish Laboratory, University of Cambridge, Cambridge, United Kingdom
[31] Department of Physics, Carleton University, Ottawa ON, Canada
[32] CERN, Geneva, Switzerland
[33] Enrico Fermi Institute, University of Chicago, Chicago IL, United States of America
[34] [(a)] Departamento de Física, Pontificia Universidad Católica de Chile, Santiago; [(b)] Departamento de Física, Universidad Técnica Federico Santa María, Valparaíso, Chile
[35] [(a)] Institute of High Energy Physics, Chinese Academy of Sciences, Beijing; [(b)] Department of Physics, Nanjing University, Jiangsu; [(c)] Physics Department, Tsinghua University, Beijing 100084, China
[36] [(a)] Department of Modern Physics and State Key Laboratory of Particle Detection and Electronics, University of Science and Technology of China, Anhui; [(b)] School of Physics, Shandong University, Shandong; [(c)] Department of Physics and Astronomy, Key Laboratory for Particle Physics, Astrophysics and Cosmology, Ministry of Education; Shanghai Key Laboratory for Particle Physics and Cosmology, Shanghai Jiao Tong University, Shanghai(also at PKU-CHEP), China
[37] Université Clermont Auvergne, CNRS/IN2P3, LPC, Clermont-Ferrand, France
[38] Nevis Laboratory, Columbia University, Irvington NY, United States of America
[39] Niels Bohr Institute, University of Copenhagen, Kobenhavn, Denmark
[40] [(a)] INFN Gruppo Collegato di Cosenza, Laboratori Nazionali di Frascati; [(b)] Dipartimento di Fisica, Università della Calabria, Rende, Italy
[41] [(a)] AGH University of Science and Technology, Faculty of Physics and Applied Computer Science, Krakow; [(b)] Marian Smoluchowski Institute of Physics, Jagiellonian University, Krakow, Poland
[42] Institute of Nuclear Physics Polish Academy of Sciences, Krakow, Poland
[43] Physics Department, Southern Methodist University, Dallas TX, United States of America
[44] Physics Department, University of Texas at Dallas, Richardson TX, United States of America
[45] DESY, Hamburg and Zeuthen, Germany

JHEP11(2017)195

[46] Lehrstuhl für Experimentelle Physik IV, Technische Universität Dortmund, Dortmund, Germany
[47] Institut für Kern- und Teilchenphysik, Technische Universität Dresden, Dresden, Germany
[48] Department of Physics, Duke University, Durham NC, United States of America
[49] SUPA - School of Physics and Astronomy, University of Edinburgh, Edinburgh, United Kingdom
[50] INFN e Laboratori Nazionali di Frascati, Frascati, Italy
[51] Fakultät für Mathematik und Physik, Albert-Ludwigs-Universität, Freiburg, Germany
[52] Departement de Physique Nucleaire et Corpusculaire, Université de Genève, Geneva, Switzerland
[53] [(a)] INFN Sezione di Genova; [(b)] Dipartimento di Fisica, Università di Genova, Genova, Italy
[54] [(a)] E. Andronikashvili Institute of Physics, Iv. Javakhishvili Tbilisi State University, Tbilisi; [(b)] High Energy Physics Institute, Tbilisi State University, Tbilisi, Georgia
[55] II Physikalisches Institut, Justus-Liebig-Universität Giessen, Giessen, Germany
[56] SUPA - School of Physics and Astronomy, University of Glasgow, Glasgow, United Kingdom
[57] II Physikalisches Institut, Georg-August-Universität, Göttingen, Germany
[58] Laboratoire de Physique Subatomique et de Cosmologie, Université Grenoble-Alpes, CNRS/IN2P3, Grenoble, France
[59] Laboratory for Particle Physics and Cosmology, Harvard University, Cambridge MA, United States of America
[60] [(a)] Kirchhoff-Institut für Physik, Ruprecht-Karls-Universität Heidelberg, Heidelberg; [(b)] Physikalisches Institut, Ruprecht-Karls-Universität Heidelberg, Heidelberg, Germany
[61] Faculty of Applied Information Science, Hiroshima Institute of Technology, Hiroshima, Japan
[62] [(a)] Department of Physics, The Chinese University of Hong Kong, Shatin, N.T., Hong Kong; [(b)] Department of Physics, The University of Hong Kong, Hong Kong; [(c)] Department of Physics and Institute for Advanced Study, The Hong Kong University of Science and Technology, Clear Water Bay, Kowloon, Hong Kong, China
[63] Department of Physics, National Tsing Hua University, Hsinchu, Taiwan
[64] Department of Physics, Indiana University, Bloomington IN, United States of America
[65] Institut für Astro- und Teilchenphysik, Leopold-Franzens-Universität, Innsbruck, Austria
[66] University of Iowa, Iowa City IA, United States of America
[67] Department of Physics and Astronomy, Iowa State University, Ames IA, United States of America
[68] Joint Institute for Nuclear Research, JINR Dubna, Dubna, Russia
[69] KEK, High Energy Accelerator Research Organization, Tsukuba, Japan
[70] Graduate School of Science, Kobe University, Kobe, Japan
[71] Faculty of Science, Kyoto University, Kyoto, Japan
[72] Kyoto University of Education, Kyoto, Japan
[73] Research Center for Advanced Particle Physics and Department of Physics, Kyushu University, Fukuoka, Japan
[74] Instituto de Física La Plata, Universidad Nacional de La Plata and CONICET, La Plata, Argentina
[75] Physics Department, Lancaster University, Lancaster, United Kingdom
[76] [(a)] INFN Sezione di Lecce; [(b)] Dipartimento di Matematica e Fisica, Università del Salento, Lecce, Italy
[77] Oliver Lodge Laboratory, University of Liverpool, Liverpool, United Kingdom
[78] Department of Experimental Particle Physics, Jožef Stefan Institute and Department of Physics, University of Ljubljana, Ljubljana, Slovenia
[79] School of Physics and Astronomy, Queen Mary University of London, London, United Kingdom
[80] Department of Physics, Royal Holloway University of London, Surrey, United Kingdom
[81] Department of Physics and Astronomy, University College London, London, United Kingdom
[82] Louisiana Tech University, Ruston LA, United States of America
[83] Laboratoire de Physique Nucléaire et de Hautes Energies, UPMC and Université Paris-Diderot and CNRS/IN2P3, Paris, France
[84] Fysiska institutionen, Lunds universitet, Lund, Sweden
[85] Departamento de Fisica Teorica C-15, Universidad Autonoma de Madrid, Madrid, Spain
[86] Institut für Physik, Universität Mainz, Mainz, Germany

JHEP11(2017)195

[87] School of Physics and Astronomy, University of Manchester, Manchester, United Kingdom
[88] CPPM, Aix-Marseille Université and CNRS/IN2P3, Marseille, France
[89] Department of Physics, University of Massachusetts, Amherst MA, United States of America
[90] Department of Physics, McGill University, Montreal QC, Canada
[91] School of Physics, University of Melbourne, Victoria, Australia
[92] Department of Physics, The University of Michigan, Ann Arbor MI, United States of America
[93] Department of Physics and Astronomy, Michigan State University, East Lansing MI, United States of America
[94] [(a)] INFN Sezione di Milano; [(b)] Dipartimento di Fisica, Università di Milano, Milano, Italy
[95] B.I. Stepanov Institute of Physics, National Academy of Sciences of Belarus, Minsk, Republic of Belarus
[96] Research Institute for Nuclear Problems of Byelorussian State University, Minsk, Republic of Belarus
[97] Group of Particle Physics, University of Montreal, Montreal QC, Canada
[98] P.N. Lebedev Physical Institute of the Russian Academy of Sciences, Moscow, Russia
[99] Institute for Theoretical and Experimental Physics (ITEP), Moscow, Russia
[100] National Research Nuclear University MEPhI, Moscow, Russia
[101] D.V. Skobeltsyn Institute of Nuclear Physics, M.V. Lomonosov Moscow State University, Moscow, Russia
[102] Fakultät für Physik, Ludwig-Maximilians-Universität München, München, Germany
[103] Max-Planck-Institut für Physik (Werner-Heisenberg-Institut), München, Germany
[104] Nagasaki Institute of Applied Science, Nagasaki, Japan
[105] Graduate School of Science and Kobayashi-Maskawa Institute, Nagoya University, Nagoya, Japan
[106] [(a)] INFN Sezione di Napoli; [(b)] Dipartimento di Fisica, Università di Napoli, Napoli, Italy
[107] Department of Physics and Astronomy, University of New Mexico, Albuquerque NM, United States of America
[108] Institute for Mathematics, Astrophysics and Particle Physics, Radboud University Nijmegen/Nikhef, Nijmegen, Netherlands
[109] Nikhef National Institute for Subatomic Physics and University of Amsterdam, Amsterdam, Netherlands
[110] Department of Physics, Northern Illinois University, DeKalb IL, United States of America
[111] Budker Institute of Nuclear Physics, SB RAS, Novosibirsk, Russia
[112] Department of Physics, New York University, New York NY, United States of America
[113] Ohio State University, Columbus OH, United States of America
[114] Faculty of Science, Okayama University, Okayama, Japan
[115] Homer L. Dodge Department of Physics and Astronomy, University of Oklahoma, Norman OK, United States of America
[116] Department of Physics, Oklahoma State University, Stillwater OK, United States of America
[117] Palacký University, RCPTM, Olomouc, Czech Republic
[118] Center for High Energy Physics, University of Oregon, Eugene OR, United States of America
[119] LAL, Univ. Paris-Sud, CNRS/IN2P3, Université Paris-Saclay, Orsay, France
[120] Graduate School of Science, Osaka University, Osaka, Japan
[121] Department of Physics, University of Oslo, Oslo, Norway
[122] Department of Physics, Oxford University, Oxford, United Kingdom
[123] [(a)] INFN Sezione di Pavia; [(b)] Dipartimento di Fisica, Università di Pavia, Pavia, Italy
[124] Department of Physics, University of Pennsylvania, Philadelphia PA, United States of America
[125] National Research Centre "Kurchatov Institute" B.P.Konstantinov Petersburg Nuclear Physics Institute, St. Petersburg, Russia
[126] [(a)] INFN Sezione di Pisa; [(b)] Dipartimento di Fisica E. Fermi, Università di Pisa, Pisa, Italy
[127] Department of Physics and Astronomy, University of Pittsburgh, Pittsburgh PA, United States of America
[128] [(a)] Laboratório de Instrumentação e Física Experimental de Partículas - LIP, Lisboa; [(b)] Faculdade

JHEP11(2017)195

de Ciências, Universidade de Lisboa, Lisboa; [c] Department of Physics, University of Coimbra, Coimbra; [d] Centro de Física Nuclear da Universidade de Lisboa, Lisboa; [e] Departamento de Fisica, Universidade do Minho, Braga; [f] Departamento de Fisica Teorica y del Cosmos, Universidad de Granada, Granada; [g] Dep Fisica and CEFITEC of Faculdade de Ciencias e Tecnologia, Universidade Nova de Lisboa, Caparica, Portugal
[129] Institute of Physics, Academy of Sciences of the Czech Republic, Praha, Czech Republic
[130] Czech Technical University in Prague, Praha, Czech Republic
[131] Charles University, Faculty of Mathematics and Physics, Prague, Czech Republic
[132] State Research Center Institute for High Energy Physics (Protvino), NRC KI, Russia
[133] Particle Physics Department, Rutherford Appleton Laboratory, Didcot, United Kingdom
[134] [a] INFN Sezione di Roma; [b] Dipartimento di Fisica, Sapienza Università di Roma, Roma, Italy
[135] [a] INFN Sezione di Roma Tor Vergata; [b] Dipartimento di Fisica, Università di Roma Tor Vergata, Roma, Italy
[136] [a] INFN Sezione di Roma Tre; [b] Dipartimento di Matematica e Fisica, Università Roma Tre, Roma, Italy
[137] [a] Faculté des Sciences Ain Chock, Réseau Universitaire de Physique des Hautes Energies - Université Hassan II, Casablanca; [b] Centre National de l'Energie des Sciences Techniques Nucleaires, Rabat; [c] Faculté des Sciences Semlalia, Université Cadi Ayyad, LPHEA-Marrakech; [d] Faculté des Sciences, Université Mohamed Premier and LPTPM, Oujda; [e] Faculté des sciences, Université Mohammed V, Rabat, Morocco
[138] DSM/IRFU (Institut de Recherches sur les Lois Fondamentales de l'Univers), CEA Saclay (Commissariat à l'Energie Atomique et aux Energies Alternatives), Gif-sur-Yvette, France
[139] Santa Cruz Institute for Particle Physics, University of California Santa Cruz, Santa Cruz CA, United States of America
[140] Department of Physics, University of Washington, Seattle WA, United States of America
[141] Department of Physics and Astronomy, University of Sheffield, Sheffield, United Kingdom
[142] Department of Physics, Shinshu University, Nagano, Japan
[143] Department Physik, Universität Siegen, Siegen, Germany
[144] Department of Physics, Simon Fraser University, Burnaby BC, Canada
[145] SLAC National Accelerator Laboratory, Stanford CA, United States of America
[146] [a] Faculty of Mathematics, Physics & Informatics, Comenius University, Bratislava; [b] Department of Subnuclear Physics, Institute of Experimental Physics of the Slovak Academy of Sciences, Kosice, Slovak Republic
[147] [a] Department of Physics, University of Cape Town, Cape Town; [b] Department of Physics, University of Johannesburg, Johannesburg; [c] School of Physics, University of the Witwatersrand, Johannesburg, South Africa
[148] [a] Department of Physics, Stockholm University; [b] The Oskar Klein Centre, Stockholm, Sweden
[149] Physics Department, Royal Institute of Technology, Stockholm, Sweden
[150] Departments of Physics & Astronomy and Chemistry, Stony Brook University, Stony Brook NY, United States of America
[151] Department of Physics and Astronomy, University of Sussex, Brighton, United Kingdom
[152] School of Physics, University of Sydney, Sydney, Australia
[153] Institute of Physics, Academia Sinica, Taipei, Taiwan
[154] Department of Physics, Technion: Israel Institute of Technology, Haifa, Israel
[155] Raymond and Beverly Sackler School of Physics and Astronomy, Tel Aviv University, Tel Aviv, Israel
[156] Department of Physics, Aristotle University of Thessaloniki, Thessaloniki, Greece
[157] International Center for Elementary Particle Physics and Department of Physics, The University of Tokyo, Tokyo, Japan
[158] Graduate School of Science and Technology, Tokyo Metropolitan University, Tokyo, Japan
[159] Department of Physics, Tokyo Institute of Technology, Tokyo, Japan
[160] Tomsk State University, Tomsk, Russia

JHEP11(2017)195

[161] Department of Physics, University of Toronto, Toronto ON, Canada
[162] [(a)] INFN-TIFPA; [(b)] University of Trento, Trento, Italy
[163] [(a)] TRIUMF, Vancouver BC; [(b)] Department of Physics and Astronomy, York University, Toronto ON, Canada
[164] Faculty of Pure and Applied Sciences, and Center for Integrated Research in Fundamental Science and Engineering, University of Tsukuba, Tsukuba, Japan
[165] Department of Physics and Astronomy, Tufts University, Medford MA, United States of America
[166] Department of Physics and Astronomy, University of California Irvine, Irvine CA, United States of America
[167] [(a)] INFN Gruppo Collegato di Udine, Sezione di Trieste, Udine; [(b)] ICTP, Trieste; [(c)] Dipartimento di Chimica, Fisica e Ambiente, Università di Udine, Udine, Italy
[168] Department of Physics and Astronomy, University of Uppsala, Uppsala, Sweden
[169] Department of Physics, University of Illinois, Urbana IL, United States of America
[170] Instituto de Fisica Corpuscular (IFIC), Centro Mixto Universidad de Valencia - CSIC, Spain
[171] Department of Physics, University of British Columbia, Vancouver BC, Canada
[172] Department of Physics and Astronomy, University of Victoria, Victoria BC, Canada
[173] Department of Physics, University of Warwick, Coventry, United Kingdom
[174] Waseda University, Tokyo, Japan
[175] Department of Particle Physics, The Weizmann Institute of Science, Rehovot, Israel
[176] Department of Physics, University of Wisconsin, Madison WI, United States of America
[177] Fakultät für Physik und Astronomie, Julius-Maximilians-Universität, Würzburg, Germany
[178] Fakultät für Mathematik und Naturwissenschaften, Fachgruppe Physik, Bergische Universität Wuppertal, Wuppertal, Germany
[179] Department of Physics, Yale University, New Haven CT, United States of America
[180] Yerevan Physics Institute, Yerevan, Armenia
[181] Centre de Calcul de l'Institut National de Physique Nucléaire et de Physique des Particules (IN2P3), Villeurbanne, France
[182] Academia Sinica Grid Computing, Institute of Physics, Academia Sinica, Taipei, Taiwan

[a] Also at Department of Physics, King's College London, London, United Kingdom
[b] Also at Institute of Physics, Azerbaijan Academy of Sciences, Baku, Azerbaijan
[c] Also at Novosibirsk State University, Novosibirsk, Russia
[d] Also at TRIUMF, Vancouver BC, Canada
[e] Also at Department of Physics & Astronomy, University of Louisville, Louisville, KY, United States of America
[f] Also at Physics Department, An-Najah National University, Nablus, Palestine
[g] Also at Department of Physics, California State University, Fresno CA, United States of America
[h] Also at Department of Physics, University of Fribourg, Fribourg, Switzerland
[i] Also at II Physikalisches Institut, Georg-August-Universität, Göttingen, Germany
[j] Also at Departament de Fisica de la Universitat Autonoma de Barcelona, Barcelona, Spain
[k] Also at Departamento de Fisica e Astronomia, Faculdade de Ciencias, Universidade do Porto, Portugal
[l] Also at Tomsk State University, Tomsk, and Moscow Institute of Physics and Technology State University, Dolgoprudny, Russia
[m] Also at The Collaborative Innovation Center of Quantum Matter (CICQM), Beijing, China
[n] Also at Universita di Napoli Parthenope, Napoli, Italy
[o] Also at Institute of Particle Physics (IPP), Canada
[p] Also at Horia Hulubei National Institute of Physics and Nuclear Engineering, Bucharest, Romania
[q] Also at Department of Physics, St. Petersburg State Polytechnical University, St. Petersburg, Russia
[r] Also at Borough of Manhattan Community College, City University of New York, New York City, United States of America

JHEP11(2017)195

[s] Also at Department of Financial and Management Engineering, University of the Aegean, Chios, Greece
[t] Also at Centre for High Performance Computing, CSIR Campus, Rosebank, Cape Town, South Africa
[u] Also at Louisiana Tech University, Ruston LA, United States of America
[v] Also at Institucio Catalana de Recerca i Estudis Avancats, ICREA, Barcelona, Spain
[w] Also at Graduate School of Science, Osaka University, Osaka, Japan
[x] Also at Fakultät für Mathematik und Physik, Albert-Ludwigs-Universität, Freiburg, Germany
[y] Also at Institute for Mathematics, Astrophysics and Particle Physics, Radboud University Nijmegen/Nikhef, Nijmegen, Netherlands
[z] Also at Department of Physics, The University of Texas at Austin, Austin TX, United States of America
[aa] Also at Institute of Theoretical Physics, Ilia State University, Tbilisi, Georgia
[ab] Also at CERN, Geneva, Switzerland
[ac] Also at Georgian Technical University (GTU),Tbilisi, Georgia
[ad] Also at Ochadai Academic Production, Ochanomizu University, Tokyo, Japan
[ae] Also at Manhattan College, New York NY, United States of America
[af] Also at Departamento de Física, Pontificia Universidad Católica de Chile, Santiago, Chile
[ag] Also at Department of Physics, The University of Michigan, Ann Arbor MI, United States of America
[ah] Also at The City College of New York, New York NY, United States of America
[ai] Also at Departamento de Fisica Teorica y del Cosmos, Universidad de Granada, Granada, Portugal
[aj] Also at Department of Physics, California State University, Sacramento CA, United States of America
[ak] Also at Moscow Institute of Physics and Technology State University, Dolgoprudny, Russia
[al] Also at Departement de Physique Nucleaire et Corpusculaire, Université de Genève, Geneva, Switzerland
[am] Also at Institut de Física d'Altes Energies (IFAE), The Barcelona Institute of Science and Technology, Barcelona, Spain
[an] Also at School of Physics, Sun Yat-sen University, Guangzhou, China
[ao] Also at Institute for Nuclear Research and Nuclear Energy (INRNE) of the Bulgarian Academy of Sciences, Sofia, Bulgaria
[ap] Also at Faculty of Physics, M.V.Lomonosov Moscow State University, Moscow, Russia
[aq] Also at National Research Nuclear University MEPhI, Moscow, Russia
[ar] Also at Department of Physics, Stanford University, Stanford CA, United States of America
[as] Also at Institute for Particle and Nuclear Physics, Wigner Research Centre for Physics, Budapest, Hungary
[at] Also at Giresun University, Faculty of Engineering, Turkey
[au] Also at CPPM, Aix-Marseille Université and CNRS/IN2P3, Marseille, France
[av] Also at Department of Physics, Nanjing University, Jiangsu, China
[aw] Also at Institute of Physics, Academia Sinica, Taipei, Taiwan
[ax] Also at University of Malaya, Department of Physics, Kuala Lumpur, Malaysia
[ay] Also at LAL, Univ. Paris-Sud, CNRS/IN2P3, Université Paris-Saclay, Orsay, France
[*] Deceased

JHEP11(2017)195